



Since January 2020 Elsevier has created a COVID-19 resource centre with free information in English and Mandarin on the novel coronavirus COVID-19. The COVID-19 resource centre is hosted on Elsevier Connect, the company's public news and information website.

Elsevier hereby grants permission to make all its COVID-19-related research that is available on the COVID-19 resource centre - including this research content - immediately available in PubMed Central and other publicly funded repositories, such as the WHO COVID database with rights for unrestricted research re-use and analyses in any form or by any means with acknowledgement of the original source. These permissions are granted for free by Elsevier for as long as the COVID-19 resource centre remains active.

Application of Heteronuclear NMR Spectroscopy to Bioinorganic and Medicinal Chemistry[☆]

Eirini Fotopoulou and Luca Ronconi, National University of Ireland Galway, Galway, Ireland

© 2018 Elsevier Inc. All rights reserved.

The present article is based on a relevant review paper entitled "Applications of heteronuclear NMR spectroscopy in biological and medicinal chemistry" by L. Ronconi and P. J. Sadler published in *Coordination Chemistry Reviews*, 252, pp. 2239–2277, in November 2008 by Elsevier Ltd. (from now on referred to as Ref. 6a). Parts of the earlier-mentioned publication are reproduced here (either as is or in a modified version) with permission from the copyright owner (Elsevier Ltd.).

Introduction	2
Pearls and Pitfalls in Metal NMR Spectroscopy	3
NMR Spectroscopy of Biologically Relevant Metals and Metalloids	5
s-Block: Alkali Metals (Li, Na, K, Rb, and Cs)	5
Lithium	5
Sodium	6
Potassium	8
Rubidium	9
Cesium	10
s-Block: Alkaline Earth Metals (Mg and Ca)	11
Magnesium	11
Calcium	12
p-Block: Group 13 (B, Al, Ga, In, and Tl)	13
Boron	13
Aluminum	14
Gallium, indium, and thallium	17
p-Block: Group 14 (Si, Ge, Sn, and Pb)	19
Silicon and germanium	19
Tin	19
Lead	20
p-Block: Group 15 (As, Sb, and Bi) and Group 16 (Te)	21
Arsenic, antimony, and bismuth	21
Tellurium	22
d-Block: Group 3 (Sc and Y) and Group 4 (Ti)	22
Scandium and yttrium	22
Titanium	23
d-Block: Group 5 (V) and Group 6 (Cr, Mo, and W)	24
Vanadium	24
Chromium, molybdenum, and tungsten	25
d-Block: Group 7 (Mn and Tc)	26
Manganese	26
Technetium	26
d-Block: Group 8 (Fe, Ru, and Os)	27
Iron	27
Ruthenium and osmium	28
d-Block: Group 9 (Co and Rh)	28
Cobalt and rhodium	28
d-Block: Group 10 (Ni, Pd, and Pt)	29
Nickel and palladium	29
Platinum	29
d-Block: Group 11 (Cu, Ag, and Au)	30
Copper	30
Silver and gold	31
d-Block: Group 12 (Zn, Cd, and Hg)	33
Zinc	33

[☆]*Change History:* April 2018. This article has been reviewed and updated by Luca Ronconi and Eirini Fotopoulou to include recent advanced relevant to the topic published from 2013 to early 2018. Compared with the original version, along with an overall revision of the script, the following specific sections have been extended: ⁶Li, ²³Na, ²⁷Al, ⁷¹Ga, ¹⁹⁵Pt, ¹⁰⁹Ag, ³³S and ⁷⁷Se NMR.

Cadmium	33
Mercury	35
f-Block: Lanthanides	36
NMR Spectroscopy of Biologically Relevant Nonmetals	36
p-Block: Group 15 (N)	36
Nitrogen	36
p-Block: Group 16 (O, S, and Se)	37
Oxygen	37
Sulfur	37
Selenium	38
p-Block: Halogens (F, Cl, Br, and I)	39
Fluorine	39
Chlorine	40
Bromine and iodine	40
Acknowledgments	41
References	41

Nomenclature

<i>A</i>	Natural abundance
<i>I</i>	Nuclear spin quantum number
<i>m</i>	Molality
<i>M</i>	Molarity
<i>Q</i>	Nuclear electric quadrupole moment
sat.	Saturated
T_1	Spin-lattice relaxation time
T_2	Spin-spin relaxation time
γ	Magnetogyric ratio
δ	Chemical shift (in ppm)

Abbreviations

DNP	Dynamic nuclear polarization
EFG	Electric field gradient
FT	Fourier transform
HMQC	Heteronuclear multiple quantum coherence
MQF	Multiple quantum filtered
MRI	Magnetic resonance imaging
NMR	Nuclear magnetic resonance
NOE	Nuclear Overhauser enhancement
PET	Positron emission tomography

Introduction

Although the list may not be complete, about 25 elements are currently believed to be essential for mammalian life, among which 14 are metals or metalloids.¹ Inorganic elements are essential components in many aspects of the biochemistry of living organisms. For instance, they can act as catalytic cores at the active sites of enzymes or as second messengers for a variety of small molecules and receptors, or they can stabilize the tertiary structure of proteins and nucleic acids.² In particular, metals in biological systems usually exist as electron-deficient cations (Lewis acids) that may interact with electron-rich biomolecules that are “natural ligands” (Lewis bases) capable of binding metal ions to perform important biological functions. Additionally, a significant number of clinical trials involve nowadays both essential and nonessential metal-based compounds to be used in either therapy or diagnosis, including anticancer, antibacterial, antiviral, antiparasitic, anti-inflammatory, antineurodegenerative, and magnetic resonance imaging (MRI) contrast agents.¹

The growing interest in understanding the coordination chemistry of biometals and the development of structure-based drug design of inorganic pharmaceuticals require suitable and reliable analytical tools to study the speciation of metal ions in biological

systems. In this context, nuclear magnetic resonance (NMR) spectroscopy is a powerful and versatile technique that can provide site-specific information about chemical bonding, structure and dynamics in molecular systems, and a description at atomic level of the intermolecular receptor–metal ion interactions responsible for molecular recognition.³ Advances in the field have been providing detailed structural information on proteins, nucleic acids, and carbohydrates, including investigations of cells and perfused organs under physiological conditions, thus allowing quantification of the dynamic properties of metabolites and kinetics of enzymatic reactions at steady state or through real-time monitoring.⁴

To date, most successful applications of NMR to biological systems have been typically carried out in aqueous solutions by exploiting nuclei with nuclear spin quantum number $I = 1/2$, such as ^1H , ^{13}C , ^{15}N , and ^{31}P (Table 1), whereas it proved less powerful when applied to quadrupolar nuclei (i.e., $I > 1/2$), that is, those having nonspherical charge distribution and a nuclear electric quadrupole moment (Q). Unfortunately, for a large number of biologically relevant elements, the only NMR-active isotopes are quadrupolar, thus giving rise to broad lines together with low detection sensitivity.⁵

When dealing with the NMR spectroscopy involving ‘exotic nuclei’ (i.e., other than ^1H , ^{13}C , ^{15}N , and ^{31}P), it is worth pointing out that:

- quadrupolar nuclides account for nearly 75% of the stable NMR-active isotopes in the periodic table;
- the inherent sensitivities of $I = 1/2$ and some quadrupolar nuclei are not similar (e.g., ^{45}Sc , ^{59}Co , ^{51}V ($I = 7/2$), and ^{93}Nb ($I = 9/2$) are much less sensitive than ^1H although being all over 99.5% naturally abundant);
- although many useful empirical correlations exist between structure and NMR parameters of $I = 1/2$ nuclei, such correlations are not so widely explored for the quadrupolar counterparts;
- from both the chemical and biological point of view, there is nothing inherently more interesting about $I = 1/2$ nuclei than there is about quadrupolar nuclei (if they were of equal practical difficulty, ^{17}O NMR would be, at least, as widely used as ^1H or ^{13}C NMR);
- if the problem of line broadening of resonances from quadrupolar nuclei could be overcome, then there would be enormously increased research activity in this area.

The aim of this article is to provide a comprehensive overview on the use of heteronuclear (in particular, metal) NMR spectroscopy to investigate the behavior of metal ions in biological systems focusing on some key results and successful applications of NMR spectroscopy involving direct detection of metals. In this regard, although there is growing interest in the applications of solid-state NMR to biological systems, this subject lies outside the scope of this work, which will be therefore limited to NMR studies carried out in solution.

Starting from some review papers published in the last few years,⁶ we will cover relevant results in the field, including the most recent findings reported in the literature to date. The present article is organized as follows:

- the first section provides an overview of metal NMR spectroscopy emphasizing the practical limitations related to quadrupolar nuclei;
- the second section describes illustrative NMR data for biologically relevant metallic and semimetallic elements belonging to s-, p-, d-, and f-block;
- the last section deals with some significant biological data obtained by exploiting nonmetallic NMR-active nuclei other than ^1H , ^{13}C , ^{15}N , and ^{31}P , whose detection to probe, indirectly, the coordination chemistry of biometals has been extensively reviewed.⁷

Nuclides reported in Table 2 are, at least in principle, observable by direct NMR spectroscopy in solution but, to the best of our knowledge, there are no relevant reports on the exploitation of their NMR properties in bioinorganic and medicinal chemistry; therefore, they will not be discussed.

For both the experimental details and the practical setup of the NMR experiments, the reader is referred to the appropriate literature cited throughout the text.

Pearls and Pitfalls in Metal NMR Spectroscopy

The development of metal (in particular transition metal) NMR spectroscopy has been very uneven because of the very small number of nuclei with favorable nuclear properties for high-resolution NMR. The majority of metal nuclei have $I > 1/2$; therefore, contrary to $I = 1/2$ counterparts (having spherical nuclear charge distribution), they show a nonspherical distribution of the nuclear electric charge (i.e., oblate or prolate spheroid). Consequently, in addition to their magnetic moment, they also possess a nuclear

Table 1 NMR properties of the most common $I = 1/2$ nuclei

Isotope	A (%)	γ ($\times 10^7 \text{ rad T}^{-1} \text{ s}^{-1}$)	Relative receptivity to ^{13}C	Reference sample
^1H	99.99	26.752	5870	$\text{Si}(\text{CH}_3)_4/\text{CDCl}_3$ (1%)
^{13}C	1.07	6.728	1	$\text{Si}(\text{CH}_3)_4/\text{CDCl}_3$ (1%)
^{15}N	0.37	2.712	0.023	$\text{CH}_3\text{NO}_2/\text{CDCl}_3$ (90%) or neat
^{31}P	100	10.839	391	$\text{H}_3\text{PO}_4/\text{D}_2\text{O}$ (85%)

Table 2 NMR properties of nuclei with no biological relevance^a

Isotope	A (%)	I	γ ($\times 10^7$ rad T ⁻¹ s ⁻¹)	Q (fm ²)	Relative receptivity to ¹³ C	Reference sample
² H	0.01	1	4.107	0.286	0.007	Si(CD ₃) ₄ /neat
⁹ Be	100	3/2	- 3.760	5.288	81.5	BeSO ₄ /D ₂ O (0.43 M)
⁸⁷ Sr	7.00	9/2	-1.164	33.5	1.120	SrCl ₂ /D ₂ O (0.5 M)
⁹¹ Zr	11.22	5/2	-2.497	-17.6	6.26	[ZrCp ₂ Cl ₂]/CD ₂ Cl ₂ (sat.)
⁹³ Nb	100	9/2	6.567	-32.0	2870	K[NbCl ₆]/CD ₃ CN (sat.)
¹³⁵ Ba	6.59	3/2	2.676	16.0	1.930	BaCl ₂ /D ₂ O (0.5 M)
¹³⁷ Ba	11.23	3/2	2.993	24.5	4.620	
¹⁷⁷ Hf	18.60	7/2	1.086	336.5	1.54	-
¹⁷⁹ Hf	13.62	9/2	-0.682	379.3	0.438	
¹⁸¹ Ta	99.99	7/2	3.244	317.0	220	K[TaCl ₆]/CD ₃ CN (sat.)
¹⁸⁵ Re	37.40	5/2	6.106	218.0	305	K[ReO ₄]/D ₂ O (0.1 M)
¹⁸⁷ Re ^b	62.60	5/2	6.168	207.0	526	
¹⁹¹ Ir	37.30	3/2	0.481	81.6	0.064	-
¹⁹³ Ir	62.70	3/2	0.523	75.1	0.137	

^aExcluding noble gases, lanthanides, actinides, and most radioactive isotopes.

^bRadioactive with a long half-life (41.2×10^9 year).

electric quadrupole moment (Q) but, whereas the orientation of the magnetic (spin) dipole is quantized relative to the external magnetic field, the orientation of Q is quantized relative to the electric field gradient (EFG) at the observed nucleus, arising from the local electronic environment (i.e., electrons and other surrounding nuclei). EFGs exert a torque on the quadrupolar nuclei and the tumbling of the molecule can then trigger transitions among the various nuclear spin states. The quadrupolar coupling constant is defined as $\chi = e^2Q(\text{EFG})/h$ where h is Planck constant (6.626070×10^{-34} J s).

The main drawback of NMR spectroscopy of quadrupolar nuclei is that the spin-lattice relaxation time (T_1) can be very short and broad lines (or even none) may be recorded. The nuclear energy levels depend on both the EFG and the applied magnetic field. In the liquid phase, rapid and isotropic molecular tumbling averages both dipolar and quadrupolar interactions. On the other hand, relaxation of Q upon fluctuations of the EFG (e.g., due to molecular collisions) relaxes the nuclear spin as well, and the fast relaxation often results in short-lived nuclear states with broad resonance lines (quadrupolar broadening).⁸

The quadrupolar relaxation rate is defined as

$$\frac{1}{T_Q} = \frac{3\pi^2(2I+3)}{10I^2(2I-1)} \left(1 + \frac{\eta^2}{2I-1}\right) \left(\frac{e^2Q(\text{EFG})}{h}\right)^2 \tau_c$$

where η is the asymmetry parameter of the EFG and τ_c is the rotational correlation time for isotropic tumbling. Anyway, it is worth reminding that this equation is valid when the molecular motion is characterized by an isotropic tumbling correlation time, and $1/T_{1Q} = 1/T_{2Q}$; $\tau_c = 4\pi\eta_0r^3/3k_B T$, where η_0 is the viscosity of the medium, k_B is Boltzmann constant ($1.3806488 \times 10^{-23}$ J K⁻¹), T is the temperature, and r is the molecular radius.

The linewidth depends on the linewidth factor

$$\frac{Q^2(2I+3)}{I^2(2I-1)}$$

Accordingly, favorable properties to metal NMR spectroscopy are the following.

- $I = 1/2$.
- For quadrupolar nuclei, larger values of I minimize Q , thus decreasing line broadening and increasing receptivity (see succeeding text).
- Large natural abundance (A) of the NMR-active nucleus (which may be accomplished by isotopic enrichment) and large magnetogyric ratio (γ , effectively the ratio of the magnetic moment to the nuclear spin quantum number) increase the intrinsic NMR receptivity (i.e., the intensity of the signal) given by $|\gamma^3|AI(I+1)$. $I = 1/2$ nuclei with low- γ values have a further problem of too slow relaxation since the rate depends on γ , so long accumulation times and/or sensitivity enhancement techniques may be required.

In general, quadrupolar nuclei display broad resonances in NMR spectra, unless they are in highly symmetrical electrical environments, which reduce the magnitude of the EFGs at the nuclei (extreme narrowing conditions). Biological macromolecules that introduce high EFGs, in conjunction with nonaveraging motional characteristics, can make quadrupolar interaction effective. However, the binding of quadrupolar metal ions can be studied by NMR spectroscopy, potentially even in the cells. This is possible

because the binding of metal ions to a biomolecule can cause a substantial increase of the effective τ_c , thus leading to a favorable change in relaxation behavior of the ions.

Another severe hindrance to the development of transition metal NMR spectroscopy is caused by the fact that some nuclei in specific oxidation states, such as high-spin Fe(II), Fe(III), Co(II), Ni(II), Cu(II), and Ru(III), are paramagnetic. Paramagnetic compounds contain unpaired electrons whose density has a drastic effect on both the chemical shift and the linewidth of signals in the NMR spectra of metalloproteins containing one or more paramagnetic transition metals.

Line broadening of NMR signals corresponding to the paramagnetic metal itself and to the nuclei in the neighborhood of the paramagnetic center is a severe limitation for high-resolution NMR spectroscopy. Relaxation of the unpaired electron(s) gives rise to the major source of line broadening of resonances for paramagnetic compounds in solution spectra, as the relative electron relaxation is sensed by the resonating nucleus through dipolar coupling. In addition, the delocalization of the unpaired electron(s) throughout the molecule is another factor that causes extreme line broadening.⁹ In some cases, extreme line broadening prevents the detection of any NMR signal.

The hyperfine shift is another factor to be taken into account when NMR studies are carried out on paramagnetic systems. It is defined as the difference in chemical shift between that of a paramagnetic molecule and that of an analogous diamagnetic system. Both contact (through-bond) and pseudo-contact (through-space) shifts are important contributors. In particular, the hyperfine shifts of nuclei in paramagnetic molecules can be well outside the window of signals for diamagnetic counterparts (even hundreds of ppm). The wide range of chemical shift values observed for paramagnetic compounds (large high-frequency and low-frequency shifts) is often attributed to the different resulting spin delocalization mechanisms.⁹

On the other hand, in some circumstances, the effects induced by a paramagnetic metal ion can be used to probe the active sites of metalloproteins and analyzed to give additional constraints for structural calculations on paramagnetic proteins, leading to NMR structures with greater precision. In fact, many NMR structures of a variety of paramagnetic metalloproteins have been reported to date.⁹

To summarize, the development of NMR techniques for the direct detection of metal ions in biological systems has been hampered by the quadrupolar and paramagnetic properties of some of the biometals of interest. Nevertheless, several successful studies have been carried out in the field, which are reported in the following sections. (*Note to chemical shift referencing:* Given a specific NMR signal recorded for the nucleus X, its chemical shift (δ) is defined as the difference between its resonance frequency ($\nu_{X, \text{sample}}$ in Hz) and the resonance frequency of the reference substance ($\nu_{X, \text{ref}}$ in Hz), divided by the operating frequency of the spectrometer ($\nu_{X, \text{spec}}$ in MHz): $\delta = (\nu_{X, \text{sample}} - \nu_{X, \text{ref}}) / \nu_{X, \text{spec}}$. Owing to the different units of numerator (Hz) and denominator (MHz), chemical shifts result in $\times 10^{-6}$ unitless figures. Therefore, for greater convenience, the factor of 10^6 difference is discarded and δ is appropriately represented by the unit ppm (parts per million). NMR referencing is a rather delicate topic, and this issue is even more pronounced in the case of metal NMR spectroscopy. In fact, different reference substances and sign conventions have been used throughout the past decades, thus making the comparison of data reported in the literature difficult and somewhat misleading. Moreover, since salts are generally used as references, the actual chemical shifts may be strongly influenced by the nature of the counterion and by the concentration of the salt itself. In this article, the reported NMR parameters, including the reference samples and conditions, are those recommended by the *International Union of Pure and Applied Chemistry* (IUPAC Recommendations 2001, revised and updated in 2008).¹⁰ Nevertheless, the reader should be aware of the existence of a number of alternative references and conventions and should refer to the individual papers cited throughout the text for a correct comparison.)

NMR Spectroscopy of Biologically Relevant Metals and Metalloids

s-Block: Alkali Metals (Li, Na, K, Rb, and Cs)

Lithium

Isotope	A (%)	I	$\gamma (\times 10^7 \text{ rad T}^{-1} \text{ s}^{-1})$	Q (fm^2)	Relative receptivity to ^{13}C	Reference sample
^6Li	7.59	1	3.937	0.081	3.79	LiCl/D ₂ O (9.7 m)
^7Li	92.41	3/2	10.398	4.01	1590	

Lithium is generally present only at trace levels within the human body, and neither nutritional nor biological roles have been undoubtedly recognized so far. On the other hand, there are several medical uses of Li(I) derivatives, in particular, for the treatment of bipolar disorders.¹¹

Naturally occurring lithium consists of the ^6Li and ^7Li isotopes, which are weakly quadrupolar (compared to other alkali metals) owing to their small quadrupole moments reflecting the small size and simple electronic structure. Both isotopes yield narrow spectral lines and long T_1 (typically 2–8 s), but the higher natural isotopic abundance and receptivity and the more favorable relaxation properties make ^7Li the isotope of choice for most studies (although ^6Li NMR has been also employed).¹² Owing to the relatively simple aqueous chemistry of the Li^+ ion, the chemical shift range is rather small and spectra usually show a single (averaged) resonance from all environments, thus complicating the interpretation of the NMR signals of the usually heterogeneous biological systems. Therefore, it is often advantageous to resolve signals from the different compartments by either exploiting

differences in relaxation properties or adding a shift reagent since each local Li(I) environment may potentially have a characteristic concentration and spin relaxation behavior.

^7Li NMR is particularly suitable for studying transmembrane transport and competitive countertransport of Li^+ and other alkali metals.¹³ Nevertheless, a major application relates to the development of noninvasive *in vivo* analytical tools to measure brain lithium concentration and speciation in humans to elucidate the mechanism(s) of therapeutic action and toxicity of lithium-based drugs in clinical practice.¹⁴ Remarkably, NMR investigations of the human brain at high magnetic field (3 T) allowed the determination of the relationship between the amount of lithium in the brain and in serum in lithium-treated bipolar patients.^{14c}

The beneficial effect of Li in mania and depression results from its action on the brain and, hence, the evaluation of its amount is an important parameter with regard to patient response. As brain lithium cannot be monitored readily at present, its concentration is measured in the serum. Moreover, due to the sedative and possible neurotoxic side effects, Li^+ concentration needs to be monitored and maintained within the safe therapeutic window by measuring it in serum or plasma. Although plasma lithium values are used to monitor the therapy, the lithium in red blood cells (RBCs) may provide a better estimate of levels in brain.¹⁵ For example, rats were treated with different amounts of Li_2CO_3 and, 24 h after administration, blood was collected, added with a Tm(III)-based shift reagent, and analyzed by ^7Li NMR, providing a clear discrimination between plasma and RBC lithium signals.¹⁶ The ^7Li spectrum (Fig. 1) shows two peaks about 13 ppm apart corresponding to plasma (extracellular) and RBC (intracellular) lithium. By comparing peak intensities with standards prepared using blood from untreated rats, it was possible to quantify the amount of lithium and results were in good agreement with other commonly employed techniques.

Hyperpolarized ^6Li NMR was recently shown to provide insights into hemoglobin oxygenation levels. Hyperpolarization by dissolution dynamic nuclear polarization (DNP) is a relatively new technique that enhances the NMR signal intensity of insensitive long- T_1 nuclei such as ^6Li .¹⁷ ^6Li is a $I = 1$ nucleus with an exceptionally small quadrupole moment that can be hyperpolarized by dissolution DNP and, subsequently, detected even *in vivo*.¹⁸ Accordingly, Mishkovsky and coworkers exploited hyperpolarized ^6Li to evaluate blood oxygenation in human and rat blood and plasma.¹⁹ Based on the assumption that ^6Li longitudinal relaxation of Li^+ ions in aqueous solution is strongly dependent on the concentration of paramagnetic species,²⁰ the measurement of the longitudinal relaxation time of $^6\text{Li}^+$ in presence of oxygenated hemoglobin (diamagnetic) and deoxyhemoglobin (paramagnetic) allowed the reproducible mapping of blood oxygenation in a number of samples, and results were fully consistent with those obtained by means of the usual oxygen gas analysis.

Sodium

Isotope	A (%)	I	γ ($\times 10^7 \text{ rad T}^{-1} \text{ s}^{-1}$)	Q (fm^2)	Relative receptivity to ^{13}C	Reference sample
^{23}Na	100	3/2	7.081	10.4	545	$\text{NaCl/D}_2\text{O}$ (0.1 M)

Sodium ions have a number of functions, including the cotransport of solutes and the maintenance of both concentration gradients across cell membranes and the pH (Na^+/H^+ transport). Moreover, Na^+ is involved in several pathological processes, such as cell death, edema formation, tumor growth, electrophysiological processes, and ion transport, all showing alterations in either intra- or extracellular sodium levels.²¹

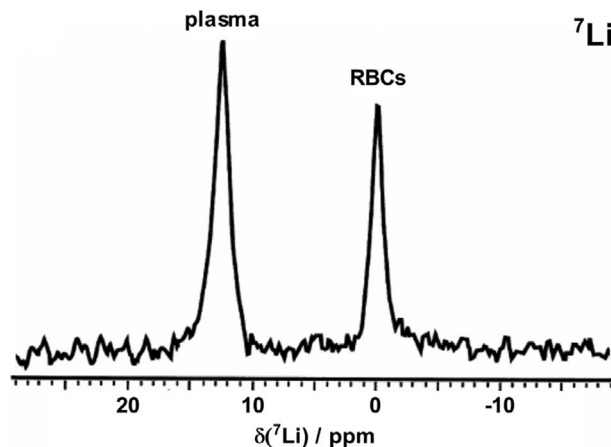


Fig. 1 ^7Li NMR spectrum of the blood sample drawn from a rat 24 h after treatment with Li_2CO_3 , recorded in 30 min at 7 T field strength. The chemical shift of lithium accumulated in RBC was set to 0 ppm. ^7Li resonances in RBC and plasma are separated by 13 ppm by the addition of 20 mg of $[\text{Tm}(\text{DOTP})]^{5-}$ (DOTP = dioctyl terephthalate) as shift reagent. Adapted from Pierson, E.; Luterbach, K.; Rzepka, E.; Ramaprasad, S. *Magn. Reson. Imaging* **2004**, *22*, 123–126, with permission.

Among the NMR-active nuclei in biological samples, ^{23}Na is favored because of its high natural abundance, relatively high sensitivity to detection, and high concentrations in tissues (5–150 mM). Notwithstanding its quadrupolar properties, lineshape analysis of ^{23}Na NMR resonances can provide information on Na^+ binding, and the study of relaxation processes can describe the dynamics of sodium ions in living systems and correlate such dynamics with the pathological or normal state of the system itself.

In most living cells, the transmembrane gradients of sodium ions are essential for proper cell function. Therefore, changes in ion concentrations at each side of the membrane may result in severe functional disorders of the cell. In this regard, ^{23}Na NMR relaxation techniques are able to discriminate between different adjacent sodium ion compartments, whether or not they are physically separated, as long as they show different molecular motions and, thus, induce different relaxation characteristics. The use of multiple echoes to provide relaxation information has greatly increased the usefulness of ^{23}Na NMR spectroscopy, and addition of paramagnetic shift reagents or contrast reagents allows the differentiation of intra- and extracellular sodium pools. The first widely used aqueous shift reagent for cations was reported by Gupta and coworkers in the attempt at finding suitable compounds impermeable to cell membrane and capable to split the NMR resonances. They succeeded with $[\text{Dy}(\text{PPP})_2]^{7-}$ (PPP = tripolyphosphate) in experiments with sequential frequency-selective radiofrequency pulses to excite selectively the well-resolved resonances of shifted and nonshifted sodium and produce separate images of the different sodium pools.²² Their discovery was followed by many other lanthanide-based shift reagents used for many different applications, including the study of ion transport and metabolism, the measurement of temperature and pH, the enantioselectivity ratio of a substance, and the encapsulation efficiency of liposomes.^{23a-f} For example, $[\text{Tm}(\text{DOTP})]^{5-}$ (DOTP = dioctyl terephthalate) was successfully used to study Na^+ transport in human erythrocytes and to quantify the movement of ions across the membrane.^{23g} Other recent examples encompass the use of ^{23}Na NMR in the evaluation of the intra- and extracellular diffusion of sodium ions in rat skeletal muscle (and its effect on ischemia),^{23h} the study of sodium ion gradients in microorganisms,²³ⁱ the investigation of complex I driven sodium transport,^{23j} and the determination of the stoichiometric relationship between Na^+ ions transported and glucose consumed in human erythrocytes.^{23k}

Multiple quantum and multiple-quantum filtered (MQF) pulse sequences were proved useful to define the interaction of quadrupolar nuclei like ^{23}Na with biologically relevant macromolecules, including in vivo NMR and MRI applications.²⁴ In particular, the relaxation profiles of specific magnetization or coherence of a quadrupolar ion can be used to determine sodium binding to biomolecules. For example, Torres and coworkers have used the relaxation properties of selected ^{23}Na magnetization coherences to determine the apparent binding constants for Na^+ and a protein (bovine serum albumin, BSA), a nucleic acid (yeast RNA), and a self-associating macroassembly (the detergent sodium dodecyl sulfate, SDS).²⁵ These three macromolecular systems were chosen as models of different classes of biomolecules that are likely to have diverse Na^+ -binding environments, and the results confirmed the occurrence of a strong binding to RNA and weak binding to BSA, whereas both strong and weak binding sites were identified in SDS.

Geraldes and coworkers used ^{23}Na MQF NMR spectroscopy to characterize the isotropic and anisotropic binding and dynamics of intra- and extracellular Na^+ ions in different cellular systems in the absence and presence of Li^+ .²⁶ This study provided a detailed evaluation of extra- and intracellular molecular sites of Na^+ and Li^+ binding, enabling the differentiation between isotropic and anisotropic Na^+ binding sites and the determination of the extent of Li^+ competition for those sites. Remarkably, this represents a solid proof-of-concept to the exploitation of ^{23}Na MQF NMR to decipher the pharmacokinetics and binding sites of lithium-based drugs in vivo.¹¹

Guanine quadruplexes (G-quadruplexes) are noncanonical nucleic acid structures present in guanine-rich nucleic acid sequences, in which four guanine bases are interconnected via Hoogsteen hydrogen bonds to form planar G-quartets that stack to each other. In the center of the cycle formed by the four guanines, completely dehydrated alkali ions (usually K^+ or Na^+) are coordinated by the buried carbonyl oxygens of the nucleotides. Stacked G-quartets form an ion channel, and the presence of the cations is crucial for the formation, stability, and function of G-quadruplexes. The presence of G-quadruplexes in different regions of the genome suggests a biological relevance for these systems.²⁷ Detection of alkali cations in G-quadruplexes has usually relied on either direct solid-state techniques, such as X-ray crystallography and solid-state NMR, or indirect methods using surrogate $I = 1/2$ probes, such as $^{15}\text{NH}_4^+$ and $^{205}\text{Tl}^+$, in solution NMR experiments.²⁸ On the basis of these studies, two types of alkali metal-binding sites were generally found in G-quadruplex structures, one type being loosely coordinated to phosphate groups and the other residing inside the G-quadruplex channel. For several years, direct detection by solution NMR of alkali ions was considered unfeasible due to low signal intensity and unfavorable quadrupolar properties. Nevertheless, Won and coworkers reported the first direct solution NMR detection of the Na^+ residing inside G-quadruplex channel structures formed by 5'-guanosinemonophosphate (5'-GMP) and the DNA oligomer, $d(\text{TG}_4\text{T})$.²⁹ Fig. 2A shows ^{29}Na NMR spectra for 0.8 M $\text{Na}_2(5'\text{-GMP})$ in an aqueous solution at pH 8. The signal centered at 0 ppm exhibits a bi-Lorentzian lineshape arising from the slow exchange of Na^+ cations between phosphate-bound and free states. The small peak at -17 ppm is due to the Na^+ cations residing inside the 5'-GMP channel. The signal intensity for the channel Na^+ cations decreases as the sample temperature increases from 278 to 308 K, an indication of "melting" of the 5'-GMP aggregates. Analogously (Fig. 2B), ^{23}Na NMR spectra of $d(\text{TG}_4\text{T})$ show the channel Na^+ signal at -17 ppm but, in this case, the total integrated area for this signal remains approximately unchanged between 278 and 293 K, indicating that the G-quadruplex structure of $d(\text{TG}_4\text{T})$ does not melt at 293 K.

These findings opened up many new possibilities in the study of cation binding and transport dynamics in G-quadruplexes including the measurement of cation binding affinity for the channel site in a direct and site-specific way.³⁰

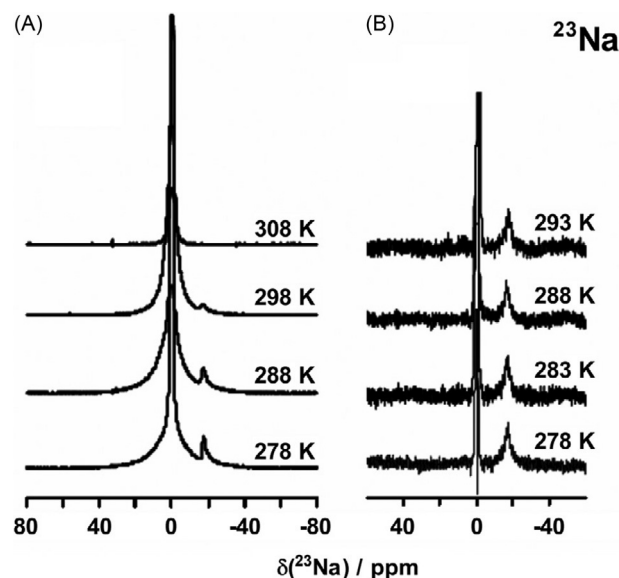


Fig. 2 Variable temperature ^{23}Na NMR spectra of (a) 0.80 M $\text{Na}_2(5'\text{-GMP})$ and (b) 8 mM $d(\text{TG}_4\text{T})$ in 10 mM sodium phosphate buffer (pH 7.1) and 100 mM NaCl. ^{23}Na chemical shifts are referenced to aqueous NaCl 1.0 M at 0.0 ppm. Adapted from Wong, A.; Ida, R.; Wu, G. *Biochem. Biophys. Res. Commun.* **2005**, *337*, 363–366, with permission.

Potassium

Isotope	A (%)	I	γ ($\times 107 \text{ rad T}^{-1} \text{ s}^{-1}$)	Q (fm^2)	Relative receptivity to ^{13}C	Reference sample
^{39}K	93.24	3/2	1.250	5.85	2.79	KCl/D ₂ O (0.1 M)
^{40}K	0.01	4	-1.554	-7.3	0.004	
^{41}K	6.73	3/2	0.686	7.11	0.033	

Together with sodium, potassium represents the most abundant monovalent cation in the cells. In particular, it is the major ion in intracellular fluids (typically ~ 140 mM), whereas Na^+ is found at higher concentration outside the cell (145 vs. 5 mM). K^+ is involved in the control of transmembrane potentials and regulates the equilibrium of cellular electrolytes and osmotic pressure. It acts primarily as counterion for negatively charged solutes and is involved in counterbalancing the high negative charge density associated with the nucleic acid phosphate backbone. The interaction with most biological ligands is weak and, as such, its direct binding is unlikely to be involved in the triggering of biological activity, although it seems to be required for the activation of a number of enzymes.²¹

Conventional analytical methods for the detection of intracellular ions (e.g., flame photometry and radioisotope tracer techniques) rely on time-consuming destructive methods to achieve separation of intra- and extracellular compartments. Furthermore, there could be uncertainty associated with the nonspecific binding of ions to the cell membrane and with ion fluxes during the separation procedure. Conversely, the possibility to develop nondestructive and noninvasive methods such as NMR spectroscopy is highly desirable. Naturally occurring potassium consists of the quadrupolar ^{39}K , ^{40}K , and ^{41}K nuclides, the former being the isotope of choice for most NMR studies because of its higher natural abundance. Unfortunately, low sensitivity (compared to ^7Li and ^{23}Na) was proved a major drawback for the development of such analytical technique, as confirmed by the relatively few data reported in the literature. Nevertheless, as technology evolves, the detectability and quantification in different tissues by means of NMR spectroscopy have been improving over time. For instance, the recent development of a triple resonant ($^{39}\text{K}/^{23}\text{Na}/^1\text{H}$) radiofrequency coil setup allowed the unprecedented acquisition of tissue images of a rat head *in vivo* by ^{39}K MRI,³¹ and, more recently, a detailed investigation of the ^{39}K magnetic resonance imaging of human muscle tissue *in vivo* has been reported.³²

Most intracellular K^+ is bound to ribosomes as it stabilizes the negatively charged ribose–phosphate backbone and specific structural motifs. In general, acting as charge screen, together with divalent metal ions, it is crucial for the establishment of the correct structure of RNAs and is also associated with DNAs. The first direct solution NMR detection of K^+ residing inside G-quadruplex channel structures formed by 5'-GMP and the DNA oligomer $d(\text{TG}_4\text{T})$ was reported by Wong and coworkers in 2005.²⁹ As shown in Fig. 3, two ^{39}K resonances are clearly observed at 278 K. The peak at 0 ppm is due to surface/free K^+ cations, whereas the signal at about 18 ppm was assigned to the channel K^+ cations, whose intensity decreases as the sample temperature is increased, thus indicating the “melting” of the 5'-GMP aggregates. It was also found that potassium ions move through the G-quadruplex channel at a much slower rate than sodium counterparts.

^{39}K NMR studies were also carried out to investigate the interaction of K^+ with ribosomes³³ and quadruplex DNA,³⁴ and attempts have been made to quantify intracellular K^+ in vitro.³⁵

K^+ transport in human erythrocytes was successfully studied by employing a Dy(III)-based paramagnetic shift reagent,³⁶ which allowed intra- and extracellular ^{39}K NMR signals to be discriminated (Fig. 4), thus establishing the suitability of NMR spectroscopy for measuring K^+ fluxes and ion concentrations in human erythrocytes.

Rubidium

Isotope	A (%)	I	γ ($\times 10^7 \text{ rad T}^{-1} \text{ s}^{-1}$)	Q (fm^2)	Relative receptivity to ^{13}C	Reference sample
^{85}Rb	72.17	5/2	2.593	27.6	45	RbCl/D ₂ O (0.01 M)
$^{87}\text{Rb}^a$	27.83	3/2	8.786	13.35	290	

^aRadioactive with a long half-life (4.81×10^{10} year, β^-)

Rubidium has two quadrupolar NMR-active isotopes and, despite the higher natural abundance of ^{85}Rb , ^{87}Rb is the isotope of choice for NMR studies because of the more favorable spectroscopic properties.

Rubidium has no acknowledged natural biological role but Rb^+ is an established probe for K^+ . Rb^+ uptake data can be used to approximate K^+ influx provided that there are no significant differences in ion selectivity of the different K^+ -transporting systems.³⁷ This implies similar ion selectivity of the systems transferring these ions inside and outside cells, thus supporting the role of Rb^+ as a mimic for K^+ . The rates of influx and efflux of Rb^+ in living tissues and isolated cells have been measured by ^{87}Rb NMR spectroscopy.³⁸ The relatively high natural abundance, low biological abundance, and high NMR sensitivity of ^{87}Rb (compared to ^{39}K) make it a good tracer for K^+ influx and efflux studies by NMR in cells and perfused organs.³⁷ With reference to Fig. 5, Rb^+ uptake rates determined by ^{87}Rb NMR spectroscopy are similar to those measured by atomic emission spectroscopy, thus allowing estimates of K^+ influx rates. The method does not require shift reagents because of the 8.5 times faster kinetics of Rb^+ equilibration in the extracellular space (compared with the intracellular space) and the much higher concentration of Rb^+ in the latter.

Cardiac sarcolemmal K_{ATP} channels are crucial in adaptation to stress caused by metabolic inhibition and moderate exercise, which requires not only downregulation of energy spending but also upregulation of mitochondrial ATP synthesis. In order to investigate sarcolemmal and mitochondrial effects of a Kir6.2 (K^+ ion-selective subunit of the channel) knockout, ^{87}Rb NMR has been used, showing that Kir6.2 knockout results in a lack of stimulation of the unidirectional potassium efflux from the heart that creates a primary defect leading to the development of non-insulin-dependent (type 2) diabetes.³⁹

During the last decade, imaging the distribution of ^{87}Rb , which mimics K^+ as a substrate for the Na^+/K^+ -ATPase pump in myocardial cells, by MRI was shown promising in distinguishing between necrotic and reversibly damaged tissue.⁴⁰ Subsequently, ^{87}Rb MRI has been moving to *in vivo* applications to monitor, upon replacement of K^+ with Rb^+ , brain potassium in animal models and to study K^+ dynamics in live rats with focal ischemic stroke.⁴¹

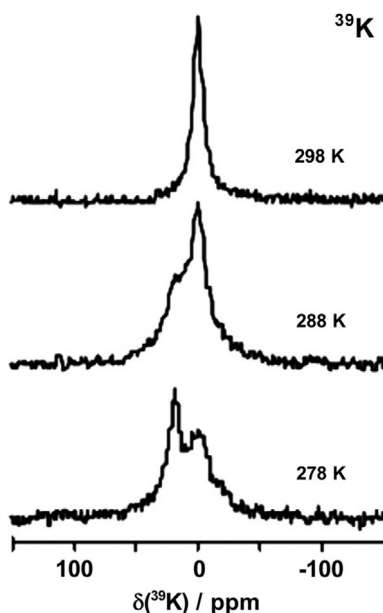


Fig. 3 Variable temperature ^{39}K NMR spectra of 0.53 M $\text{Na}_2(5'-\text{GMP})$ treated with 0.10 M KCl. ^{39}K chemical shifts are referenced to aqueous KCl 1.0 M at 0.0 ppm. Adapted from Wong, A.; Ida, R.; Wu, G. *Biochem. Biophys. Res. Commun.* **2005**, *337*, 363–366, with permission.

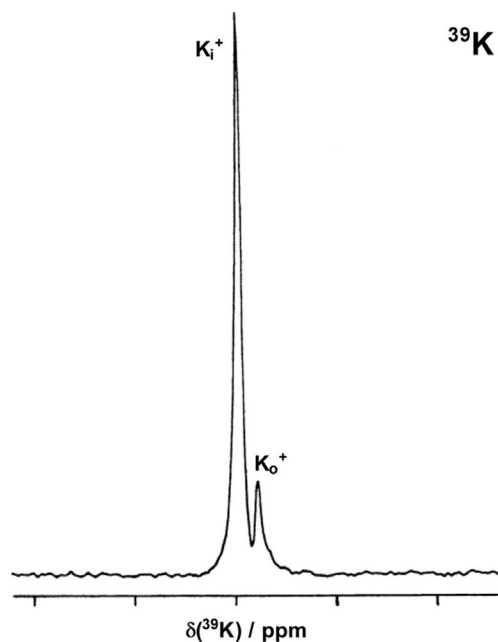


Fig. 4 ^{39}K NMR spectrum (one axis division equal to 50 ppm) of human erythrocytes (hematocrit 61.2%) resuspended in the NMR buffer (65 mM NaCl, 20 mM KCl, 1 mM NaH_2PO_4 , 2 mM MgCl_2 , 10 mM glucose, 5 mM $\text{Na}_7[\text{Dy}(\text{P}_3\text{O}_{10})_2]$, 50 mM HEPES, pH 7.4) at 37°C. K_i^+ and K_o^+ represent the intra- and extracellular ^{39}K peaks, respectively. Adapted from Ronconi, L.; Sadler, P. J. *Coord. Chem. Rev.* **2008**, *252*, 2239–2277, with permission.

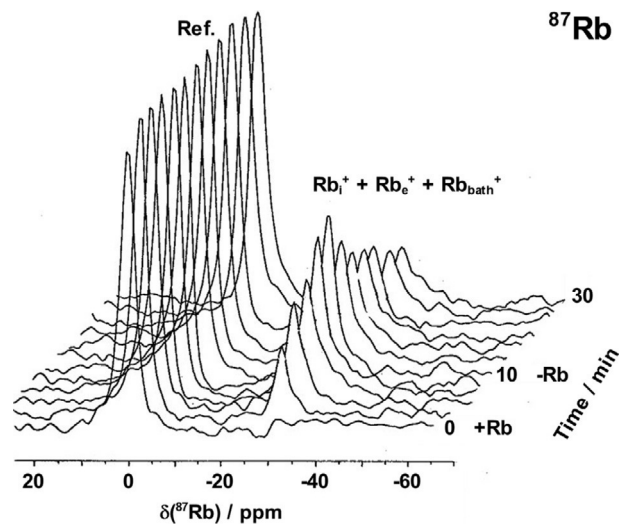


Fig. 5 ^{87}Rb NMR spectra (referenced to internal aqueous Rb^+ at 0.0 ppm) of perfused rat heart during Rb^+ load and washout. The hearts were perfused with phosphate-free Krebs–Henseleit buffer. The perfusate was equilibrated with 95% O_2 /5% CO_2 , and the pH maintained at 7.4. The buffer used for Rb^+ loading contained 0.94 mM Rb^+ and 3.76 mM K^+ . Adapted from Ronconi, L.; Sadler, P. J. *Coord. Chem. Rev.* **2008**, *252*, 2239–2277, with permission.

Cesium

Isotope	A (%)	I	γ ($\times 10^7 \text{ rad T}^{-1} \text{ s}^{-1}$)	Q (fm^2)	Relative receptivity to ^{13}C	Reference sample
^{133}Cs	100	7/2	3.533	0.343	284	$\text{CsNO}_3/\text{D}_2\text{O}$ (0.1 M)

Interest in the biological roles of cesium ions arises from three areas: (i) applications related to alkali metal ion transport and enzyme activation, (ii) toxicological considerations related to the uptake and passage through food chains of radioactive ^{137}Cs produced in fission reactions, and (iii) applications of cesium derivatives in the treatment of behavioral depression.² The

development of ^{133}Cs NMR spectroscopy for Cs^+ analysis has triggered the interest in the biochemistry and physiology of Cs^+ in biological systems. It accumulates in the intracellular space, primarily through the action of Na^+/K^+ -ATPase, thus making it a valuable tool for noninvasively probing of its congener K^+ .

A major advantage of ^{133}Cs NMR is that the chemical shift range is much larger than the other alkali metals, and ^{133}Cs signals are extremely sensitive to changes in chemical environment, solvents, temperature, and counterions present.⁴² ^{133}Cs has a small quadrupole moment, resulting in narrow NMR lines and a relaxation rate approximately 200 times smaller than the other NMR-active alkali metal nuclei. Cs^+ is 100% visible by NMR spectroscopy and its biomedical applications have been extensively reviewed.⁴³

Intra- and extracellular ^{133}Cs NMR resonances in Cs^+ -loaded cell suspensions can be distinguished without the addition of shift reagents (required to resolve resonances of other alkali metal ions such as ^7Li , ^{23}Na , and ^{39}K). In this regard, intra- and extracellular resonances were readily resolved for suspended human erythrocytes treated with CsCl , the resulting spectra exhibiting two resonances separated by 1.0–1.4 ppm (Fig. 6).⁴⁴

In addition, it is possible to resolve the NMR signals of ^{133}Cs in different tissue compartments on the basis of chemical shift or relaxation properties. This compartmental resolution applies not only to the intra- and extracellular spaces but also to the subcellular compartments. For example, Cs^+ binding to human RBC was evaluated by means of relaxation measurements, showing that it binds more strongly to 2,3-bisphosphoglycerate and RBC membranes than to any other intracellular component in RBC at physiological concentrations.⁴⁵

^{133}Cs NMR spectroscopy was also proved useful to evaluate the ion transport across membranes and the kinetic/chemical environment of the intracellular space in systems ranging from RBC to rat brain.^{43,46}

s-Block: Alkaline Earth Metals (Mg and Ca)

Magnesium

Isotope	A (%)	I	γ ($\times 10^7 \text{ rad T}^{-1} \text{ s}^{-1}$)	Q (fm^2)	Relative receptivity to ^{13}C	Reference sample
^{25}Mg	10.00	5/2	1.639	19.94	1.58	$\text{MgCl}_2/\text{D}_2\text{O}$ (11 M)

Together with K^+ , Mg^{2+} is one of the major intracellular ions (typically 30 mM) and is 90% bound to the ribosomes. It is regarded as a natural RNA cofactor and, besides acting as charge screener to allow proper folding and correct establishment of RNA tertiary interactions, it was shown to be also directly involved in ribozyme catalysis.⁴⁷ Moreover, magnesium is an essential cofactor for many RNA- and DNA-processing enzymes and for enzymes using ATP, ADP, or AMP as substrates.² As metallotherapeutic drugs, magnesium salts are frequently prescribed to treat diseases such as gestational hypertension, preeclampsia and eclampsia, asthma, strokes, acute myocardial infarction, and arrhythmias.⁴⁸ Mg^{2+} readily forms complexes with biological substrates to either define peculiar conformations or catalytically activate specific chemical functionalities, and its role is critically dependent on the coordination mode adopted in a defined biological context.

The interaction of ^{25}Mg quadrupole moment with EFGs provides a very effective relaxation mechanism.⁴⁹ The observed lineshapes are sensitive to the motion and exchange dynamics of the Mg^{2+} ions, thus providing insights into the interaction with various biomolecules. Owing to the low natural abundance and low receptivity, only the use of isotopically enriched $^{25}\text{Mg}^{2+}$ allowed a total lineshape analysis of ^{25}Mg NMR spectra to determine the association constant (K_a), the free energy of activation

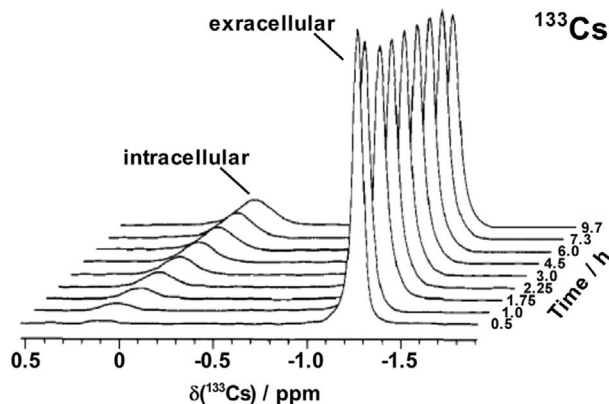


Fig. 6 ^{133}Cs NMR spectra of human erythrocytes suspended in a buffer containing 140 mM NaCl and 10 mM CsCl . The origin of the chemical shift scale is arbitrary. Adapted from Davis, D. G.; Murphy, E.; London, R. E. *Biochemistry* **1988**, *27*, 3547–3551, with permission.

(ΔG^\ddagger), outer-sphere association (K_{os}), and off-rate (k_{off}) and on-rate (k_{on}) constants for magnesium binding to several biologically relevant macromolecules, as summarized in Table 3.⁵⁰

Indirect methods have also been used to study RNA–Mg(II) interactions. Normally, such investigations rely on changes of ^1H chemical shifts upon titration with Mg^{2+} , allowing Mg(II)–RNA affinity constants to be determined. Moreover, the different binding modes of Mg^{2+} to RNA (i.e., inner- and outersphere coordination) can be mimicked by employing different probes like Mn^{2+} , $[\text{Co}(\text{NH}_3)_6]^{3+}$, and Cd^{2+} .⁵¹

^{25}Mg NMR was also proved useful to investigate the interaction between Mg^{2+} and calmodulin (a calcium-binding protein that can bind to and regulate a multitude of different protein targets), thereby affecting a number of cellular functions.⁵² Tsai and coworkers demonstrated that Mg^{2+} shows opposite site preference relative to Ca^{2+} and binds to sites I and II of calmodulin with a binding constant of $\sim 2000 \text{ M}^{-1}$, whereas it binds weakly to sites III and IV. Since the intracellular concentration of Mg^{2+} is higher than that of Ca^{2+} , they hypothesized that sites I and II are constantly occupied by Mg^{2+} at the resting state.

Analogously, the interactions between Mg^{2+} and other biomolecules, such as adenylate kinase (a phosphotransferase enzyme requiring Mg^{2+} to catalyze the production of ATP from ADP)⁵³ and several biological polyelectrolytes,⁵⁴ have been studied by ^{25}Mg NMR spectroscopy. In both cases, it was demonstrated that magnesium ions bind loosely to the investigated actin filaments and, thus, show a behavior typical of counterions.

Calcium

Isotope	A (%)	I	γ ($\times 10^7 \text{ rad T}^{-1} \text{ s}^{-1}$)	Q (fm^2)	Relative receptivity to ^{13}C	Reference sample
^{43}Ca	0.135	7/2	−1.803	4.08	0.051	$\text{CaCl}_2/\text{D}_2\text{O}$ (0.1 M)

Calcium is an important element in the human body and is located principally in bones and teeth as apatite, a calcium phosphate mineral. It is distributed throughout all tissues where it plays special roles in controlling blood pressure, nerve impulse transmission, muscle action, blood clotting, and cell permeability.²¹ Together with Na^+ , Ca^{2+} is a major extracellular ion (typically 4 mM). Its fundamental role in initiating biological reactions results from rapid exchange kinetics and strong ligand binding capability. Many processes of signal transduction involve the release of Ca^{2+} as part of an interconnected set of pathways. Increased intracellular levels are sensed by a family of calcium-binding proteins, including calmodulin, which use changes in the intracellular calcium concentration to activate a variety of enzymes, such as protein kinases, NAD kinase, and phosphodiesterases, and some Ca^{2+} -ATPases.²

Calcium supplements (usually carbonate, citrate, gluconate, or lactate salts) are administered to protect against osteopenia, osteoporosis, and hypertension, and calcium-based drugs may be used to prevent from high blood cholesterol, diabetes, and major pregnancy complications. CaCO_3 is also marketed as antacid to relief the pain and discomfort of indigestion, heartburn, and other symptoms related to excess stomach acidity.⁵⁵

^{43}Ca is the only NMR-active calcium isotope and its NMR properties are rather unfavorable due to the low resonance frequency, low natural abundance, and strong quadrupolar relaxation, thus explaining the paucity of data available. In this regard, the most recent biologically related application of ^{43}Ca NMR in solution appears to date back to 2008 when Kwan and coworkers reported the first direct NMR evidence for Ca^{2+} ion binding to G-quartets by combining natural abundance ^{43}Ca NMR spectroscopy with extensive quantum chemical calculations.⁵⁶

In the past three decades, such technique had provided a few insights into the structural and motional characteristics of calcium-binding sites in a number of calcium-binding proteins.⁵⁷ For example, the ^{43}Ca NMR signals from Ca^{2+} ions bound to the Ca-binding proteins parvalbumin, troponin C, and calmodulin have been detected⁵⁸ by using isotopically enriched ^{43}Ca -calcium. The signals of $^{43}\text{Ca}^{2+}$ bound to all three proteins were recorded at similar chemical shifts, and all showed similar magnitude of the

Table 3 Determination of kinetic and thermodynamic parameters for Mg^{2+} binding to phosphate-containing ligands by ^{25}Mg NMR spectroscopy

Ligand	K_a (M^{-1})	ΔG^\ddagger (kcal mol^{-1})	k_{off} ($\times 10^{-3} \text{ s}^{-1}$)	k_{on} ($\times 10^{-3} \text{ s}^{-1}$)	K_{os} (M^{-1})
tRNA (native)	220	12.8	2.5	5.5×10^5	220
tRNA (non-native)	250	13.1	1.6	4.0×10^5	250
[Glucose-1-P] $^{2-}$	15	12.7	2.9	4.3×10^4	0.43
[Glucose-6-P] $^{2-}$	8	12.7	3.1	2.5×10^4	0.25
$\text{CH}_3\text{CO}_2\text{PO}_3^{2-}$	9	13.1	1.5	1.4×10^4	0.14
AMP^{2-}	18	12.7	3.4	6.2×10^4	0.62
ADP^{3-}	2.2×10^3	12.8	2.5	5.5×10^6	55
ADPH^{2-}	13	12.1	7.7	8.5×10^4	0.85
ATP^{4-}	3.0×10^3	12.4	5.0	1.5×10^7	150
ATPH^{3-}	6	12.5	4.2	5.1×10^4	0.51

Adapted from Cowan, J. A. *Inorg. Chem.* **1991**, *30*, 2740–2747, with permission.

quadrupole coupling constant. This observation supported the hypothesis that the Ca-binding sites have the same arrangements of oxygen donors coordinated to the Ca^{2+} ion. An analogous study has been carried out to evaluate the exchange rates and the binding constants of Ca^{2+} ions to the high-affinity and low-affinity binding sites on calmodulin.⁵⁹

The calcium-binding properties of equine and pigeon lysozyme and those of bovine and human α -lactalbumin have been also investigated.⁶⁰ An example is shown in Fig. 7. Upon addition of isotopically enriched $^{60}\text{Ca}^{2+}$ to equine lysozyme, a broad peak ($\Delta\nu_{1/2} = 253$ Hz) appears at -5.3 ppm, and the signal intensity increases linearly up to 1 equiv. of metal ion. This resonance corresponds to calcium bound to the single high-affinity calcium site. In the presence of excess metal ion, a sharp signal ($\Delta\nu_{1/2} = 10$ Hz) is also observed at 1 ppm, in the proximity of that of free calcium. All proteins were found to contain one high-affinity calcium-binding site, and a second weak calcium-binding site was observed for bovine α -lactalbumin only. The chemical shifts, linewidths, relaxation times, and quadrupolar coupling constants for the respective ^{43}Ca NMR signals associated with high-affinity binding sites were quite similar, indicative of a high degree of homology between those sites in the four proteins. On the other hand, both the chemical shifts and the quadrupolar coupling constants are quite distinct from those observed for typical EF-hand calcium-binding proteins, thus suggesting a different geometry for the calcium-binding loops.

p-Block: Group 13 (B, Al, Ga, In, and Tl)

Boron

Isotope	A (%)	I	γ ($\times 10^7$ rad T^{-1} s^{-1})	Q (fm^2)	Relative receptivity to ^{13}C	Reference sample
^{10}B	19.90	3	2.875	8.459	23.2	$\text{BF}_3 \cdot \text{OEt}_2 / \text{CDCl}_3$ (15%)
^{11}B	80.10	3/2	8.585	4.059	777	

Boron is regarded as a nonessential element for mammalian life, although it may turn out to be a necessary “ultratrace” element. The main medicinal application of boron is the tumor-targeted delivery of boron derivatives for boron neutron capture therapy (BNCT).⁶¹ The therapy is based on the nuclear reaction that occurs when the stable isotope ^{10}B is irradiated with neutrons at appropriate energy to produce ^{11}B in an unstable form, which then undergoes instantaneous nuclear fission to produce high-energy alpha particles and recoiling ^7Li nuclei ($^{10}\text{B} + n_{\text{th}} \rightarrow [^{11}\text{B}] \rightarrow \alpha + ^7\text{Li}$). These heavy charged particles have pathlengths of approximately one cell diameter (10–14 μm) and deposit most of their energy within the boron-containing cells. Provided that boron-based therapeutics are delivered and accumulate preferentially in tumors and enough low energy thermal neutrons (n_{th}) reach the target site, cancer cells undergo necrosis as a result of the $^{10}\text{B}(n, \alpha)^7\text{Li}$ capture reaction. BNCT has been used clinically to treat patients with brain cancers, such as glioblastoma multiforme, with high-grade gliomas, and a much smaller number with primary and

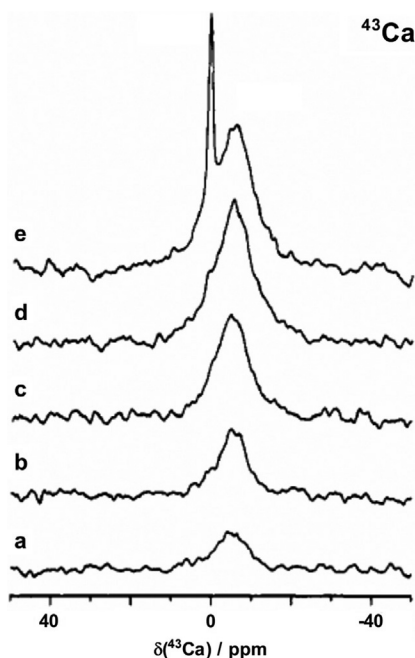


Fig. 7 ^{43}Ca NMR spectra recorded upon titration of 0.33 mM equine apolysozyme with (a) 0.23 equiv., (b) 0.46 equiv., (c) 0.69 equiv., (d) 0.92 equiv., and (e) 1.15 equiv. of $^{43}\text{Ca}^{2+}$ at pH 6.0. Adapted from Aramini, J. M.; Drakenberg, T.; Hiraoki, T.; Ke, Y.; Nitta, K.; Vogel, H. J. *Biochemistry* **1992**, *31*, 6761–6768, with permission.

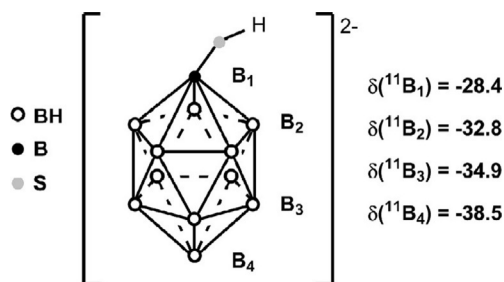


Fig. 8 Schematic illustration of the borocaptate anion. There is a net double negative charge in the boron–hydride cage. $\delta(^{11}\text{B})$ of free BSH is referenced to saturated H_3BO_3 at 0.0 ppm. Adapted from Zhu Tang, P.-P. P.; Schweizer, M. P.; Bradshaw, K. M.; Bauer, W. F. *Biochem. Pharmacol.* **1995**, *49*, 625–632, with permission.

metastatic melanoma. Delivery vehicles synthesized for this application include sodium borocaptate (BSH, $\text{Na}_2\text{B}_{12}\text{H}_{11}\text{SH}$), borano phosphonates and borano bis(phosphonates), borano phosphate oligodeoxynucleotides, in which BH_3 is linked to the phosphate backbone of antisense oligodeoxynucleotides,^{61b} and carboranes.^{61d}

Boron NMR is a suitable technique to study the pharmacokinetics of boron-based therapeutics and to evaluate their binding to biologically relevant molecules. Both ^{10}B and ^{11}B are NMR-active, but ^{11}B has higher sensitivity and natural abundance. Therefore, although ^{10}B is the nucleus used in BNCT treatment, the more sensitive ^{11}B is more appropriate for NMR studies, since the isotopic difference does not alter the structure, binding, or the pharmacokinetic effects of the BNCT agents. Both isotopes are quadrupolar and their relaxation times are rather short. NMR research efforts have been primarily moved toward two directions: first, to investigate the metabolism and pharmacokinetics of BNCT agents in vivo and, second, to use localized NMR spectroscopy and/or MRI for noninvasive mapping of the administered molecules. While the first goal can be accomplished by ^{11}B NMR for natural abundance samples, molecules used in BNCT are generally enriched (>95%) in the less favorable (in terms of NMR properties) ^{10}B nucleus. Anyway, the use of ^{10}B MRI was proved successful to evaluate the distribution in vivo of these agents⁶² and, in this regard, much attention has been recently given to the exploitation of boron nitride nanotubes containing Fe paramagnetic impurities⁶³ and to dual gadolinium/boron compounds as contrast agents.⁶⁴

The first attempts to investigate the interaction between boron derivatives and biomolecules by ^{11}B NMR spectroscopy date back to 1990s. Peptide boronic acids are exceptionally potent inhibitors of serine proteases, which are well known to play crucial roles in biological systems. Therefore, the high affinity and specificity of boronic acid-based inhibitors make them considerably interesting as both research tools and potential therapeutic agents. ^{11}B chemical shifts are very sensitive to changes in the coordination geometry of the boron atom, and resonances belonging to trigonal species appear downfield compared to tetraordinated ones. Accordingly, for a number of such boron-containing inhibitors, ^{11}B signals were recorded at about 17 ppm, consistent with the formation of boron–histidine and boron–serine adducts with α -lytic protease in a tetrahedral geometry.⁶⁵

^{11}B chemical shift and relaxation rate changes can be also used to monitor the interaction of BNCT agents with proteins. An example of such application of ^{11}B NMR spectroscopy is the study of the reaction between BSH (Fig. 8) and serum albumin, the latter likely being involved in its pharmacokinetics.⁶⁶

Similarly, the binding of borate ions to cytochrome *c* surface has been investigated by ^{11}B NMR spectroscopy. Cytochrome *c* is a globular heme protein acting as electron carrier in the cell mitochondria. It has a positively charged surface that is believed to bind mitochondrial enzymes, small anions, and metabolites. Such surface interaction influences the efficiency of the proton transfer and the mobility of the protein itself. Borate ions were shown by ^{11}B NMR to bind specifically to cytochrome *c* surface, and this interaction could be used as a model for anion–protein surface interaction.⁶⁷ Fig. 9A shows the ^{11}B spectrum at 11.4 T of a 100 mM borate solution in presence of 4 mM ferricytochrome *c* at pH 9.7 at 5°C. The large peak at 7.1 ppm (peak *z*) represents the weighted average resonance arising from 70% $\text{B}(\text{OH})_4^-$ exchanging with 30% $\text{B}(\text{OH})_3$. The peaks at 2.1 ppm (peak *y*) and 1.8 ppm (peak *x*) were assigned to $\text{B}(\text{OH})_4^-$ specifically bound to two conformations of ferricytochrome *c* coexisting at pH 9.7, whereas the shoulder at around 6 ppm (peak *w*) is still unassigned. When MQF NMR experiments were carried out (Fig. 9B), two narrow signals related to the specific binding sites of ferricytochrome *c* and a broad peak owing to the borate/boric acid were detected (at ~2 and 7.1 ppm, respectively), suggesting two different types of binding sites designated as I (for slowly exchanging borate ion) and II (for fast exchanging borate ion and boric acid).

Finally, a recent paper reports on the use of ^{11}B NMR spectroscopy to study boron-induced enzyme inhibition. ^{11}B chemical shift analysis was used to prove the formation of ternary complexes between boronic acids, sugars, and α -chymotrypsin as model enzyme.⁶⁸

Aluminum

Isotope	A (%)	I	γ ($\times 10^7 \text{ rad T}^{-1} \text{ s}^{-1}$)	Q (fm^2)	Relative receptivity to ^{13}C	Reference sample
^{27}Al	100	5/2	6.976	14.66	1220	$\text{Al}(\text{NO}_3)_3/\text{D}_2\text{O}$ (1.1 m)

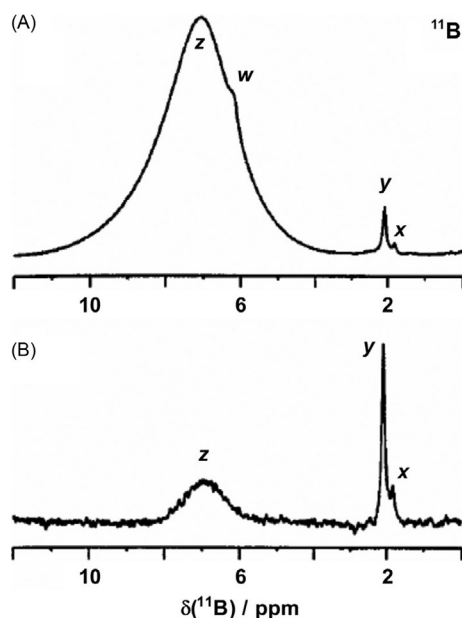


Fig. 9 The ^{11}B (a) single quantum and (b) MQF ($\tau = 1.4$ ms) NMR spectra of 100 mM borate solution in the presence of 4 mM ferricytochrome *c* at 5°C, 11.4 T, and pH 9.7. Adapted from Taler, G.; Eliav, U.; Navon, G. *J. Magn. Reson.* **1999**, *141*, 228–238, with permission.

Aluminum is the third most abundant metal in the Earth's crust, representing approximately 8% of total weight, and the natural element consists entirely of the ^{27}Al isotope. The concentration in blood plasma is about 0.005 mg L^{-1} , corresponding to about 1% of the aluminum body burden, 80% of which is bound to proteins. It accumulates mainly in the liver, bones, and spleen of humans and animals. It is a nonessential element nowadays recognized as potential toxic element linked to neurological problems, especially dialysis encephalopathy and Alzheimer's disease, and also to some bone disorders and problems in the hematopoietic system, muscles, and joints.⁶⁹ For a long time, owing to the low solubility under physiological conditions, aluminum was regarded as a nontoxic element, so its biological effects have not been investigated until recently. In particular, due to the increasing acidity of the environment and the concomitant increased dissolution of aluminum minerals, the concentration of this element in freshwaters has become a considerable issue. On the other hand, aluminum-based drugs are sold as antacids ($\text{Al}(\text{OH})_3$ and $\text{Al}_2(\text{CO}_3)_3$) and for the treatment of malaria ($\text{Al}(\text{OH})_3$). Three aluminum salts (alum, $\text{Al}(\text{OH})_3$, and $\text{Al}(\text{PO}_4)$) have also been added to many vaccines, including widely used formulations for diphtheria, hepatitis B, and tetanus, as adjuvant ('vaccine boosters').^{70a} Moreover, the magnetic resonance characteristics of this nuclide also make it potentially suitable for medical applications (^{27}Al -based MRI is feasible).^{70b}

^{27}Al is amenable to NMR studies owing to the relatively high receptivity, the existence of only one isotope, and the relatively small quadrupole moment associated with its high nuclear spin. The latter two favorable factors result in a much higher relative peak height (by one order of magnitude or higher compared to the other elements belonging to group 13), thus allowing to achieve sufficient signal-to-noise ratios even for dilute ($\sim 0.01 \text{ M}$) solutions of aluminum compounds. ^{27}Al linewidths may vary from 3 to several kHz, and the signals may even completely vanish into the baseline noise in some instances. This negative aspect of quadrupolar relaxation is counterbalanced by the fact that the magnitude of the quadrupolar line broadenings provides information about the coordination geometry of the aluminum center.

The major metal transport protein in blood plasma is the bilobal glycoprotein transferrin, and ^{27}Al NMR can be used to investigate directly the metal in the specific binding sites and to reveal subtle intersite differences.⁷¹ Human serum transferrin (Fig. 10) is a member of a small group of monomeric nonheme proteins (MW ~ 76 –81 kDa), which includes lactoferrin, ovotransferrin, and melanotransferrin. It has two binding sites for Fe^{3+} ions in a six-coordinate, distorted octahedral coordination geometry identified as C- and N-terminal sites. Two tyrosines, one histidine, and one aspartate constitute four protein ligands for the metal ion, which requires a synergistic anion for the formation of stable transferrin complexes. The bidentate CO_3^{2-} serves this purpose by coordinating directly to the metal in the fifth and sixth coordination positions *in vivo*. Since serum transferrin is normally only about 30% saturated with iron, it retains a relatively high capability for binding to other metal ions.

Vogel and Aramini demonstrated the feasibility of ^{27}Al NMR to probe the binding of Al^{3+} to ovotransferrin and its half-molecules in the presence of carbonate or oxalate as synergistic anions.⁷² The ovotransferrin-bound ^{27}Al NMR signals have some rather unusual properties related to quadrupolar nuclei bound in slow exchange to large macromolecules far from extreme narrowing conditions. First, the maximum intensity of the protein-bound ^{27}Al signal is substantially lower than that observed for equimolar solutions of the free metal ion. Secondly, the signals exhibit a unique pulse angle dependence where a maximum in peak intensity is attained at pulse lengths that are less than half the 90 degrees pulse for aqueous Al^{3+} solutions. Third, ^{27}Al signals for

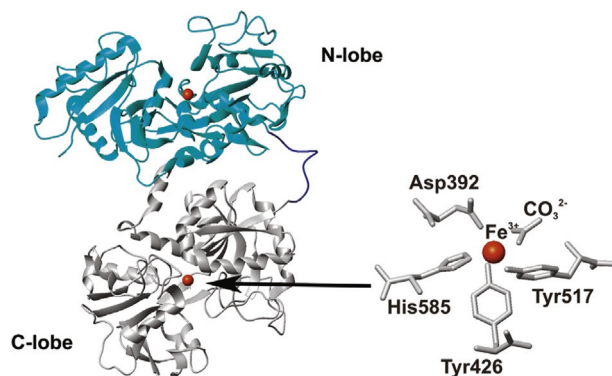


Fig. 10 Ribbon representation of the structure of diferric human serum transferrin (Fe^{III} , Fe^{III} - hTf) with C-lobe in gray, N-lobe in cyan, peptide linker in blue, and the two Fe(III) ions in orange. The coordination sphere of the Fe(III) center in the C-lobe is magnified. The pictures were prepared with MOLMOL (Koradi, R.; Billeter, M.; Wüthrich, K. *J. Mol. Graphics* **1995**, *14*, 19–32, 51–55) using the PDB ID 3QYT.

Al^{3+} bound to the half-molecules of ovotransferrin are much broader than those for the intact protein, thus reflecting the importance of molecular motion on the detectability of quadrupolar nuclei. Finally, the increase of the external magnetic field strength causes line narrowing and a 2–4 ppm downfield dynamic frequency shift (Fig. 11).⁷³ The chemical shifts of the ^{27}Al signals from Al_2 -ovotransferrin were found from +40 to –46 ppm, which is in accordance with a six-coordinate (octahedral) Al(III) complex. From these assignments and titration experiments, it was found that, in the presence of carbonate, the N-terminal site of ovotransferrin binds Al^{3+} with a higher affinity than the C-terminal site. Interestingly, changing the synergistic anion to oxalate alters the specificity (Fig. 12).^{72a}

Aluminum neurotoxicity involves also the inhibition of certain enzymes, such as ATPase. It is believed that the Al^{3+} ion, once bound to ATP, interferes with Mg^{2+} so that any consequent reactions requiring Mg^{2+} -ATP complex participation are inhibited.²¹ This has prompted the study of the binding of Al^{3+} to ATP by ^{27}Al NMR. The linewidths of these complexes typically fall within the range 150–500 Hz. Detellier and coworkers⁷⁴ studied these interactions at pH 7.4 using multinuclear NMR spectroscopy. Such ^{27}Al NMR investigations allowed them to identify two complexes coexisting in equilibrium: 2:1 { $\text{Al}(\text{ATP})_2$ } and 1:1 { $\text{Al}(\text{ATP})$ } species.

More recently, the involvement of glutathione (GSH) in aluminum toxicity was evaluated by detailed spectroscopic studies, including ^{27}Al NMR.⁷⁵ GSH turned out to form various mono- and dinuclear Al-containing species by coordinating the metal center through the Gly and Glu carboxylate groups, although the Glu amino group, the peptide imino, and carbonyl moieties also appeared to be involved in the bidentate and tridentate derivatives.

^{27}Al NMR spectroscopy has been also employed to study aluminum-containing species present in natural waters. For example, Casey and coworkers studied the rates of solvent exchange in aqueous Al^{3+} -maltolate complexes.⁷⁶ Maltolate is a natural product that can be isolated from larch trees but is now widely used as a food additive. It is soluble in water, and the corresponding trisderivatives of Al^{3+} are toxic and may cause brain disease. A variable temperature ^{27}Al NMR investigation showed that maltolate can replace the inner-sphere water molecules bound to Al^{3+} and labilize the remaining coordinated water molecules. In particular, coordination of a single maltolate ligand into the inner-coordination sphere of $[\text{Al}(\text{H}_2\text{O})_6]^{3+}$ increases the exchange rate of the

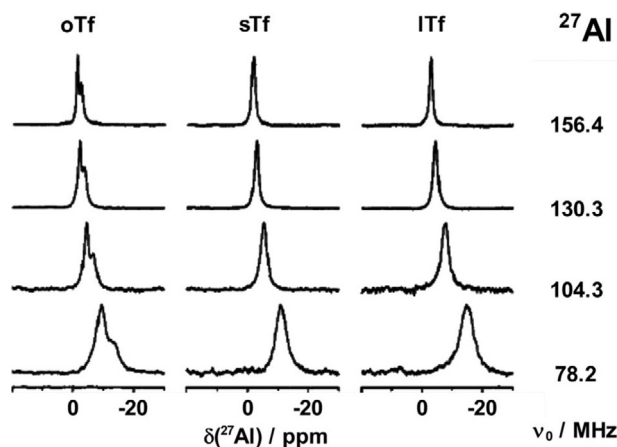


Fig. 11 ^{27}Al NMR spectra (referenced to external 1.0 M $\text{Al}(\text{NO}_3)_3$ in D_2O at 0.0 ppm) of ovotransferrin (oTf, 1.13 mM, pH 7.5), serotransferrin (sTf, 1.09 mM, pH 7.3), and lactoferrin (lTf, 0.73 mM, pH 7.5) in the presence of 20 mM Na_2CO_3 and 2.0 equiv. of Al^{3+} (75% H_2O /25% D_2O , 150 mM KCl, 25°C) at four magnetic fields (7.0, 9.4, 11.7, and 14.1 T). Adapted from Aramini, J. M.; Germann, M. W.; Vogel, H. J. *J. Am. Chem. Soc.* **1993**, *115*, 9750–9753, with permission.

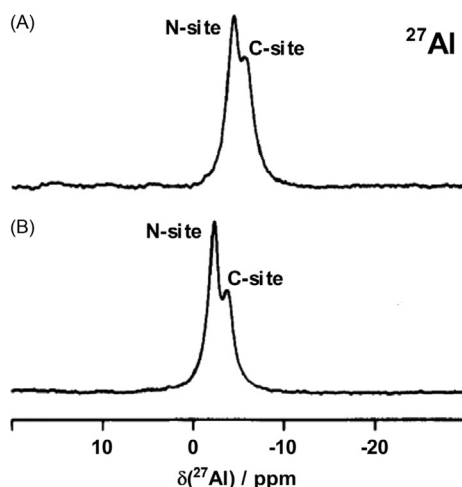


Fig. 12 ^{27}Al NMR spectra (referenced to external 1.0 M $\text{Al}(\text{NO}_3)_3$ in D_2O at 0.0 ppm) of (a) 1.20 mM ovotransferrin in the presence of 5 mM $\text{Na}_2\text{C}_2\text{O}_4$ and 2.0 equiv. of Al^{3+} (75% $\text{H}_2\text{O}/25\%$ D_2O , 150 mM KCl, pH 7.4, 25°C) and (b) 1.13 mM ovotransferrin in the presence of 20 mM $\text{Na}_2\text{C}_2\text{O}_4$ and 2.0 equiv. of Al^{3+} (75% $\text{H}_2\text{O}/25\%$ D_2O , 150 mM KCl, pH 7.6, 25°C) at a magnetic field strength of 11.7 T. Adapted from Aramini, J. M.; Vogel, H. J. *J. Am. Chem. Soc.* **1993**, *115*, 245–252, with permission.

other bound water molecules with bulk solution by a factor of about 10^2 . Remarkably, the addition of a second ligand, to form the bis-derivative $[\text{Al}(\text{maltolate})_2(\text{H}_2\text{O})_2]^+$, increases the rate by an additional factor of 6–7.

Apart from investigating the biological role of aluminum, ^{27}Al NMR has been also exploited to assess the binding environment and ligands coordination modes in Al(III)-containing potential biologically active scaffolds, such as bionanomaterials.⁷⁷

Gallium, indium, and thallium

Isotope	A (%)	I	γ ($\times 10^7 \text{ rad T}^{-1} \text{ s}^{-1}$)	Q (fm^2)	Relative receptivity to ^{13}C	Reference sample
^{69}Ga	60.11	3/2	6.439	17.1	246	$\text{Ga}(\text{NO}_3)_3/\text{D}_2\text{O}$ (1.1 M)
^{71}Ga	39.89	3/2	8.181	10.7	335	
^{113}In	4.29	9/2	5.885	79.9	88.5	$\text{In}(\text{NO}_3)_3/\text{D}_2\text{O}$ (0.1 M)
$^{115}\text{In}^a$	95.71	9/2	5.897	81.0	1980	332
^{203}Tl	29.52	1/2	15.539	–	340	$\text{Tl}(\text{NO}_3)_3/\text{D}_2\text{O}$ (1%)
^{205}Tl	70.48	1/2	15.692	–	836	332

^aRadioactive with a long half-life (4.41×10^{14} year, β^-).

Although none of the group 13 elements is considered essential to life, their trivalent ions are of great biological interest. Gallium is present in human tissues at a level of only 10^{-4} – 10^{-3} ppm.⁷⁸ It has two naturally occurring isotopes and 13 radioactive nuclides. ^{67}Ga (γ , $t_{1/2} = 3.25$ days) and ^{68}Ga (β^+ , $t_{1/2} = 68$ min) are two radioisotopes with appropriate energies and half-lives for γ -scintigraphy and positron emission tomography (PET), respectively. Together with imaging applications, the Auger electrons emitted by ^{67}Ga possess potent cytotoxicity pointing toward potential therapeutic applications of the radionuclide, whereas the positrons emitted by ^{68}Ga may also have therapeutic applications in the prevention of restenosis by intracoronary radiation therapy.⁷⁹ Although most reports on gallium pharmaceutical chemistry relate to applications of its radioisotopes, the tumor-seeking and antineoplastic properties of nonradioactive Ga^{3+} salts were already recognized in the 1970s when, for example, safety and activity of intravenous gallium(III) nitrate were extensively studied in clinical trials.⁸⁰ The development of gallium-based anticancer agents has been pursued as a strategy to circumvent the limitations faced with simple gallium salts. In particular, efforts to improve bioavailability via the oral route have recently led to the selection of the complexes *tris*(8-quinolinolato)gallium(III) (KP46) and *tris*(3-hydroxy-2-methyl-4H-pyran-4-onato)gallium(III) (gallium maltolate) for clinical studies.⁸¹

Despite the nonideal imaging characteristics of its gamma emissions, ^{111}In (γ , $t_{1/2} = 2.82$ days) is also a popular radiolabel for targeting biomolecules and is widely employed in nuclear medicine for γ -imaging, probably because of the simplicity of its bioconjugate chemistry. Its radioisotopes are administered to the patients in the form of stable chelates.⁷⁹

$^{69/71}\text{Ga}$ and $^{113/115}\text{In}$ are quadrupolar NMR-active isotopes. They are characterized by high sensitivity to detection by NMR and large chemical shift ranges, two factors that make their study relatively easy. ^{71}Ga has higher receptivity and narrower linewidths than ^{69}Ga , which makes it usually the more favorable isotope for direct NMR observations despite the lower natural abundance.

^{113}In and ^{115}In have large quadrupole moments so their linewidths are very sensitive to the environmental symmetry around the indium nuclei. The low receptivity of ^{113}In accounts for the lack of NMR studies based on this nuclide. Gallium- and indium-based

radiopharmaceuticals are generally chelated with suitable ligands, such as triazamacrocyclic ligands with different types of pendant arms, that form kinetically and thermodynamically stable complexes in vivo. The thermodynamic stability of gallium and indium complexes with potential applications in imaging and radioimmunotherapy has been widely investigated in vitro and in vivo by NMR (some examples are summarized in Table 4), and recent advances have been focusing on the development of new generation chelators, including the tripodal 3-hydroxy-4-pyridinone and the quinazoline-derivative DOTA-like ligands.⁸²

Given the potential imaging applications of Ga(III), recent studies have focused on the exploitation of ⁷¹Ga NMR spectroscopy to gain insights into the structure, internal dynamics and stability in aqueous solution of the corresponding “cold” (i.e., non-radioactive) gallium derivatives. These include, for example, chelates of mixed phosphonates-carboxylate triazamacrocyclic ligands relevant to nuclear medicine⁸³ and some heterobimetallic Ga(III)-Ru(II) complexes containing histidyl-alanyl-valinyl (HAV) sequences for tumor targeting of potential theranostic agents (combining the anticancer activity of the Ru(II) unit with the imaging properties of ⁶⁷Ga(III) labeling).^{83b}

The redox chemistry of thallium is considerably different from the other elements of the group. In fact, under physiological conditions, the most stable oxidation state is +1, although Tl³⁺ may also exist.⁶⁹ Thallium salts are poisonous due to the capability of the thallos ion to mimic alkali metal ions, especially K⁺.⁸⁴

Interestingly, both ²⁰³Tl and ²⁰⁵Tl nuclides are NMR-active and nonquadrupolar. They have high receptivity, ²⁰³Tl being only slightly less receptive than ³¹P, whereas ²⁰⁵Tl is the third most receptive $I = 1/2$ nuclide. Because of its similarity to the alkali metal ions, Tl⁺ has potential as probe for Na⁺ and K⁺ in biological systems. ²⁰⁵Tl NMR can be used to investigate directly the specific binding sites of transferrins. Due to its high receptivity, ²⁰⁵Tl NMR signals of protein-bound Tl³⁺ ions can be observed even at mM concentrations. The first ²⁰⁵Tl NMR study of human serum transferrin was reported over 40 years ago by Bertini and coworkers.⁸⁵ They showed that ²⁰⁵Tl NMR is a suitable probe to monitor the occupancy of the two available transferrin binding sites, thus characterizing both the dithallium- and the monothallium-transferrin derivatives with carbonate as synergistic anion. The high affinity of the protein for trivalent metal ions was thought to be responsible for the stabilization of the +3 oxidation state of the metal. Two distinct ²⁰⁵Tl NMR signals (at +2075 and +2055 ppm downfield from aqueous Tl⁺) of similar shape were found for the Tl(III)₂-transferrin derivative at physiological pH. The two signals are relatively broad ($\Delta\nu_{1/2} \sim 100$ Hz) and show a different pH dependence (the signal at +2055 ppm proved more resistant to acidification). At physiological pH, the Tl³⁺ ion was shown to bind sequentially to the two sites; the signal at +2055 ppm appeared first and was assigned to Tl³⁺ bound to the acid-resistant C-terminal site. The signal at +2075 ppm was assigned to Tl³⁺ bound to the N-terminal site. By using ¹³C NMR spectroscopy to study the ¹³CO₃⁻²⁰⁵Tl-transferrin derivative, it was shown that the ¹³C nucleus of the synergistic anion is strongly magnetically coupled to the ²⁰⁵Tl nucleus so that its ¹³C signal is split into a doublet. Analogously, in the ¹³C NMR spectrum of (¹³CO₃⁻²⁰⁵Tl)₂ transferrin, two superimposed doublets are recorded, the extent of the coupling constants (290 and 265 Hz) being typical of a ²J(²⁰⁵Tl-¹³C) coupling. This result provided evidence of carbonate coordination to the metal.⁸⁶ Similar experiments were carried out by Aramini and coworkers to investigate the binding of ²⁰⁵Tl to chicken ovotransferrin in the presence of carbonate as the synergistic anion.⁸⁷ Two ²⁰⁵Tl NMR signals due to the bound metal ion in the two high-affinity iron-binding sites of the protein were detected and, from titration studies, it was demonstrated that Tl³⁺ shows no site preference in ovotransferrin. Again, when ¹³C-labeled carbonate was used, two closely spaced doublets in the carbonyl region of the ¹³C NMR spectrum of ovotransferrin were recorded due to the coupling between the bound metal ion and carbonate (²J(²⁰⁵Tl-¹³C)) ranging from 270 to 290 Hz).

The interaction of monovalent thallium with yeast pyruvate kinase was investigated by ²⁰⁵Tl NMR.⁸⁸ Pyruvate kinase from almost all sources requires mono- and divalent metal ions. Potassium is the physiologically relevant monovalent cation, but several other +1 cations, including Tl⁺, can activate this enzyme. Compared to KCl, TlNO₃ was shown to activate pyruvate kinase to

Table 4 ⁷¹Ga and ¹¹⁵In NMR chemical shifts and linewidths ($W_{1/2}$) of some derivatives with potential applications in imaging and radioimmunotherapy

Ligand ^a	⁷¹ Ga		¹¹⁵ In	
	δ (ppm)	$W_{1/2}$ (Hz)	δ (ppm)	$W_{1/2}$ (Hz)
H ₂ O	0	53	0	375–18,000
NOTA	+171	201	–	–
NOTA	+171	201	–	–
NODASA	+165	1000	–	–
NODASA	+165	1000	–	–
NOTP	+110	434	–	–
H ₃ ppma	62.3	50	14.7	1630
TAMS	+34	3400	–	26,000
TAPS	+57	1230	–	22,000

^aLigands: NOTA, 1,4,7-triazacyclononane-1,4,7-triacetate; NODASA, 1,4,7-triazacyclononane-1-succinic acid-4,7-diacetate; NOTP, 1,4,7-triazacyclononane-1,4,7-tris-(methylenephosphonate); H₃ppma, tris(4-(phenylphosphinato)-3-methyl-3-azabutyl)amine; TAMS, 1,1,1-tris((2-hydroxy-5-sulfobenzyl)-amino)methyl ethane; TAPS, 1,2,3-tris((2-hydroxy-5-sulfobenzyl)-amino)propane.

Adapted from André, J. P.; Mäcke, H. R. *J. Inorg. Biochem.* **2003**, *97*, 315–323, with permission.

80%–90% activity, in combination with $\text{Mn}(\text{NO}_3)_2$ as the activating divalent cation. At higher Tl^+ concentrations, enzyme inhibition occurs, and the extent of such inhibition is also dependent on the nature and concentration of the divalent cation. In this regard, the effect of Mn^{2+} on the relaxation properties of $^{205}\text{Tl}^+$ was determined by ^{205}Tl NMR spectroscopy. The distance between Tl^+ and Mn^{2+} at the active site of yeast pyruvate kinase was calculated from the paramagnetic contribution of Mn^{2+} to the longitudinal relaxation rates of the bound Tl^+ . Similar measurements were performed to monitor structural alterations introduced at the active site of yeast pyruvate kinase by mutation of Thr298⁸⁹ and showed that the mutation influences the interaction between the mono- and the divalent cations, both interacting with the phosphoryl group of the substrate at the active site of the enzyme.

p-Block: Group 14 (Si, Ge, Sn, and Pb)

Silicon and germanium

Isotope	A (%)	I	γ ($\times 10^7 \text{ rad T}^{-1} \text{ s}^{-1}$)	Q (fm^2)	Relative receptivity to ^{13}C	Reference sample
^{29}Si	4.68	1/2	-5.319	-	2.16	$\text{Si}(\text{CH}_3)_4/\text{CDCl}_3$ (1%)
^{73}Ge	7.73	9/2	-0.936	19.6	-0.642	$\text{Ge}(\text{CH}_3)_4/\text{neat}$

Silicon is a highly abundant element in minerals and soils, but its role in living systems, if any, is poorly understood and it is currently debatable whether it is essential for human life. Silicon is not particularly toxic but finely divided silicates or silica can cause major damage to the lungs.²

^{29}Si is the only NMR-active isotope of silicon, and ^{29}Si NMR can be employed to study the biological and medicinal chemistry of silicon, although low natural abundance and low receptivity have hindered the development of this technique so far. Accordingly, to the best of our knowledge, only a very few studies were recently reported on the use of ^{29}Si NMR in solution to characterize organosilicon derivatives of biological interest, that is, showing antifungal, antibacterial or cytotoxic activity.⁹⁰ On the other hand, solid-state ^{29}Si NMR studies applied to biocompatible materials have been reported, including the development of silicon-containing monocomposites for the controlled release of pharmaceuticals⁹¹ and of bioactive silicon-based hybrids for bone regeneration.^{91d,92} Additionally, ^{29}Si MRI has potential for imaging silicone prostheses in humans.⁹³ ^{29}Si relaxation times of silicone gels average $T_1 = 21.2 \pm 1.5 \text{ s}$ and $T_2 = 207 \pm 40 \text{ ms}$, with no significant difference between virgin and explanted gels. Three volunteers with silicone gel-filled breast implants and one subject with an intraocular silicone oil injection were thus examined with a total acquisition time of 10–15 min per image. In all ^{29}Si images, the shape of the silicone object is well depicted and, although conventional proton images are superior in resolution and signal-to-noise ratio, ^{29}Si imaging has the advantage of optimal specificity, since only the silicone itself is visible.

Germanium has no biological role but it is believed to stimulate the metabolism. Nevertheless, organogermanium compounds may exert some biological activity.⁹⁴ For example, spirogermanium, a germanium-containing azaspirane derivative, is reported to have in vitro and in vivo cytotoxicity toward a number of preclinical tumor models and to exhibit antiarthritic and immunoregulatory activities.⁹⁵ It underwent phase I and II clinical trials but turned out to be poorly active for further clinical use.

The natural abundance of ^{73}Ge is slightly higher than ^{29}Si , but recording of ^{73}Ge resonances is very difficult because of the low value of γ , along with its nuclear spin of 9/2 and large quadrupole moment. EFGs around ^{73}Ge lead to excessive broadening of the signals. Symmetrical germanium complexes give sharp signals in the ^{73}Ge NMR, whereas the signal broadens as the symmetry lowers. For instance, the halfwidth of the ^{73}Ge peak for tetramethylgermanium, a compound with high geometric symmetry, is only 1.4 Hz, whereas the corresponding values of germacyclohexane, 1-methylgermacyclohexane, and 1,1-dimethylgermacyclohexane are 15.4, 22.3, and 15.6 Hz, respectively. When either halogen or oxygen atoms are asymmetrically substituted, as in 1-bromo-1-methylgermacyclohexane, excessive broadening takes place to such an extent that observation of signals is impossible.⁹⁶ To the best of our knowledge, no ^{73}Ge NMR studies on biologically relevant systems have been reported to date.

Tin

Isotope	A (%)	I	γ ($\times 10^7 \text{ rad T}^{-1} \text{ s}^{-1}$)	Q (fm^2)	Relative receptivity to ^{13}C	Reference sample
^{115}Sn	0.34	1/2	-8.801	-	0.711	$\text{Sn}(\text{CH}_3)_4/\text{C}_6\text{D}_6$ (90%)
^{117}Sn	7.68	1/2	-9.589	-	20.8	
^{119}Sn	8.59	1/2	-10.032	-	26.6	

Tin may be an essential element for human beings. The chemistry of organotin compounds has attracted much attention during the last 60 years, owing to potential biological and industrial applications. Tin is regarded as the third most important pollutant in the ecosystem, which has raised the concern that it may enter the human food chain and be accumulated in the environment and in other biological systems.⁹⁷ Organotin(IV) derivatives have interest as potential metallopharmaceuticals since some exhibit in vitro

antitumor activity against a number of human tumor cell lines and antimicrobial, anti-inflammatory, cardiovascular, trypanocidal, antiherpes, and antituberculosis agents.^{79c,98}

The merits of tin NMR in assessing structural characteristics of organotin compounds (e.g., substitution pattern on tin, coordination number, influence of solvent, and speciation under physiologically relevant conditions) were recognized in the early 1970s, owing to the reasonably favorable magnetic properties of tin nuclei. Tin has ten natural isotopes, of which three have $I = 1/2$. Among them, ^{115}Sn is the least NMR favorable isotope, because of its extremely low natural abundance. As a result, it has been only rarely studied, for example, to overcome difficulties in unraveling strongly coupled homonuclear $^2J(^{119}\text{Sn}-^{119}\text{Sn})$ scalar coupling satellites in di-tin compounds.⁹⁹ The “twins” ^{117}Sn and ^{119}Sn nuclei have rather similar properties, but ^{119}Sn NMR spectroscopy is, by far, the most widely used in tin chemistry because of both its slightly higher magnetic moment and natural abundance. Thus, not surprisingly, the use of NMR in tin chemistry has been widely reviewed.¹⁰⁰ In particular, the use of $^{117/119}\text{Sn}$ NMR spectroscopy to investigate the interaction between organotin complexes and biomolecules such as amino acids, peptides, carbohydrates, and nucleic acids has been extensively reviewed, including equilibrium, structural, and biological studies.¹⁰¹

Nowadays, ^{119}Sn NMR is mainly used as a routine analytical tool to characterize tin complexes, in particular Schiff bases derivatives, as potential antimicrobial and anticancer agents.¹⁰²

Lead

Isotope	A (%)	I	γ ($\times 10^7 \text{ rad T}^{-1} \text{ s}^{-1}$)	Q (fm^2)	Relative receptivity to ^{13}C	Reference sample
^{207}Pb	22.10	1/2	5.580	–	11.8	$\text{Pb}(\text{CH}_3)_4/\text{C}_6\text{D}_6$ (90%) or neat

Lead is probably nonessential for man but its toxicology is of great interest since it is a ubiquitous environmental contaminant. Although the use of lead (as PbEt_4) in gasoline and paint has now been banned in most developed countries, lead is still among the ten most common contaminants.¹⁰³ On the other hand, lead has been investigated for its possible applications in medicine. The potentially therapeutic radioisotope ^{212}Pb has a number of interesting features including α -emission by short-lived daughter radionuclides, and its use is encouraged by the development of state-of-the-art generator systems¹⁰⁴ and by the observation that when ^{212}Pb -conjugated antibodies are internalized, radioactivity is retained inside the cells.¹⁰⁵

^{207}Pb is the only NMR-active ($I = 1/2$) lead isotope and has excellent receptivity, relatively high natural abundance, and large chemical shift range. Although ^{207}Pb NMR spectroscopy has been used extensively to characterize $\text{Pb}(\text{IV})$ -alkyl derivatives, relatively few spectroscopic studies have been carried out on the aqueous coordination chemistry of soluble $\text{Pb}(\text{II})$ complexes.¹⁰⁶

The toxicological implications of lead derivatives have spurred a number of studies aimed at investigating their interaction with various proteins.¹⁰⁷ For example, Pb^{2+} can bind very tightly to, and even displace Ca^{2+} from, calmodulin, calbindin, and troponin C. Moreover, it can replace calcium in the activation of several enzymes, including protein kinase C, phosphodiesterase, and myosin light chain kinase, the latter two in a calmodulin-dependent way. Therefore, model systems are needed for lead bound to Ca-binding sites in proteins, as these interactions are thought to account for lead's toxicity. For example, the high-affinity Ca^{2+} -binding sites of carp (pI 4.25) and pike (pI 5.0) parvalbumins, as well as those of mammalian calmodulin and its C-terminal tryptic half-molecule (TR_2C), have been investigated by ^{207}Pb NMR spectroscopy.¹⁰⁸ For the parvalbumins, two ^{207}Pb signals are observed, with chemical shifts ranging from +750 to +1260 ppm downfield of aqueous $\text{Pb}(\text{NO}_3)_2$, corresponding to $^{207}\text{Pb}^{2+}$ bound to the two high-affinity helix-loop-helix Ca^{2+} -binding sites. Four ^{207}Pb signals, recorded in the same chemical shift window, can be discerned for calmodulin (Fig. 13). Experiments on TR_2C allowed the assignment of each signal due to $^{207}\text{Pb}^{2+}$ occupying a helix-loop-helix site in either the N- or the C-lobe of the intact protein. ^{207}Pb and ^1H NMR titration studies on calmodulin have provided evidence that Pb^{2+} binding to all four sites occurs simultaneously, in contrast to the behavior of the same protein in the presence of Ca^{2+} . The large chemical shift dispersion observed for the ^{207}Pb signals of the three investigated proteins illustrates the remarkable sensitivity of this parameter to subtle differences in the chemical environment of the protein-bound ^{207}Pb nucleus.

Pb^{2+} can replace calcium and sometimes zinc in both the “hard” oxygen- and nitrogen-rich protein active sites and in the “soft” ones, such as all-sulfur-containing zinc ion coordination sites. Among the sulfur-rich targets for Pb^{2+} are GSH and metallothioneins, which cause perturbations of essential metal ion homeostasis and are likely to be involved in human lead poisoning. ^{207}Pb NMR signals for the thiol-rich binding sites are expected to be shifted downfield to oxygen- and nitrogen-rich ones, thus allowing to distinguish $\{\text{PbS}_3\}$ versus $\{\text{PbS}_3\text{O}\}$ coordination environments.¹⁰⁹ In this regard, Pecoraro and coworkers presented the first report on ^{207}Pb NMR spectroscopy used to directly probe the binding of Pb^{2+} to a Cys₃-motif in thiolate-rich metalloprotein by utilizing three-strand coiled-coil peptides, showing the preferred $\{\text{PbS}_3\}$ homoleptic trigonal pyramidal geometry for Pb^{2+} .¹¹⁰ Such evidence has been recently confirmed by performing ^{207}Pb NMR experiments aimed at revealing the coordination behavior of Pb^{2+} toward GSH and zinc-finger proteins.¹¹¹

Claudio and coworkers¹¹² have reported on the first 2D [$^1\text{H}, ^{207}\text{Pb}$] heteronuclear multiple quantum coherence (HMQC) spectrum (Fig. 14) and demonstrated that this experiment can provide useful information about the lead coordination environment in aqueous $\text{Pb}(\text{II})$ complexes. This technique allows ^{207}Pb - ^1H couplings through up to three bonds to be identified and could prove useful for the investigation of Pb^{2+} ions in more complex systems, such as biological and environmental samples.

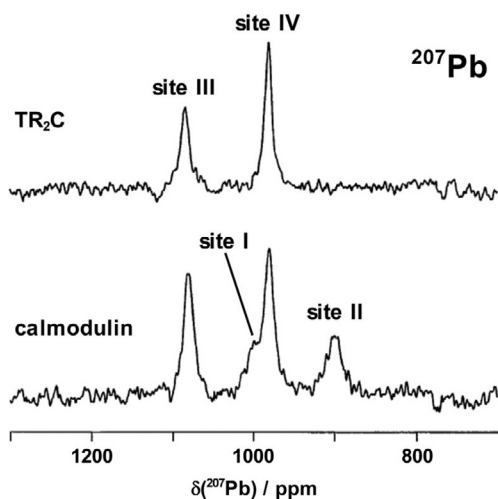


Fig. 13 ^{207}Pb NMR spectra of the $^{207}\text{Pb}^{2+}$ forms of bacterially expressed mammalian calmodulin (1.47 mM, 4.0 equiv. $^{207}\text{Pb}^{2+}$, 100 mM KCl, pH 7.1) and its C-terminal domain fragment TR₂C (1.11 mM, 2.0 equiv. $^{207}\text{Pb}^{2+}$, 100 mM KCl, pH 7.0). Adapted from Aramini, J. M.; Hiraoki, T.; Yazawa, M.; Yuan, T.; Zhang, M.; Vogel, H. J. *J. Biol. Inorg. Chem.* **1996**, *1*, 39–48, with permission.

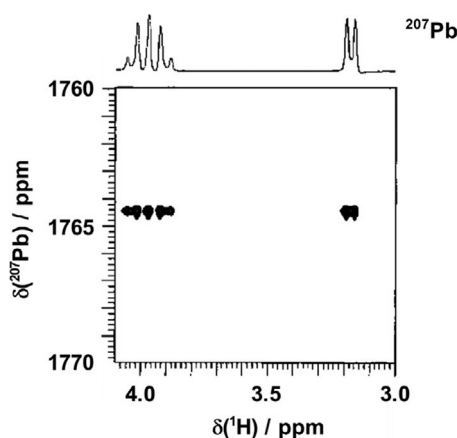


Fig. 14 2D [^1H , ^{207}Pb] HMQC NMR spectrum of $[\text{}^{207}\text{Pb}(\text{EDTA}-N_4)]^{2+}$ (EDTA = ethylenediaminetetraacetic acid, 99.9% D₂O, pH 6.1, 25°C). Coupling is observed from ^{207}Pb to ^1H through three bonds. ^{207}Pb chemical shifts are referenced to external 1.0 M $\text{Pb}(\text{NO}_3)_2$ in 99.9% D₂O at pH 3.3. Adapted from Claudio, E. S.; ter Horst, M. A.; Forde, C. E.; Stern, C. L.; Zart, M. K.; Godwin, H. A. *Inorg. Chem.* **2000**, *39*, 1391–1397, with permission.

p-Block: Group 15 (As, Sb, and Bi) and Group 16 (Te)

Arsenic, antimony, and bismuth

Isotope	A (%)	I	γ ($\times 10^7 \text{ rad T}^{-1} \text{ s}^{-1}$)	Q (fm^2)	Relative receptivity to ^{13}C	Reference sample
^{75}As	100	3/2	4.596	31.4	149	$\text{NaAsF}_6/\text{CD}_3\text{CN}$ (0.5 M)
^{121}Sb	57.21	5/2	6.444	36.0	548	$\text{K}[\text{SbCl}_6]/\text{D}_2\text{O}$ (sat.)
^{123}Sb	42.79	7/2	3.489	49.0	117	
^{209}Bi	100	9/2	4.375	51.6	848	$\text{Bi}(\text{NO}_3)_3/\text{D}_2\text{O}$ (sat. in HNO_3)

Despite arsenic reputation as a highly toxic substance, this element may actually be necessary for good health. Studies on animals such as chickens, rats, goats, and pigs showed that it is necessary for proper growth, development, and reproduction. In these reports, the main symptoms of arsenic deficiency were retarded growth and development. Arsenic compounds occur naturally in marine organisms, such as arsenobetaines in flat fish, and are used as growth promoters for farm animals. It is suspected, but not yet proven, that arsenic may be an essential element necessary for the functioning of the nervous system and for growth. Arsenic trioxide

(As₂O₃, Trisenox) has been approved by the Food and Drug Administration to treat a rare and deadly form of leukemia called acute promyelocytic leukemia.¹¹³

Antimony appears to have no known role in the body. Sb(III) compounds cause damage to the liver and are used in some cases to induce vomiting and sweating. Some Sb(V) derivatives are used to treat the parasitic disease leishmaniasis.¹¹⁴

Bismuth has no known natural biological role and is relatively nontoxic. However, it has been used for some time as a medicine (e.g., as tripotassium dicitratobismuthate) for treatment of gastrointestinal disorders. Nowadays, it is used for the treatment of stomach ulcers since it is effective against the bacterium *Helicobacter pylori*^{115a} and can be added in antihemorrhoid creams, such as Anusol and Hemocane, as bismuth oxide and in Anusol ointment as bismuth subgallate.^{115b} Finally, it was recently reported that bismuth complexes may inhibit the severe acute respiratory syndrome coronavirus.¹¹⁶

⁷⁵As, ^{121/123}Sb, and ²⁰⁹Bi are the corresponding NMR-active isotopes and are characterized by a high sensitivity and large quadrupole moments, which make their linewidths very sensitive to the environmental symmetry of the nuclei. Although both their natural abundances and receptivities are favorable, recording NMR spectra of these nuclei is known to be very difficult due to their very broad signals, especially for ²⁰⁹Bi. As far as we are aware of, no NMR studies concerning the involvement of As, Sb, or Bi in biologically relevant systems have been reported to date.

Tellurium

Isotope	A (%)	I	γ ($\times 10^7$ rad T ⁻¹ s ⁻¹)	Q (fm ²)	Relative receptivity to ¹³ C	Reference sample
¹²³ Te	0.89	1/2	7.059	–	0.96	Te(CH ₃) ₂ /C ₆ D ₆ (90%) or neat
¹²⁵ Te	7.07	1/2	8.51	–	13.4	

Tellurium is a noble metalloid that can act as either a Lewis acid or a Lewis base. It has no known biological role and most tellurium compounds are highly toxic. Organotellurium derivatives are potent immunomodulators (both in vitro and in vivo) with a variety of potential therapeutic applications. For example, ammonium trichloro(dioxoethylene-O,O')tellurate (AS101) is known to be effective in the treatment of AIDS and cancer. It confers protection against side effects of both radiotherapy and chemotherapy by protecting the bone marrow and preventing from alopecia. It also exhibits synergistic effects with a variety of other drugs and is reported to be effective against systemic lupus erythematosus and psoriasis.¹¹⁷

Tellurium has two naturally occurring NMR-active isotopes, ¹²³Te and ¹²⁵Te, both having $I = 1/2$. ¹²⁵Te has higher receptivity and natural abundance, thus making it the more favorable isotope for direct NMR observations. The use of ¹²⁵Te NMR spectroscopy to probe the ligand chemistry of tellurium has been widely reviewed.¹¹⁸

Tellurium coordination chemistry is dominated by sulfur ligands. Owing to the strong affinity of Te(IV) for thiols, tellurium has been investigated as a selective cysteine protease inhibitor. In this regard, AS101 was shown to inhibit cysteine proteases in a time- and concentration-dependent way but no inhibitory activity of serine, metalloprotease, or aspartic proteases was observed. Remarkably, the capability of Te(IV) to interact with cysteine thiol groups is believed to correlate with its inhibitory activity. ¹²⁵Te NMR has been used to follow the interaction between cysteine and Te(IV) or Te(VI) compounds.¹¹⁹ Although the resonances are highly sensitive to the environment (e.g., solvent, concentration, and temperature), they can be divided into well-defined frequency ranges corresponding to the tellurium oxidation state. Data reported in this study demonstrated a clear distinction in reactivity of Te(IV) and Te(VI) complexes toward thiol nucleophiles. Whereas the latter do not interact with the thiols, all the investigated Te(IV) derivatives exhibited significant shifts upon interaction with cysteine. For example, AS101 experienced a downfield shift from +1700 to +1807 ppm, respectively, attributable to the formation of [Te(Cys)₄].

d-Block: Group 3 (Sc and Y) and Group 4 (Ti)

Scandium and yttrium

Isotope	A (%)	I	γ ($\times 10^7$ rad T ⁻¹ s ⁻¹)	Q (fm ²)	Relative receptivity to ¹³ C	Reference sample
⁴⁵ Sc	100	7/2	6.509	–22.0	1780	Sc(NO ₃) ₃ /D ₂ O (0.06 M)
⁸⁹ Y	100	1/2	–1.316	–	0.700	Y(NO ₃) ₃ /D ₂ O (sat.)

Scandium has no known biological role. It is relatively nontoxic, although there have been suggestions that some of its compounds might be carcinogenic and can cause lung embolisms, especially upon long-term exposure.²¹

Yttrium is not normally found in human tissues and plays no known biological role. Targeted radionuclide therapy of cancer using the high-energy β -emitting isotope ⁹⁰Y is now in advanced clinical trials (using the conjugates of somatostatin receptor binding peptides), with promising results, at least at a palliative level.¹²⁰

Both ⁴⁵Sc and ⁸⁹Y are NMR-active nuclides with 100% natural abundance. ⁴⁵Sc has high resonance frequency, high receptivity, and a relatively small quadrupole moment but, despite these favorable features, ⁴⁵Sc NMR spectroscopy has been scarcely exploited

for biological studies of scandium derivatives to date. As already shown for ^{27}Al (see text earlier), ^{45}Sc NMR can be used to probe metal-binding sites in large proteins. The solution chemistry of scandium is based entirely on Sc^{3+} , which forms almost exclusively six-coordinate complexes. The ionic radius of Sc^{3+} is only slightly larger than Fe^{3+} (0.75 vs. 0.65 Å), thus making it a suitable probe for the Fe(III)-binding sites of transferrins in which the metal ion is coordinated by six donor atoms, four from the side chains of four protein residues and two from the synergistic anion (i.e., carbonate), in a distorted octahedral geometry. In this regard, the binding of Sc^{3+} to chicken ovotransferrin has been investigated by ^{45}Sc and ^{13}C NMR spectroscopy.¹²¹ In the presence of carbonate, both ^{45}Sc and ^{13}C NMR spectra show two signals assigned to the bound $^{45}\text{Sc}^{3+}$ and $^{13}\text{CO}_3^{2-}$ groups in the N- and C-binding sites of the protein (Fig. 15). Several properties of the transferrin-bound ^{45}Sc signals, such as their dependence on pulse length, magnetic field, protein size, and temperature, are consistent with the detection of only the central transition of the quadrupolar nucleus in conditions far away from the extreme narrowing ones. Additionally, from the ^{45}Sc chemical shift and linewidth data recorded at four magnetic fields, the quadrupolar coupling constants and the rotational correlation time have been calculated for the bound metal ion in each site of the protein. Remarkably, this work represented the first, and so far the only, ^{45}Sc NMR study of a metalloprotein. More recent relevant reports have been dealing with the use of ^{45}Sc NMR spectroscopy for the characterization of Sc(III) derivatives as potential PET agents and radiopharmaceuticals.¹²²

^{89}Y has $I = 1/2$ and, as such, it should be attractive for NMR study. Nevertheless, it is not routinely used in the characterization of yttrium complexes owing to the low receptivity and resonance frequency, and long relaxation times, which lead to problems with detection and to the necessity for lengthy experiments. The use of ^{89}Y NMR spectroscopy for the characterization of organometallic and coordination compounds containing yttrium has been previously reported.¹²³ On the contrary, fewer biologically related reports exist on the exploitation of this technique. For example, it was shown that yttrium complexes can be successfully hyperpolarized,^{124,125} so as to overcome the intrinsic detectability issues of ^{89}Y itself. As such, owing to the long longitudinal relaxation time, ^{89}Y derivatives seem promising as MRI agents.¹²⁵ Moreover, yttrium and gadolinium have similar ionic radii and coordination chemistry, so the former can be used as model for gadolinium-based contrast agents (see text later). In this regard, a recent paper reports on the use of hyperpolarized ^{89}Y NMR to monitor slow complexation processes.¹²⁶

Titanium

Isotope	A (%)	I	γ ($\times 10^7 \text{ rad T}^{-1} \text{ s}^{-1}$)	Q (fm^2)	Relative receptivity to ^{13}C	Reference sample
^{47}Ti	7.44	5/2	-1.511	30.2	0.918	$\text{TiCl}_4/\text{C}_6\text{D}_{12}$ (90%) or neat
^{49}Ti	5.41	7/2	-1.511	24.7	1.2	4612

Titanium is believed to be a nonessential element, although some observations indicate that Ti^{4+} may have a variety of biological roles. In medicine, titanium is used to make hip and knee replacements, pacemakers, bone plates, and screws and cranial plates for skull fractures, and it has been also used to attach false teeth. Two Ti(IV) derivatives (budotitan and titanocene dichloride) have been investigated as potential metallodrugs.^{79c,127} In particular, titanocene dichloride, $[\text{TiCl}_2\text{Cp}_2]$ (Cp = cyclopentadienyl), entered phase I clinical trials in 1993 and, although nephrotoxicity was identified as a major issue, the absence of any effect on the proliferative activity of the bone marrow suggested that titanocene dichloride might have significant potential for possible use in combination therapy. Subsequently, two phase II clinical trials involving patients with advanced renal cell carcinoma and breast metastatic carcinoma have been reported. However, outcomes were not sufficiently promising compared to other treatment regimes to warrant further studies, and titanocene dichloride was discontinued from further clinical trials.¹²⁸

Titanium has two naturally occurring quadrupolar NMR-active isotopes, ^{47}Ti and ^{49}Ti , the latter having slightly higher receptivity and narrower linewidths, thus usually making it the more favorable isotope for direct NMR observations in spite of the lower natural abundance. The $^{47/49}\text{Ti}$ chemical shifts of titanocene dichloride were determined over 30 years ago,¹²⁹ but, to the best of our knowledge, no further biological investigations have been performed by means of Ti NMR spectroscopy.

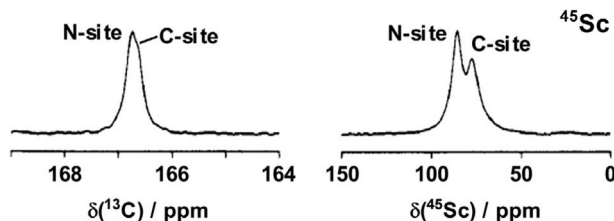


Fig. 15 ^{13}C and ^{45}Sc NMR spectra (referenced to external neat TMS and 1.0 M ScCl_3 in D_2O , respectively, at 0.0 ppm) of 1.05 mM ovotransferrin in the presence of 10 mM $\text{Na}_2^{13}\text{CO}_3$ and 1.9 equiv. of Sc^{3+} (75% $\text{H}_2\text{O}/25\%$ D_2O , 150 mM KCl, pH 7.6, 25°C). Adapted from Aramini, J. M.; Vogel, H. J. *J. Am. Chem. Soc.* **1994**, *116*, 1988–1993, with permission.

d-Block: Group 5 (V) and Group 6 (Cr, Mo, and W)**Vanadium**

Isotope	A (%)	I	γ ($\times 10^7 \text{ rad T}^{-1} \text{ s}^{-1}$)	Q (fm^2)	Relative receptivity to ^{13}C	Reference sample
$^{50}\text{V}^a$	0.25	6	2.67	21.0	0.818	$\text{VOCl}_3/\text{C}_6\text{D}_6$ (90%)
^{51}V	99.75	7/2	7.046	-5.2	2250	

^aRadioactive with a long half-life (1.4×10^{17} year, β^+).

Vanadium exists in a variety of oxidation states, from -3 to +5. In vivo, owing to the constraints of standard physiological conditions (pH 3–7, aerobic aqueous solution, room temperature), oxidation states +4 and +5 prevail, with thermodynamically plausible species including vanadate, a mixture of $[\text{HVO}_4]^{2-}$ and $[\text{H}_2\text{VO}_4]^-$, and vanadyl, $[\text{VO}]^{2+}$. Vanadium is normally present at very low concentrations ($<10^{-8}$ M) in virtually all cells in plants and animals. In the oxidation states +3, +4, and +5, it readily forms V–O bonds and binds N- and S-donors as well, forming robust coordination compounds. From a coordination chemistry point of view, vanadium is remarkably flexible. For example, V(V) has nonrigid stereochemical requirements and can form coordination complexes in geometries ranging from tetrahedral and octahedral to trigonal and pentagonal bipyramidal. On the contrary, V(IV) is much less flexible, with square pyramidal or, if a sixth position is occupied, distorted octahedral geometries. Vanadium derivatives readily undergo redox reactions under physiological conditions and form both cationic and anionic complexes. The interplay between V(V) and V(IV) represents the key redox process of vanadium complexes in vivo, and the two oxidation states coexist in equilibrium both intra- and extracellularly.¹³⁰

The biological relevance of vanadium was confirmed by the discovery of two naturally occurring vanadium proteins, a V-bromoperoxidase and a V-nitrogenase.¹³¹ In addition, vanadium has received much attention in recent years due to the discovery of many therapeutic properties. Several vanadium salts and their complexes have shown insulin-mimetic pharmacological properties, including stimulation of glucose transport into the cells and its oxidation via glycolysis, glycogen synthesis, and lipogenesis, and inhibition of gluconeogenesis and glycogenolysis. The antidiabetic properties of vanadium compounds, demonstrated both in vitro and in vivo, have attracted much interest as potential therapeutic agents for diabetes mellitus. They can be administered orally and promote glucose uptake in animal models of type 1 and type 2 diabetes. Phase I clinical trial of bis(ethylmaltolato)oxovanadium(IV) was completed in 2000, and the results of the phase II clinical trial were first published in 2009.^{79b,132} Moreover, the anticancer potential of, for example, vanadocene derivatives and a vanadium(IV)–aspirin complex is currently being investigated.¹³³ Coordination compounds of vanadium, which may have pharmacological relevance, include not only vanadate $[\text{VO}_x\text{L}_y]$ and vanadyl $[\text{VOL}_z]$ derivatives but also the peroxovanadates $[\text{VO}(\text{O}_2)(\text{H}_2\text{O})(\text{L}-\text{L}')]^n-$ ($n = 0, 1$) and $[\text{VO}(\text{O}_2)_2(\text{L}-\text{L}')]^n-$ ($n = 1, 2, 3$).¹³⁴

^{51}V NMR is a powerful and selective probe of vanadium in biological systems. Unlike many other biologically relevant isotopes, the NMR receptivity of the quadrupolar ^{51}V nucleus is rather high due to a large magnetic moment, a small quadrupole moment, a relatively large γ , a high natural abundance, and a rapid quadrupolar relaxation in solution. ^{51}V chemical shifts are quite sensitive to changes in the nature of the ligands, thereby providing an excellent diagnostic tool for detailed investigations of vanadium speciation and binding to macromolecules.¹³⁵

In particular, the speciation of vanadate and vanadium(V)-based coordination compounds under physiologically relevant conditions and in presence of selected biomolecules has been probed by Pettersson and coworkers, and results were reviewed recently.¹³⁶

Inorganic vanadium salts were the first compounds for which insulin-enhancing behavior was detected in vivo, but several vanadium complexes with organic ligands were found to be more potent and less toxic than vanadium salts, likely owing to the increased selectivity. In this regard, speciation studies of vanadate–ligand and peroxovanadate–ligand systems in aqueous media and under physiological conditions have been carried out by means of ^{51}V NMR spectroscopy in order to provide insights into their insulin-mimetic behavior.¹³⁷

^{51}V NMR spectroscopy has been successfully employed to probe the solution chemistry and stability under physiologically relevant conditions of several vanadium-based chemotherapeutic agents, such as the leading compound bis(maltolato)oxovanadium(IV),^{138a} its kojato analog,^{138b} and a prodrug of peroxovanadate insulin-mimetic *hexakis*-(benzylammonium)decavanadate(V) dihydrate.^{138c} An example of the suitability of this technique is illustrated in Fig. 16, in which the variable pH ^{51}V NMR spectra of a solution of $[\text{VO}(\text{maltolato})_2]$ (Fig. 16A) and of genuine $[\text{VO}_2(\text{maltolato})_2]^-$ (Fig. 16B) are reported. As shown in Fig. 16A, in basic solution, only one peak (V_1) at -537 ppm was observed and assigned to mixed protonation states of vanadate. As the pH was lowered, peaks V_2 ($[\text{VO}_2(\text{maltolato})_2]^-$) and V_3 ($[\text{VO}_2(\text{maltolato})(\text{OH})(\text{H}_2\text{O})]^-$) appeared at -496 and -510 ppm, respectively. As the acidity of the solution increased, peak V_1 shifted downfield and disappeared below pH 5.5. By comparison with the variable pH ^{51}V NMR spectra of $\text{NH}_4[\text{VO}_2(\text{maltolato})_2]$ (Fig. 16B), it was proved that some V(V) complexes form in a solution of $[\text{V}^{\text{IV}}\text{O}(\text{maltolato})_2]$, even under relatively acidic conditions.

Other applications of the favorable spectroscopic properties of ^{51}V include: the use of ^{51}V NMR to probe the interaction of vanadium derivatives with proteins, such as transferrins¹³⁹ and actin,¹⁴⁰ the study of the uptake, intracellular reduction, and binding of the aerobic oxidation products of oxovanadium(IV) compounds in human erythrocytes,¹⁴¹ and the interactions of vanadium(V)–citrate complexes with the sarcoplasmic reticulum calcium pump¹⁴² have been reported.

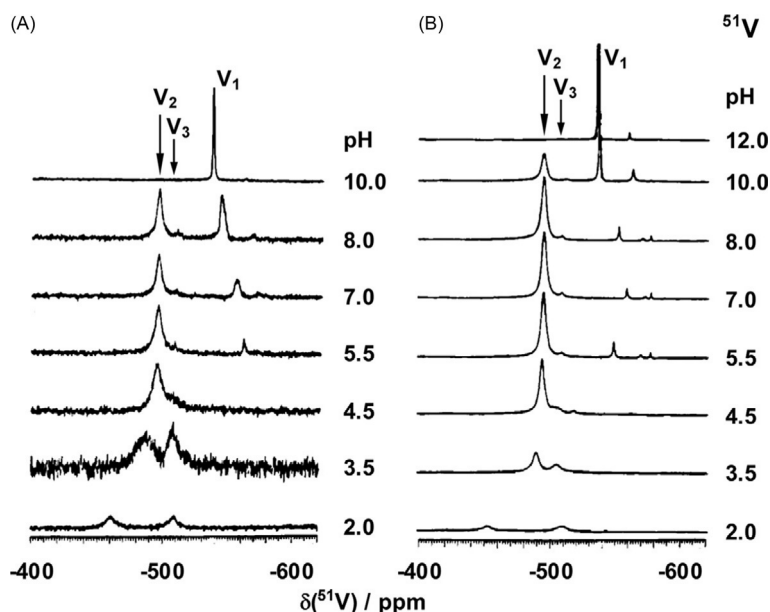


Fig. 16 Variable pH ^{51}V NMR spectra (referenced to external neat $[\text{VOCl}_3]$ at 0.0 ppm) of a 0.15 M NaCl aqueous solution of (a) $[\text{VO}(\text{maltolato})_2]$ (10 mM) and (b) $\text{NH}_4[\text{VO}_2(\text{maltolato})_2]$ (10 mM) at 25°C. Adapted from Caravan, P.; Gelmini, L.; Glover, N.; Herring, F. G.; Li, H.; McNeill, J. H.; Rettig, S. J.; Setyawati, I. A.; Shuter, E.; Sun, Y.; Tracey, A. S.; Yuen, V. G.; Orvig, C. *J. Am. Chem. Soc.* **1995**, *117*, 12759–12770, with permission.

Vanadium derivatives are currently under intense investigation for their potential medicinal applications other than insulin mimetics, including their anticancer,^{143a,143b} antimoebic,^{143c} antiparasitic^{143d} and biological catalytic (peroxidase mimicking)^{143e} activities. In most cases, ^{51}V NMR proved useful not only to characterize the novel vanadium-based derivatives and study their stability in aqueous systems but also to probe their binding to DNA.^{143a}

In recent years, VO_2 films have been attracting growing attention as thermochromic materials for applications in intelligent windows.^{144a} Although most studies focus on the optimization of preparation methods and enhancement of energy-saving efficiency, metal oxide nanomaterials might be toxic to human health and the environment.^{144b} In this regard, Jin and coworkers have successfully exploited ^{51}V NMR to evaluate the potential toxicity of VO_2 films.^{144c} Spectra recorded on extracts of VO_2 films in PBS solution showed the formation over time of a ^{51}V peak at -560 ppm (corresponding to mononuclear tetrahedral vanadate) and, subsequently, the appearance of a signal at -580 ppm (associated with the corresponding divanadate species). The study demonstrated the release of vanadium under physiological-like conditions as V(V) and this was linked to the potential toxic mechanism of VO_2 -based nanomaterials due to the vanadate disturbing ATP synthesis as a phosphate analogue through a vanadate-phosphate antagonism.

Chromium, molybdenum, and tungsten

Isotope	A (%)	I	γ ($\times 10^7 \text{ rad T}^{-1} \text{ s}^{-1}$)	Q (fm^2)	Relative receptivity to ^{13}C	Reference sample
^{53}Cr	9.50	3/2	-1.515	-15.0	0.507	$\text{K}_2\text{CrO}_4/\text{D}_2\text{O}$ (sat.)
^{95}Mo	15.92	5/2	-1.751	-2.2	3.06	$\text{Na}_2\text{MoO}_4/\text{D}_2\text{O}$ (2 M)
^{97}Mo	9.55	5/2	-1.788	25.5	1.95	
^{183}W	14.31	1/2	1.128	-	0.063	$\text{Na}_2\text{WO}_4/\text{D}_2\text{O}$ (1 M)

Chromium may be an essential trace element for mammals and be involved in the maintenance of proper carbohydrate and lipid metabolism, and its mild dietary deficiency is sometimes associated with possible heart disease. Recent studies revealed that the chromium-binding oligopeptide chromodulin may play a role in the autoamplification of insulin signaling. Attempts to develop chromium-containing nutritional supplements and therapeutics have been made.¹⁴⁵ Nevertheless, in anything other than trace amounts, chromium compounds are regarded as highly toxic. The health effects of chromium are at least partially related to the oxidation state of the metal at the time of exposure. Cr(III) and Cr(VI) compounds are thought to be the most biologically significant. Cr(VI) is generally considered much more toxic than Cr(III), and prolonged exposure to Cr(VI) has been associated with increased incidence of lung cancer.²

Molybdenum is an essential trace element for virtually all life forms. In humans, upon binding to a unique pterin, molybdenum functions as a cofactor that, in different variants, is the active compound at the catalytic site of two families of molybdenum containing enzymes, that is, sulfite oxidase and xanthine oxidase.¹⁴⁶ As a metallopharmaceutical, molybdocene dichloride, an analog of titanocene dichloride (see preceding text), and its derivatives are still under investigation as anticancer agents,^{147,148} and tetrathiomolybdate has been developed as an effective anticopper therapy for the initial treatment of Wilson's disease, an autosomal recessive disorder that leads to abnormal copper accumulation.¹²⁸

Opinions are mixed about the need for tungsten in plant and animal life processes. It is not known whether humans need tungsten for good health although it was proved necessary for certain bacteria. Additionally, polyoxotungstate clusters have been evaluated as insulin mimetics in animal models.¹⁴⁸

There are several practical problems involved in the routine chromium NMR spectroscopy. ⁵³Cr, the only NMR-active isotope, has a small magnetic moment, resulting in low Larmor frequency and sensitivity, and a relatively large quadrupole moment, which leads to short nuclear relaxation times and large experimental linewidths. The low natural isotope abundance combined with the small overall receptivity results in extremely low sensitivity to detection by NMR spectroscopy. To date, only a few ⁵³Cr solution NMR measurements have been reported, and none is of any biological interest.¹⁴⁹

Molybdenum has two naturally occurring NMR-active isotopes, ⁹⁵Mo and ⁹⁷Mo, both quadrupolar and characterized by low sensitivity to detection by NMR and low natural abundance. ¹⁸³W is the only nonquadrupolar NMR-active nucleus in group 6 family, but it is also characterized by low natural abundance and extremely low receptivity. Thus, despite the potentially interesting biological properties of molybdenum and tungsten, only a few biologically relevant data on the application of ^{95/97}Mo and ¹⁸³W NMR spectroscopy have been reported. For example, ⁹⁵Mo NMR was used to detect the binding of tetraoxo- and tetrathiomolybdate to BSA by exploiting ⁹⁵Mo-enriched species.¹⁵⁰ More recently, the cleavage of the phosphoester in a DNA model promoted by a polyoxomolybdate was probed by ⁹⁵Mo NMR spectroscopy.¹⁵¹ As far as ¹⁸³W NMR is concerned, such technique was exploited to characterize some heteropolytungstates tested as anti-HIV¹⁵² and anticancer¹⁵³ agents' and some organoantimony(III)-containing heteropolytungstates with potential applications as antimicrobial agents.¹⁵⁴

d-Block: Group 7 (Mn and Tc)

Manganese

Isotope	A (%)	I	γ ($\times 10^7$ rad T ⁻¹ s ⁻¹)	Q (fm ²)	Relative receptivity to ¹³ C	Reference sample
⁵⁵ Mn	100	5/2	6.645	33.0	1050	KMnO ₄ /D ₂ O (0.82 m)

Manganese has many roles in biological systems. It can exist in 11 oxidation states (from +7 to -3), more than any other element, but its aqueous chemistry is dominated by Mn(II) complexes. Both Mn(II) and Mn(III) ions are found in enzymes. The ionic radius of 0.9 Å places Mn²⁺ in between Mg²⁺ and Ca²⁺, so that it is not surprising that there is overlap in function with these two ions in providing structural charge stabilization of enzymes and, in some cases, substrates, such as Mn-ATP. In this regard, manganese has been useful in substituting Mg²⁺ and Ca²⁺ as a probe of divalent metal ion binding and function in enzymes¹⁵⁵ and ribozymes.⁴⁷ Manganese also acts as a superacid catalyst in several hydrolytic enzyme-catalyzed reactions.¹⁵⁶ The classes of enzymes that have manganese cofactors are very broad and include oxidoreductases, transferases, hydrolases, lyases, isomerases, ligases, lectins, and integrins. The Mn superoxide dismutase enzyme is probably one of the most ancient, as nearly all aerobic organisms use it to deal with the toxic effects of superoxide.¹⁵⁷ In addition to its important biological role, manganese may have several therapeutic uses, including the treatment of arthritis, cancer, cardiovascular diseases, and HIV.¹⁵⁸

Consequently, to the biological relevance of manganese, NMR spectroscopy might be a potential analytic tool to investigate its behavior. ⁵⁵Mn is quadrupolar and has a natural abundance of 100%, a Larmor frequency close to ¹³C, and a chemical shift range of approximately 3500 ppm, but because of the large Q, ⁵⁵Mn NMR spectroscopy has found limited applications and mainly for Mn (I)-carbonyl derivatives,¹⁵⁹ owing to their potential use as CO-releasing molecules (CORMs). Moreover, both Mn(II) and Mn(III) ions are paramagnetic, thus preventing the direct detection of these nuclei in solution. On the other hand, their paramagnetism can be used to probe indirectly the active sites of metallobiomolecules via paramagnetic shifts and line broadening analysis.¹⁶⁰

Technetium

Isotope	A (%)	I	γ ($\times 10^7$ rad T ⁻¹ s ⁻¹)	Q (fm ²)	Relative receptivity to ¹³ C	Reference sample
⁹⁹ Tc ^a	"100" ^b	9/2	6.046	12.9	–	(NH ₄)TcO ₄ /D ₂ O (sat.)

^aRadioactive with a long half-life (2.1 × 10⁵ year, β⁻).

^bArtificially produced.

Technetium does not occur naturally on Earth and it was the first element to be produced artificially. ⁹⁹Tc is a β-emitting radionuclide with a long half-life (2.13 × 10⁵ years) and is generated as a by-product of nuclear power plants and atomic weapon

tests. Interest in technetium chemistry arises from the application in nuclear medicine. Radiopharmaceuticals containing ^{99m}Tc linked to a variety of carrier biomolecules are in clinical use.^{79b} Therefore, such extensive use of this radionuclide in medicine calls for more detailed structural information to design more effective and selective radiopharmaceuticals.

^{99}Tc chemical shifts and linewidths may provide insights into technetium oxidation states and into the composition and structure of its derivatives. The ^{99}Tc nuclide is extremely convenient for NMR spectroscopy due to its high receptivity and to the 100% abundance. Although ^{99}Tc has a significant quadrupole moment, the effect of line broadening in solution is attenuated by a large spin. In fact, its resonances are among the narrowest for quadrupolar nuclei. However, due to the presence of unpaired electrons in Tc(II), Tc(IV), and Tc(VI) compounds, the metal cannot be detected directly by ^{99}Tc NMR spectroscopy. A review on ^{99}Tc NMR spectroscopy has been published in 2005¹⁶¹ and, although this technique has not been used yet to specifically investigate the behavior of technetium in biological systems, the reported examples show that ^{99}Tc NMR can be successfully used in studying both complex formation and the kinetics of reactions in solution.

d-Block: Group 8 (Fe, Ru, and Os)

Iron

Isotope	A (%)	I	γ ($\times 10^7 \text{ rad T}^{-1} \text{ s}^{-1}$)	Q (fm^2)	Relative receptivity to ^{13}C	Reference sample
^{57}Fe	2.12	1/2	0.868	–	0.004	$[\text{Fe}(\text{CO})_5]/\text{C}_6\text{D}_6$ (80%)

Iron is the fourth most abundant element in the Earth's crust, but only a trace element in biological systems, making up only 0.004% of the body's mass. Yet, it is an essential component or cofactor of numerous metabolic reactions. Approximately 70% of this iron in man is contained in hemoglobin, and the remaining 30% is stored in the bone marrow, spleen, liver, and muscles. Myoglobin and enzymes contain about 15% of the iron, and ferritin almost as much (14%), whereas only about 1% is in transit in serum. Iron distribution is heavily regulated in mammals and a major component of this regulation is the protein transferrin, which binds iron absorbed from the duodenum and carries it in the blood to cells. Biologically relevant iron may exist in low- and high-spin configurations in both +2 and +3 oxidation states. The energy difference between the two spin configurations for given oxidation state can be very small, accounting for the facile interconversion and the subsequent important biochemical implications.²¹

Despite the importance of iron in biological chemistry, only limited studies of Fe NMR have been reported. ^{57}Fe , the only isotope of iron suitable for NMR study, has favorable $I = 1/2$ nuclear spin but also a very low sensitivity when investigated at natural abundance. Fe(III) and high-spin Fe(II) centers are paramagnetic, so the diamagnetic low-spin ferrous ion $^{57}\text{Fe}^{2+}$ is the only NMR-observable iron isotope. However, use of ^{57}Fe -enriched material and high fields combined with the very large chemical shift range have yielded useful information especially about heme proteins. Ferrocenes and porphyrins have been used as model compounds to obtain chemical shift data and to provide insights into the relaxation mechanisms.¹⁶² ^{57}Fe NMR spectra are available for myoglobins and cytochrome *c* (Fig. 17),¹⁶³ and, in general, ^{57}Fe NMR proved powerful to probe iron–ligand interactions in these proteins, particularly for porphyrin derivatives.^{162a,164}

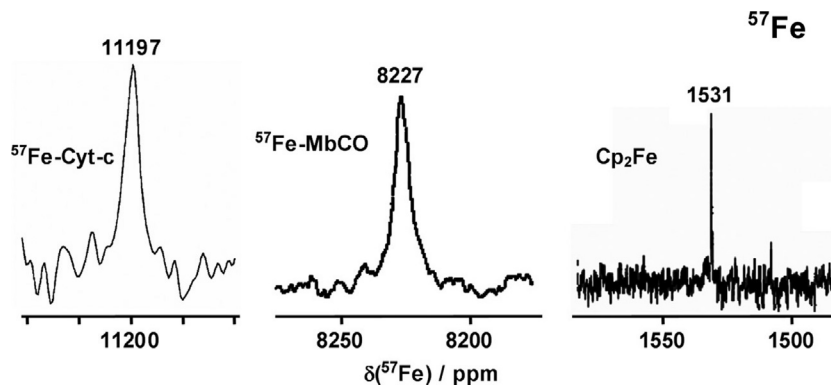


Fig. 17 ^{57}Fe NMR spectra (referenced to external $[\text{Fe}(\text{CO})_5]$ at 0.0 ppm) of ^{57}Fe -cytochrome *c* (^{57}Fe -Cyt *c*, 3 mM in 50 mM phosphate buffer, pH 7.0, 298 K), ^{57}Fe -carbonmonoxymyoglobin (^{57}Fe -MbCO, 15 mM in 50 mM phosphate buffer, pH 7.1, 296 K), and ferrocene (Cp_2Fe , 0.8 M in C_6H_6). Adapted from Ronconi, L.; Sadler, P. J. *Coord. Chem. Rev.* **2008**, *252*, 2239–2277, with permission.

Ruthenium and osmium

Isotope	A (%)	I	γ ($\times 10^7 \text{ rad T}^{-1} \text{ s}^{-1}$)	Q (fm^2)	Relative receptivity to ^{13}C	Reference sample
^{99}Ru	12.76	5/2	-1.229	7.9	0.848	$\text{K}_4[\text{Ru}(\text{CN})_6]/\text{D}_2\text{O}$ (0.3 M)
^{101}Ru	17.06	5/2	-1.377	45.7	1.59	
^{187}Os	1.96	1/2	0.619	-	0.001	$\text{OsO}_4/\text{CCl}_4$ (0.98 M)
^{189}Os	16.15	3/2	2.107	85.6	2.32	

Both ruthenium and osmium have no known natural biological function. However, during the last decades, ruthenium and osmium complexes have aroused great interest for their potential use as anticancer agents. Two Ru(III) complexes, namely, *trans*-[RuCl₄(Im)(DMSO)]ImH (NAMI-A) and *trans*-[RuCl₄(Ind)₂]IndH (KP1019), are currently undergoing phases I and II clinical trials, respectively, thus boosting the development of other ruthenium-based metallopharmaceuticals.¹⁶⁵ In this regard, also the activity of Ru(II) complexes is currently being explored. In particular, since arenes are known to stabilize ruthenium in the +2 oxidation state, the potential of Ru(II)-(η^6 -arene) derivatives as anticancer agents is under investigation.¹⁶⁶ Additionally, owing to the strict similarity with Ru(II), the design of Os(II)-(η^6 -arene) chemotherapeutics has been also taken into account.¹⁶⁷

Among the two quadrupolar ruthenium NMR-active isotopes, despite the slightly lower natural abundance, ^{99}Ru nuclide is favored for NMR spectroscopy due to the smaller quadrupole moment. Anyway, a major issue of ^{99}Ru NMR is the low resonance frequency, resulting in acoustic ringing that causes distorted baselines. Very little is known about the dependence of $\delta(^{99}\text{Ru})$ on structure and temperature; thus, it is not surprising that few ^{99}Ru NMR spectroscopic studies have been reported.¹⁶⁸ In addition, due to the presence of unpaired electrons, Ru(III) compounds cannot be directly detected by ^{99}Ru NMR spectroscopy, so ^{99}Ru (II) is the only NMR-observable ruthenium isotope. To date, ^{99}Ru NMR spectroscopy has been successfully employed for Ru(II) complexes having highly symmetrical environments around the metal nucleus.¹⁶⁹

Like ruthenium, also for osmium only one of its two magnetically receptive nuclei is useful for NMR measurements, the other possessing a large quadrupole moment. Nevertheless, although having $I = 1/2$, the ^{187}Os nuclide has very low natural abundance of only 1.96% and is the most insensitive nucleus in the periodic table, making its observation by conventional NMR techniques extremely difficult. In fact, for many years, the only known chemical shift was that of the reference compound OsO₄.¹⁷⁰ However, the advent of polarization transfer techniques, which require a nonzero scalar $^nJ(\text{M}-\text{X})$ coupling, has improved the detection of low- γ nonquadrupolar nuclei. ^{187}Os NMR data have been reported for some Os(II)-(η^6 -arene) and sandwich-type complexes, using inverse 2D [^{31}P , ^{187}Os] and [^1H , ^{187}Os] NMR spectroscopy,¹⁷¹ showing the potential of this technique.

d-Block: Group 9 (Co and Rh)**Cobalt and rhodium**

Isotope	A (%)	I	γ ($\times 10^7 \text{ rad T}^{-1} \text{ s}^{-1}$)	Q (fm^2)	Relative receptivity to ^{13}C	Reference sample
^{59}Co	100	7/2	6.332	42.0	1640	$\text{K}_3[\text{Co}(\text{CN})_6]/\text{D}_2\text{O}$ (0.56 M)
^{103}Rh	100	1/2	-0.847	-	0.186	$[\text{Rh}(\text{acac})_3]/\text{CDCl}_3$ (sat.)

Despite the low biological abundance, cobalt plays a unique role in the metabolism of several living organisms. Cobalt derivatives contain the metal ion in the oxidation states +1, +2, and +3. A major acknowledged biological role of cobalt is its participation in the vitamin B₁₂ family of compounds, whose active forms are responsible for catalyzing a wide variety of processes related to nucleic acid, protein, and lipid syntheses and for maintaining the normal function of epithelial and nervous cells. Cobalamins also stand out as nature's most complex nonpolymeric structures and the first discovered biomolecule containing a metal-carbon bond. In addition to vitamin B₁₂ and its derivatives, several different types of cobalt-containing enzymes have been also identified.¹⁷²

The NMR detection of ^{59}Co nucleus should be, in principle, easy. It is 100% naturally abundant, it possesses a relatively high magnetogyric ratio and, owing to the magnetic mixing of its occupied and excited d orbitals, it may experience substantial paramagnetic deshieldings that can reveal even subtle changes in chemical environments. On the other hand, the $I = 7/2$ is associated with a quadrupole moment that provides an efficient relaxation mechanism, thus leading to broadened resonances in solution.¹⁷³ ^{59}Co NMR spectroscopy has been used to study naturally occurring cobalamins. Targets of these investigations included vitamin B₁₂, B₁₂ coenzyme (adenosylcobalamin), methylcobalamin, and dicyanocobyrinic acid heptamethylester.¹⁷⁴ Illustrative ^{59}Co NMR spectra are shown in Fig. 18. Solid-state ^{59}Co NMR spectroscopy was used in similar studies and, owing to a favorable combination of different factors, the resulting spectra were of much higher quality than their solution counterparts.¹⁷⁴ Solid-state ^{59}Co NMR spectroscopy has been successfully employed also to study a single crystal of vitamin B₁₂ and in the analysis of vitamin B₁₂ in its different polymorphic forms.¹⁷⁵

In contrast to cobalt, rhodium has no known biological function. Recently, rhodium complexes have been investigated for their possible applications in medicine as antitumor, antibacterial, and antiparasitic agents.¹⁷⁶ As a monoisotopic nonquadrupolar species with a wide chemical shift range, the ^{103}Rh nucleus is attractive for NMR studies. Unfortunately, low receptivity, negative

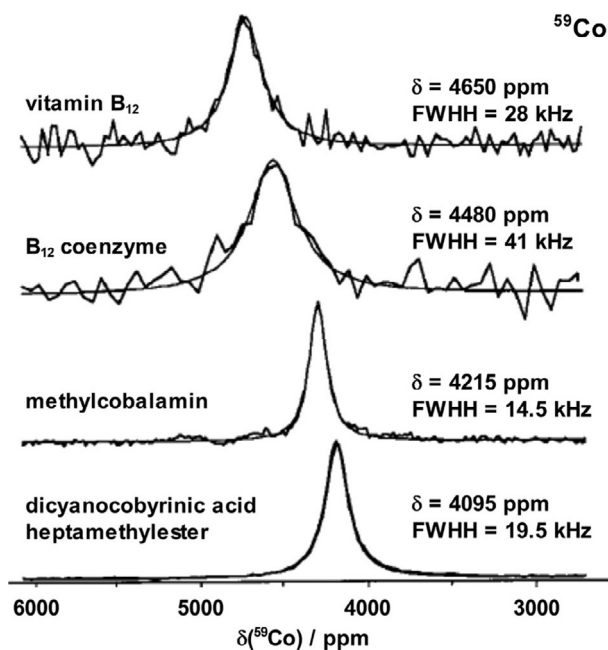


Fig. 18 ^{59}Co NMR spectra of natural B_{12} derivatives in solution (externally referenced to 1 M aqueous $[\text{Co}(\text{NH}_3)_6]\text{Cl}_3$ and subsequently converted to ppm downfield from 1 M aqueous $\text{K}_3[\text{Co}(\text{CN})_6]$ for the sake of literature consistency). Superimposed on the experimental traces are best Lorentzian fits characterized by the isotropic shift δ and full-width-at-half-height (FWHH) values indicated on the right. Adapted from Medek, A.; Frydman, V.; Frydman, L. *Proc. Natl. Acad. Sci. U.S.A.* **1997**, *94*, 14237–14242, with permission.

magnetogyric ratio, and very long relaxation times (>50 s) are major drawbacks. A recent survey of ^{103}Rh NMR spectroscopy has been published,¹⁷⁷ but, to the best of our knowledge, no studies of biological relevance have been reported.

d-Block: Group 10 (Ni, Pd, and Pt)

Nickel and palladium

Isotope	A (%)	I	γ ($\times 10^7 \text{ rad T}^{-1} \text{ s}^{-1}$)	Q (fm^2)	Relative receptivity to ^{13}C	Reference sample
^{61}Ni	1.14	3/2	-2.395	16.2	0.240	$[\text{Ni}(\text{CO})_4]/\text{C}_6\text{D}_6$ (80%)
^{105}Pd	22.33	5/2	-1.23	66.0	1.49	$\text{K}_2[\text{PdCl}_6]/\text{D}_2\text{O}$ (sat.)

Often found in the +2 oxidation state, nickel in biological systems plays a role acknowledged only since 1975, when urease was shown to be a nickel enzyme. Since then, other nickel-containing enzymes have been discovered in bacteria and/or Archaea, including hydrogenase, methyl-S-coenzyme-M-reductase, carbon monoxide dehydrogenase, nickel superoxide dismutase, glyoxylase I, and a putative nickel *cis-trans* isomerase.¹⁷⁸

^{61}Ni is the only naturally occurring NMR-active isotope of nickel. It is a quadrupolar nucleus characterized by low sensitivity to detection by NMR and low natural abundance. The ^{61}Ni chemical shifts of several Ni(0) organometallic derivatives have been recently reported,¹⁷⁹ whereas octahedral and tetrahedral Ni(II) derivatives cannot be studied directly by NMR because they are paramagnetic.

Palladium is a nonessential element for life. Pharmaceutical interest in Pd(II) compounds is driven by analogy to antitumor Pt(II) complexes (see text later) and antiviral, antifungal, and antimicrobial metalloterapeutics.¹⁸⁰

Palladium has one naturally occurring NMR-active isotope, ^{105}Pd . Although it has high natural abundance, this quadrupolar nucleus is characterized by a low sensitivity to detection by NMR, low resonance frequency, and extremely fast relaxation times ($<10^{-5}$ s). As far as we are aware of, no ^{105}Pd NMR studies in solution of biological relevance have been reported.

Platinum

Isotope	A (%)	I	γ ($\times 10^7 \text{ rad T}^{-1} \text{ s}^{-1}$)	Q (fm^2)	Relative receptivity to ^{13}C	Reference sample
^{195}Pt	33.83	1/2	5.839	–	20.7	$\text{Na}_2[\text{PtCl}_6]/\text{D}_2\text{O}$ (1.2 M)

Platinum is a relatively inert metal and has no natural biological role. Nevertheless, platinum complexes are now among the most widely used drugs for the treatment of cancer.¹⁸¹

Table 5 ^{195}Pt chemical shifts of platinum antitumor complexes and adducts with different donor atoms

Complex	δ (^{195}Pt) (ppm)
cis-Pt(II) complexes	
<i>cis</i> -[PtCl ₂ (NH ₃) ₂] (cisplatin)	-2149
[Pt(CBDCA- <i>O,O</i>)(NH ₃) ₂] (carboplatin)	-1705/-1715 (in vivo)
<i>cis</i> -[Pt(NH ₃) ₂ (O) ₂]	-1460 to -1590
<i>cis</i> -[Pt(NH ₃) ₂ Cl(O)]	-1806 to -1841
<i>cis</i> -[Pt(NH ₃) ₂ (N)(O)]	-2067 to -2147
<i>cis</i> -[Pt(NH ₃) ₂ Cl(N)]	-2295 to -2369
<i>cis</i> -[Pt(NH ₃) ₂ (N) ₂]	-2434 to -2660
<i>cis</i> -[Pt(NH ₃) ₂ (O)(S)]	-2618 to -2800
<i>cis</i> -[Pt(NH ₃) ₂ (N)(S)]	-2800 to -3218
<i>cis</i> -[Pt(NH ₃) ₂ (S) ₂]	-3200 to -3685
<i>cis</i> -[Pt(NH ₃) ₂ Cl(DMSO)] ⁺	-3120 to -3145
[PtCl(N)(DACH)]	-2514 to -2579
trans-Pt(II) complexes	
<i>trans</i> -[PtCl ₂ (NH ₃) ₂] (transplatin)	-2101
<i>trans</i> -[Pt(GS) ₂ (NH ₃) ₂]	-3226
[[<i>trans</i> -Pt(GS)(NH ₃) ₂] ₂ - μ -GS]	-3186
(1,1/ <i>t,t</i>) ^a	-2437
<i>trans</i> -[Pt(NH ₃) ₂ (NH ₂ R)(S)]	-2977 to -2987
<i>trans</i> -[Pt(NH ₃) ₂ (NH ₂ R)(N)]	-2568 to -2573
BBR3464 ^b	-2417 (PtN ₃ Cl)/-2648 (PtN ₄)
Pt(IV) complexes	
<i>cis</i> -[Pt(NH ₃) ₂ Cl ₄]	-145
<i>cis</i> -[Pt(NH ₃) ₂ Cl ₂ (OH) ₂]	+860
<i>trans</i> -[Pt(DACH)(OH) ₂ Cl(N)]	+784 to +563
<i>trans</i> -[Pt(DACH)(AcO) ₂ Cl(N)]	+875 to +739

^a[[*trans*-PtCl(NH₃)₂]₂(μ -NH₂(CH₂)₆NH₂)₂]²⁺.

^b[[*trans*-PtCl(NH₃)₂]₂(μ -*trans*-Pt(NH₃)₂(NH₂(CH₂)₆NH₂)₂)⁴⁺ (1,0,1/*t,t,t*).

Adapted from Berners-Price, S. J.; Ronconi, L.; Sadler, P. J. *Prog. Nucl. Magn. Reson. Spectrosc.* **2006**, *49*, 65–98, with permission.

NMR methods proved useful in the investigation of platinum drugs from the time that cisplatin was first introduced into the clinic over 40 years ago. ^{195}Pt is a reasonably sensitive nucleus for NMR detection having high natural abundance and relative receptivity. However, the detection limit in the millimolar range makes the observation of natural abundance ^{195}Pt signals in physiological fluids rather difficult, although Bachert and coworkers successfully used in vivo ^{195}Pt NMR (at 2.0 T) in rats to monitor local disposition kinetics of carboplatin in intact tissue following a subcutaneous injection.¹⁸²

An attractive feature of ^{195}Pt NMR for studies of platinum anticancer drugs is the very large chemical shift range, which allows ready differentiation between Pt(II) and Pt(IV), having chemical shifts at the high-field and low-field ends of the range, respectively. The resonances for square planar Pt(II) complexes span some 4000 ppm and ligand substitutions produce predictable chemical shift ranges. The ^{195}Pt chemical shifts of some platinum antitumor complexes and various adducts are listed in Table 5 with the ^{195}Pt chemical shift ranges illustrated pictorially in Fig. 19.

Both 1D ^{195}Pt and 2D [¹H, ¹⁵N] NMR techniques have been providing a major contribution in the understanding of the molecular mechanism of action of platinum-based anticancer drugs, including kinetic studies on the interaction with biomolecules by using ^{195}Pt isotopically enriched platinum complexes. The overall topic has been extensively reviewed elsewhere.^{79,183}

Moreover, the use of state-of-the-art computational methods, allowed the prediction of ^{195}Pt NMR chemical shifts for a number of Pt(II) and Pt(IV) cytotoxic agents, and the subsequent use of ^{195}Pt NMR parameters to generate reliable quantitative structure-activity relationship (QSAR) models for platinum-based antitumor compounds.¹⁸⁴

Notwithstanding ^{195}Pt NMR is commonly used as a routine analytical tool to characterize novel platinum anticancer agents, recent papers also reported on its use to probe platinum binding to glutathione and plasma,^{185a} to DNA^{185b,185c} and the HIV NCP7 protein,^{185d} and even the release of cisplatin encapsulated into carbon nanotubes as drug delivery systems.^{185e}

d-Block: Group 11 (Cu, Ag, and Au)

Copper

Isotope	A (%)	I	γ ($\times 10^7 \text{ rad T}^{-1} \text{ s}^{-1}$)	Q (fm^2)	Relative receptivity to ^{13}C	Reference sample
⁶³ Cu	69.17	3/2	7.112	-22.0	382	[Cu(CH ₃ CN) ₄](ClO ₄)/CD ₃ CN (sat.)
⁶⁵ Cu	30.83	3/2	7.604	-20.4	208	

Copper is the third most abundant transition metal element in biological systems after iron and zinc. The bioinorganic chemistry of copper is dominated by +1 and +2 oxidation states. Almost all of the copper in the human body is bound to transport proteins

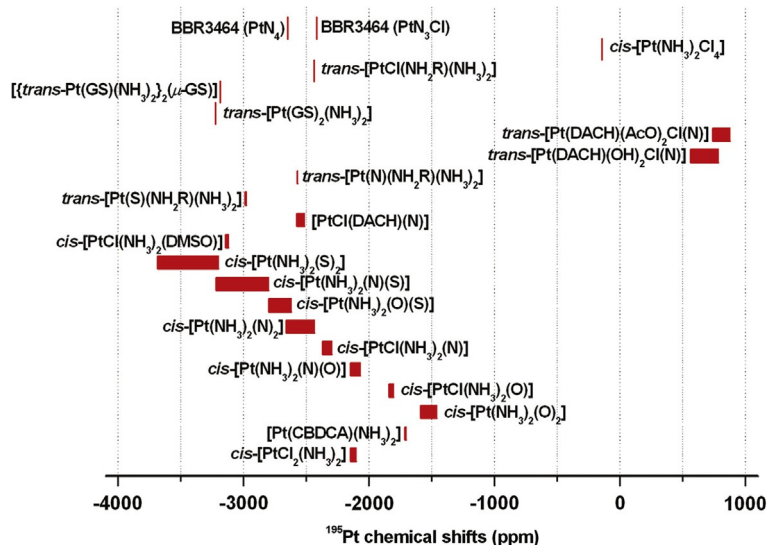


Fig. 19 ^{195}Pt chemical shifts ranges for diam(m)ino platinum antitumor complexes. Adapted from Berners-Price, S. J.; Ronconi, L.; Sadler, P. J. *Prog. Nucl. Magn. Reson. Spectrosc.* **2006**, *49*, 65–98, with permission.

(ceruloplasmin and copper–albumin), storage proteins (metallothioneins), or copper-containing enzymes, whereas unbound free copper is not found in large quantities. Copper is essential for the proper functioning of copper-dependent enzymes, including cytochrome *c* oxidase (energy production), superoxide dismutase (antioxidant protection), tyrosinase (pigmentation), dopamine hydroxylase (catecholamine production), lysyl oxidase (collagen and elastin formation), clotting factor V (blood clotting), and ceruloplasmin (antioxidant protection, iron metabolism, and copper transport). In addition to its enzymatic roles, copper is used for biological electron transport. The “blue copper” proteins (named after their intense blue color arising from a ligand-to-metal charge-transfer absorption band at ~ 600 nm) that participate in electron transport include azurin and plastocyanin.²¹ Copper is a redox active nucleus and may be also involved in the formation of reactive oxygen species. In this regard, the interaction of copper complexes with nucleic acids and their capability to damage DNA have been investigated.¹⁸⁶ In addition, some artificial DNA enzymes were shown to have Cu^{2+} -dependent activity.¹⁸⁷ Finally, some copper complexes are currently being investigated for their potential anticancer and anti-inflammatory activity.¹⁸⁸

The NMR-active copper isotopes ^{63}Cu and ^{65}Cu are quadrupolar and couple strongly to local EFGs. Since the quadrupole moments cause a significant line broadening when the charge is unevenly distributed, only copper derivatives with regular tetrahedral or cubic symmetry may be observable by direct NMR detection.¹⁸⁹ ^{63}Cu is by far most used in copper NMR spectroscopy because of both the higher receptivity and natural abundance compared to ^{65}Cu .

For the past decades, the structures, electronic states, and reactivity of Cu(II) complexes have been widely investigated by various spectroscopic methods, such as UV–vis, Raman, and electron paramagnetic resonance spectroscopy because of their characteristic absorptions resulting from d–d transitions, ligand-to-metal charge transfers, and unpaired electrons on the copper(II) ion. On the other hand, these analytic techniques have not been applied extensively to Cu(I) derivatives because of featureless spectroscopic properties resulting from the closed shell d^{10} electron configuration. For diamagnetic Cu(I) complexes, ^{63}Cu NMR spectroscopy appears to have the greatest potential for characterizing their structures and electronic states, because most Cu(I) complexes prefer a tetrahedral configuration, thus giving rise to relatively sharp resonance lines,¹⁹⁰ whereas the paramagnetism of Cu(II) center prevents its detection by ^{63}Cu NMR spectroscopy.

Silver and gold

Isotope	A (%)	I	γ ($\times 10^7$ rad T^{-1} s $^{-1}$)	Q (fm^2)	Relative receptivity to ^{13}C	Reference sample
^{107}Ag	51.84	1/2	−1.089	–	0.205	$\text{AgNO}_3/\text{D}_2\text{O}$ (sat.)
^{109}Ag	48.16	1/2	−1.252	–	0.290	
^{197}Au	100	3/2	0.473	54.7	0.162	–

Both silver and gold have no known natural biological role in humans, but interest in the medicinal applications of silver and gold derivatives has increased in recent years. Historical treatments with Ag(I) salts as antiseptic agents are well documented. Although the introduction of modern antibiotics greatly reduced their use in antimicrobial drugs, the increasing development of bacterial resistance toward antibiotics currently marketed has renewed the interest in novel and more efficient silver-based

antimicrobial agents.¹⁹¹ Chrysotherapy (i.e., the therapeutic use of gold compounds) has been established for centuries for the treatment of rheumatoid arthritis, owing to the known immunosuppressive and anti-inflammatory properties of some gold salts. In particular, late-stage disease was treated with various Au(I) drugs, such as solganal, myocrisin, sanocrysin, allocrysin, and auranofin, and some are still in clinical use.¹⁹² In addition, both Au(I) and Au(III) derivatives are emerging as a new class of metal-based anticancer agents.¹⁹³

All naturally occurring silver is found in two NMR-active isotopic forms, ^{107}Ag and ^{109}Ag , both having $I = 1/2$. Despite its lower natural abundance, ^{109}Ag is normally preferred for NMR studies because of the slightly higher sensitivity. Difficulties in obtaining ^{109}Ag NMR spectra with good signal-to-noise ratio are due to the extremely long T_1 and relatively poor receptivity, both stemming from the very low γ . ^{109}Ag chemical shift is strongly affected by several factors, including the type and number of coordinating atoms, the number of bridging versus terminal donor atoms, bond distances and bond angles, the solvent and the nature of the counterion, and also the concentration. For example, the ^{109}Ag chemical shift differs from about 50 ppm for 1 and 9 M (nearly saturated) AgNO_3 aqueous solutions,¹⁹⁴ and since aqueous AgNO_3 is frequently used as reference and often its concentration is not stated, this makes the direct comparison of ^{109}Ag NMR chemical shifts reported in the literature rather difficult.

Notwithstanding all the limitations, ^{109}Ag NMR spectroscopy is a potentially useful tool to characterize silver-containing compounds since both the chemical shifts and the coupling constants are very sensitive to the coordination geometry of the Ag(I) center.¹⁹⁵ For example, ^{109}Ag NMR spectroscopy was successfully employed to characterize silver-based antimicrobial and antifungal agents¹⁹⁶ and to investigate the solution behavior of the anticancer agent $[\text{Ag}(\text{d}2\text{pype})_2]\text{NO}_3$ ($\text{d}2\text{pype} = 1,2$ -bis (di-2-pyridylphosphino)ethane), the latter by exploiting 2D [^{31}P , ^{109}Ag] HMQC technique.¹⁹⁷

NMR spectroscopy occupies a major role in probing protein metal-binding sites where the native quadrupolar metal ions, for example, Zn(II), Ca(II), Fe(II), Mg(II), Cu(II), and Cu(I), can be replaced by $I = 1/2$ metal isotopes. In spite of the attractiveness of Ag(I) as a redox stable analog for Cu(I), ^{109}Ag NMR has so far found limited applications in biological systems due to the poor sensitivity of the nucleus, thus making direct detection impractical for most biological systems. Relatively few biologically relevant examples have been reported to date,¹⁹⁸ and the only known metalloprotein studied by 2D [^1H , ^{109}Ag] HMQC spectroscopy to date is the ^{109}Ag -substituted yeast metallothionein (Fig. 20).¹⁹⁹

Since the interaction between Ag(I) ions and cysteine-rich proteins seems to play a key role in bacterial inactivation, an in-depth investigation of the behavior of Ag(I) in the presence of cysteine, GSH, and penicillamine was carried out by means of ^{109}Ag NMR spectroscopy, demonstrating the strong tendency of the thiolate sulfur atoms to form bridges between silver ions.²⁰⁰

Ag(I) may be also used to induce metal-mediated base pairs in nucleic acids, that is, two opposite nucleobases (either artificial or natural) coordinated to a metal ion incorporated in the core of the helix. Nucleic acids have interesting applications in nanotechnology, their potential relying on their iterative structural motifs and self-assembly properties, together with the possibility to incorporate specific nucleosides designed on purpose. Modified nucleic acids resulting from the site-specific incorporation of metal ions may be exploited as nanomaterials, for example, by increasing the conductive properties of the natural analogues.²⁰¹ In this regard, a recent paper reports on the use of the NMR properties of silver to confirm the incorporation of Ag(I) ions in a DNA duplex bearing three imidazole (Im) moieties by forming stable $\text{Im-Ag}^+-\text{Im}$ base pairs. Intriguingly, although no ^{109}Ag signal could be detected in the [^1H , ^{109}Ag] HMQC spectrum, a direct coupling between silver and the coordinated Im nitrogen atoms was observed, thus confirming the occurrence of a strong binding of Ag(I) ions to the artificial nucleobases.²⁰²

Similarly, ^{109}Ag NMR (in conjunction with DFT calculations) confirmed the formation of the Ag^+ -mediated cytosine-cytosine base pair within a DNA duplex in solution.²⁰³ In fact, the ^{109}Ag chemical shift recorded at 442 ppm, together with the observation of

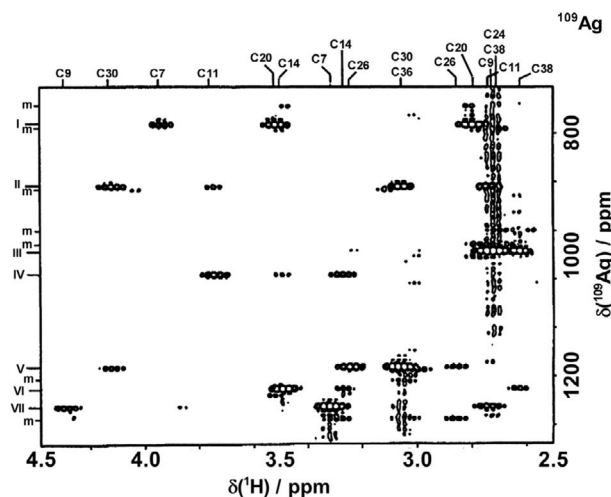


Fig. 20 2D [^1H , ^{109}Ag] HMQC spectrum (referenced to external 1 M AgNO_3 at 0.0 ppm) of yeast ^{109}Ag -metallothionein (6 mM in 18 mM phosphate buffer in D_2O , pD 6.5, 298 K). The spectrum shows the connectivity of all seven silver atoms with the cysteine H_β protons of the yeast Ag-metallothionein. Adapted from Narula, S. S.; Mehra, R. K.; Winge, D. R.; Armitage, I. M. *J. Am. Chem. Soc.* **1991**, *113*, 9354–9358, with permission.

$^1J(^{15}\text{N}, ^{109}\text{Ag}) = 83$ and 84 Hz, supported the presence of $\text{N}^3\text{-Ag}^+\text{-N}^3$ linkages within two opposed cytosines, and allowed the full 3D NMR structure the Ag^+ -DNA adduct to be obtained.

Naturally occurring gold has a single isotope, ^{197}Au , characterized by a large quadrupole moment. As a result of fast quadrupole relaxation, the resonances are extremely broad and weak. Due to the low NMR receptivity of ^{197}Au combined with the fast relaxation, no NMR studies of gold have been reported in the literature to date.²⁰⁴

d-Block: Group 12 (Zn, Cd, and Hg)

Zinc

Isotope	A (%)	I	γ ($\times 10^7 \text{ rad T}^{-1} \text{ s}^{-1}$)	Q (fm^2)	Relative receptivity to ^{13}C	Reference sample
^{67}Zn	4.10	5/2	1.677	15.0	0.692	$\text{Zn}(\text{NO}_3)_2/\text{D}_2\text{O}$ (sat.)

Zinc is an essential element in humans and, under physiological conditions, exists in the +2 oxidation state. It has catalytic, structural, or regulatory functions in more than 200 zinc metalloenzymes, and it is estimated that around 3000 proteins in the human body contain zinc prosthetic groups. In particular, zinc plays a structural role in the formation of the so-called zinc fingers, proteins exploited by transcription factors for interacting with DNA and regulating gene activity. Another function of zinc is in the maintenance of the integrity of biological membranes resulting in their protection against oxidative injury. In addition, there are over a dozen types of cells in the human body that secrete zinc ions, and the consequences of these secreted zinc signals in medicine and health are now being actively studied. Over 95% of the total body zinc is bound to proteins within cells and cell membranes. Most of the zinc in blood is found in the RBC bound to the metalloenzyme carbonic anhydrase, whereas plasma contains only 0.1% of the total zinc (of which approximately 18% bound to α_2 -macroglobulin, 80% to albumin, and 2% to such proteins as transferrin and ceruloplasmin).²¹

^{67}Zn , the only naturally occurring NMR-active isotope of zinc, has $I = 5/2$ and a large quadrupole moment responsible for high relaxation rates. This quadrupolar nucleus is characterized by low sensitivity and low resonance frequency. The required concentration for Zn^{2+} to be detected by NMR is typically high (>0.1 M) but lower concentrations can be utilized following isotopic enrichment. Anyway, due to the quadrupolar nature of the nuclide, even if solution NMR methods afforded observable zinc resonances in a metalloprotein, the resulting linewidths would likely obscure the determination of site-specific isotropic chemical shifts. Consequently, it is not surprising that the literature of ^{67}Zn NMR data in solution is scarce and, among those reports, only a very few are biologically relevant. In this regard, ^{67}Zn NMR has been used to study the environment and/or behavior of Zn^{2+} interacting with proteins, such as concanavalin, calmodulin, thermolysin, and S100.²⁰⁵

Given the unfavorable NMR properties of ^{67}Zn , the method of choice for the study of zinc in biological systems in solution remains its replacement with ^{113}Cd (see succeeding text). On the other hand, the exploitation of solid-state techniques may represent a reliable alternative. Historically, solid-state ^{67}Zn NMR spectroscopy has been undesirable due to broad quadrupolar lineshapes and low sensitivity. In recent years, however, dramatic improvements in the solid-state NMR of quadrupolar nuclides have occurred. A general strategy for the observation of low- γ half-integer quadrupolar nuclides has been developed, involving a combination of low temperature (4–100 K) with cross-polarization experiments employing specific spin-echo sequences.²⁰⁶ Nevertheless, although such methodology affords sufficient sensitivity to examine Zn^{2+} -binding sites, as far as we are aware of, still few reports are available to date in the literature describing the use of solid-state ^{67}Zn NMR for the study of zinc in metalloproteins or in zinc complexes as models for active sites of metalloproteins.²⁰⁷

Cadmium

Isotope	A (%)	I	γ ($\times 10^7 \text{ rad T}^{-1} \text{ s}^{-1}$)	Q (fm^2)	Relative receptivity to ^{13}C	Reference sample
^{111}Cd	12.80	1/2	-5.968	-	7.27	$\text{Cd}(\text{CH}_3)_2/\text{neat}$
$^{113}\text{Cd}^a$	12.22	1/2	-5.961	-	7.94	32

^aRadioactive with a long half-life (7.61×10^{15} year, β^-)

Cadmium belongs to a category of heavy metal ions that have increasingly attracted attention over the years, due to their toxic effect toward the environment and various living organisms, including man.²⁰⁸ Although nonessential in the human physiology, Cd(II) is largely associated with Zn(II), and Cd/Zn competition in binding to biomolecules is associated with cadmium-related toxicity.²¹

In spite of the similar magnetic properties and natural occurrence of the two $I = 1/2$ cadmium isotopes, the large majority of the biological NMR studies have used ^{113}Cd due to its slightly higher relative sensitivity compared to ^{111}Cd .²⁰⁹ The sensitivity of ^{113}Cd at natural abundance is about eight times that of ^{13}C , putting it on the fringe of accessibility for biological applications using modern high-field spectrometers. However, an approximate eightfold enhancement can be obtained by using ^{113}Cd -enriched

starting materials, thus allowing reasonable quality spectra to be acquired, for example, on as little as 0.5 mM of a ^{113}Cd -substituted protein sample in a few hours of data accumulation.

The adaptable ligand coordination number and geometry of Cd(II) are the most commonly cited reasons why cadmium can be used to replace an extensive range of biologically relevant metal ions and mimic essential elements such as Zn(II) and Cu(II) in metallothioneins and the natural cofactor Mg(II) in nucleic acids.

Metallothioneins (MTs) are small cysteine-rich proteins that are present in several living organisms, including vertebrate, bacteria, fungi, and plants. Due to the high content of cysteines, they bind preferentially soft metal ions, forming metal–thiolate clusters. In particular, they show high affinity toward the toxic metal ions Zn(II), Cu(I), Cd(II), and Hg(II) and are believed to be involved in metal detoxification. The suitable NMR properties of ^{113}Cd make it a reliable probe to study these metal cluster arrangements. In particular, it can be used to mimic the tetrahedral coordination geometry of Zn(II), whose NMR properties are less favorable (see earlier text).^{6b}

^{113}Cd chemical shifts span a 900 ppm range and are extremely sensitive to number, nature, and coordination geometry of the ligands, as clearly summarized in Fig. 21. Remarkably, the broad chemical shift dispersion of the ^{113}Cd resonances allows to not only provide information about the ligand type(s) at a particular metal site but also assess the selectivity in the presence of multiple metal-binding sites with identical ligand coordination.

Owing to the capability of the Cd^{2+} ion to replace a number of metal ions in a variety of metalloproteins and to the sensitivity of the ^{113}Cd resonances to changes in the chemical environment around the metal center, ^{113}Cd NMR spectroscopy is regarded as a powerful and straightforward method to identify the metal-binding sites and to define the coordination geometry. In this regard, a number of data have been reported providing insights into cadmium coordination in metalloproteins,²¹⁰ in protein active core model compounds,²¹¹ and in de novo designed metalloproteins and polypeptides.²¹²

Cd(II) is regarded as “softer” than Mg(II) and it is normally used in thio-rescue experiments to identify metal ion-binding sites within large RNAs⁴⁷ and, owing to its coordination properties, it can be used as mimic of Mg(II) to study its binding properties in

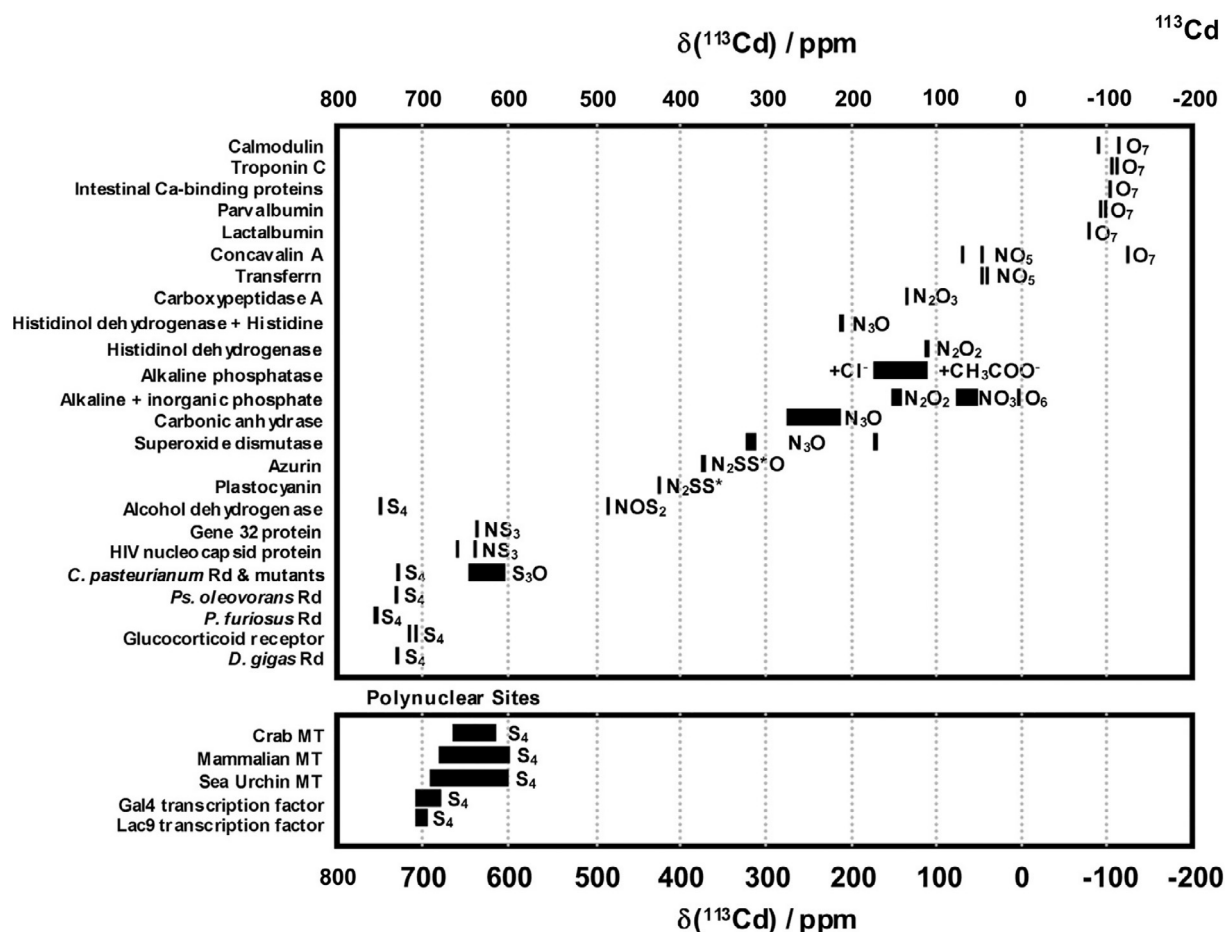


Fig. 21 Observed ^{113}Cd chemical shifts for structurally characterized ^{113}Cd -substituted mononuclear (top) and polynuclear (bottom) metalloproteins. All chemical shifts are relative to external aqueous 0.1 M $\text{Cd}(\text{ClO}_4)_2$. The chemical shift position is correlated to ligand composition, where S represents sulfur from cysteine, S represents sulfur from methionine, O represents oxygen from carboxylate or water, and N represents nitrogen from histidine. Adapted from Ronconi, L.; Sadler, P. J. *Coord. Chem. Rev.* **2008**, *252*, 2239–2277, with permission.

RNA–metal ion interactions.²¹³ Direct ¹¹³Cd NMR detection was used to study the interaction of Cd(II) with a small ribozyme. The addition of an excess of Cd(NO₃)₂ caused a downfield shift and broadening of ¹¹³Cd signal, indicating a fast exchange between free and bound cadmium.²¹⁴ Several papers report on the indirect observation of cadmium bound to RNA. For example, upon titration of a hammerhead ribozyme metal-binding site model with Cd(II), strong perturbations in ¹H, ¹³C, and ¹⁵N resonances were observed, in particular a strong upfield shift (c. 20 ppm) of a ¹⁵N signal, resulting from the direct coordination of Cd(II) to a specific guanine N (7). The authors also investigated the one-bond ¹¹³Cd–¹⁵N scalar coupling, but no coupling could be detected due to the fast exchange between free and bound Cd(II). Nevertheless, according to literature data, if the chemical exchange could be lowered down, a ¹J(¹¹³Cd,¹⁵N) coupling of 78–216 Hz should be observed in the NMR spectra.²¹⁵

¹¹³Cd chemical shifts are strongly influenced by the concentration and the nature of the counterion and care should be taken when choosing the Cd(II) salt to be used for titration studies. A detailed multinuclear NMR study of the CdCl₂–ATP and the Cd(CLO₄)₂–ATP systems as a function of pH has been reported, showing how the affinity of the counterion to Cd(II) influences the nature of cadmium–ATP interaction. In fact, the different behavior of Cd²⁺ and CdCl⁺ toward ATP has a direct strong effect also on the observed ¹¹³Cd resonances.²¹⁶

Mercury

Isotope	A (%)	I	γ ($\times 10^7$ rad T ⁻¹ s ⁻¹)	Q (fm ²)	Relative receptivity to ¹³ C	Reference sample
¹⁹⁹ Hg	16.87	1/2	4.846	–	5.89	Hg(CH ₃) ₂ /neat
²⁰¹ Hg	13.18	3/2	1.789	38.6	1.16	

Mercury has no known natural biological role. Hg(0) is volatile and relatively nontoxic, whereas Hg(II) is toxic to most living organisms because of its avid coordination to thiol groups within biological systems. Hg(II) is known to undergo biological methylation to methylmercury and dimethylmercury, both of which are extremely toxic to humans.²¹⁷

Mercury has two NMR-active isotopes, ¹⁹⁹Hg and ²⁰¹Hg, the latter being quadrupolar. The *I* = 1/2 nuclide ¹⁹⁹Hg has a chemical shift range of 2500 ppm and a relative sensitivity 5.9 times that of ¹³C, which should make it, at least in principle, an excellent probe for direct NMR detection of organomercury adducts, but its inherent insensitivity is a major drawback for biologically related studies. In fact, by means of conventional NMR direct detection techniques, including large (10–15 mm) sample tubes and long accumulation times, concentrations exceeding the solubility limits of most proteins and nucleic acids would be necessary to obtain reasonable ¹⁹⁹Hg NMR spectra. Consequently, a variety of indirect detection techniques have been devised to improve the observation of this insensitive nucleus,²¹⁸ together with the use of ¹⁹⁹Hg-enriched mercury precursors.

¹¹³Cd NMR is still the method of choice to probe metal-binding sites in metalloproteins (see preceding text) but ¹⁹⁹Hg NMR spectroscopy has been increasingly employed. In fact, although the number of applications where the Hg(II) ion can replace isostructurally the native metal ions is limited owing to the 1.10 Å ionic radius and the preference for either linear or trigonal coordination geometry, ¹⁹⁹Hg NMR spectra of ¹⁹⁹Hg-substituted metalloproteins, for example, carbonic anhydrase, azurin, plastocyanin, rusticyanin, rubredoxin, Gal4, MerR and MerP, and a number of mercury model complexes, have been reported.²¹⁹ Much of these data are a result of the studies of O'Halloran and coworkers and have revealed ¹⁹⁹Hg chemical shifts indicative of certain coordination environments. For example, two-coordinate aliphatic Hg(II) thiolates {HgS₂} show chemical shifts at c. –800 ppm, whereas the range for three-coordinate {HgS₃} species is reported to be from –80 to –160 ppm for the trigonalplanar geometry and around –360 ppm for the distorted trigonal one. The chemical shifts of Hg(II) bound to four cysteine thiolates {HgS₄} fall within the range –300 to –500 ppm, whereas coordination by four histidines {HgN₄} is observed at the other extreme of chemical shift at about –1200 ppm. In addition, ¹⁹⁹Hg exhibits scalar couplings to ¹H, ¹³C, and ¹⁵N that are slightly larger than those observed with ¹¹³Cd, thus allowing heteronuclear correlation experiments to be carried out to confirm the ligand type(s) and stoichiometry.

Recently, Pecoraro and coworkers extended such studies to probe the metal ion coordination in other native proteins and in *de novo* designed polypeptides.^{212b,220} For example, it was shown by ¹⁹⁹Hg NMR spectroscopy that at pH 7.5 Hg(II) is bound to a monomeric human copper chaperone (HAH1) as a two-coordinate linear complex {HgS₂}, whereas upon increasing the pH Hg²⁺ promotes HAH1 association, leading to formation of {HgS₃} and {HgS₄} complexes, which are in exchange on the μs–ns time scale.²²¹

¹⁹⁹Hg NMR spectroscopy was also shown to be a useful tool to assess the capability of different molecules to act as mercury detoxification agents. Recent reports include the formation of Hg(II) adducts with penicillamine in alkaline solution and with GSH at alkaline and physiological pH and with cysteine-containing pseudopeptides to be used as possible mercury-sequestering agents in water.²²²

Mercury can interact with nucleic acids, and the study of these interactions may shed light on the genotoxicity of this heavy metal. Several groups in the past used NMR spectroscopy to characterize mercury adducts with model nucleotides, polynucleotides, and oligonucleotides, but the effect of Hg(II) binding was probed only indirectly by evaluating its impact on ¹H, ¹³C, and ¹⁵N chemical shifts.²²³ On the other hand, ¹⁹⁹Hg NMR spectroscopy was used to follow the interaction of Hg²⁺ with the model nucleobase 1,3-dimethyluracil (1,3-DimeU).²²⁴ Starting from the species [(1,3-DimeU-C (5))Hg(OAc)], the replacement of the acetate with different ligands was investigated in terms of the overall effect on both the ¹⁹⁹Hg chemical shifts and ³J(¹H–¹⁹⁹Hg)

coupling constants. It was found that both parameters decrease as a function of the ligand according to the following order $\text{NO}_3^- > \text{OAc}^- > \text{Cl}^- \sim \text{Br}^- > \text{I}^- > \text{SCN}^- > \text{CN}^- > 1, 3 - \text{DimeU} - \text{C}(5)$. The last species of this series is $[\text{Hg}(1,3\text{-DimeU-C}(5))_2]$, in which the central mercury is coordinated to two model nucleobases and can be regarded as a metal-modified base pair.

As previously reminded (see text earlier), the study of metal-modified base pairs represents the starting point to obtain nucleic acids functionalized with metal ions (including Hg^{2+}) to be used as nanomaterials. In this regard, NMR was used to probe indirectly the presence of linear $\{\text{T-Hg(II)-T}\}$ base pairs in DNA duplexes containing mismatched thymidine residues (T). The authors treated DNA duplexes containing differently ^{15}N -labeled mismatched thymidines with natural abundance Hg(II) showing that, in addition to a strong shift of the ^{15}N resonances upon metallation ($\Delta\delta > 30$ ppm), a mercury-mediated coupling was clearly observed between the two metal-coordinated N (3) atoms of the opposite thymidine involved in the artificial base pairing ($^2J(^{15}\text{N}, ^{15}\text{N}) = 2.4$ Hz).²²⁵ Similarly, Hg(II) was reacted with RNA duplexes containing up to 20 uridine mismatches, leading to the formation of mercury-mediated base pairs of the type $\{\text{U-Hg(II)-U}\}$.^{6b,226} The authors focused on a 22-nucleotide long palindromic sequence containing six successive uracil residues and could prove the incorporation of Hg(II) by means of a combination of NMR methods, including ^1H , ^{15}N , ^{199}Hg , and ^1H diffusion-ordered spectroscopy NMR experiments. Interestingly, the only detectable ^{199}Hg was that originated by free Hg(II) ions in solution, most likely accounting for the kinetically labile metal binding and the strong line broadening owing to ^{199}Hg chemical shift anisotropy relaxation. Anyway, the last examples showed that even if direct observation of ^{199}Hg may be somehow elusive, the incorporation of Hg^{2+} in nucleic acids can be confidently assessed by a combination of different more classical NMR techniques.

f-Block: Lanthanides

Although considered as nonessential elements for life, lanthanides are biologically active and have several important medicinal applications in both diagnosis and therapy,²²⁷ the most successful being the use of Gd(III) complexes as MRI contrast agents.²²⁸ The latest positive outcomes are mainly related to gadolinium derivatives of polydentate aminocarboxylate. Gadolinium also has potential for use in neutron capture therapy with the advantage that its uptake can be monitored by MRI. There are two main goals for future development. One is to control the biological behavior (cellular uptake and retention, tissue targeting, and in vivo stability) by incorporating Gd(III) into bioconjugates, such as lipids with acid labile bonds. The other is to improve the efficiency with which the complexes induce spin relaxation in protons of water molecules, by designing chelators to control exchange rates of coordinated, or hydrogen-bonded water molecules, and by controlling the mobility and rotation (e.g., through molecular size) of complexes. These two goals can be merged by designing agents whose spin relaxation properties are dependent on the physiological environment, so that MRI scans can provide biochemical/physiological and structural information.²²⁹

The paramagnetic trivalent lanthanide cations (Ln(III)) have been exploited as shift reagents in NMR spectroscopy for a long time.²³⁰ Applications have been both qualitative, to simplify the spectrum, and quantitative, by comparison of the lanthanide-induced shift and relaxation rate enhancements with values calculated for a proposed structure. Currently, the main application of Ln(III) complexes as shift reagents include the NMR separation of enantiomers (chiral shift reagents), the identification of NMR resonances from intra- and extracellular alkali metal ions (see preceding text), and their exploitation as paramagnetic probes tagging metalloproteins to determine their 3D structure in solution by NMR spectroscopy.²³¹

NMR Spectroscopy of Biologically Relevant Nonmetals

p-Block: Group 15 (N)

Nitrogen

Isotope	A (%)	I	$\gamma (\times 10^7 \text{ rad T}^{-1} \text{ s}^{-1})$	Q (fm^2)	Relative receptivity to ^{13}C	Reference sample
^{14}N	99.63	1	1.934	2.044	5.90	$\text{CH}_3\text{NO}_2/\text{CDCl}_3$ (90%) or neat

The overall more favorable nuclear properties of the $I = 1/2$ ^{15}N isotope, together with the development of ^{15}N -enrichment methods, have prevented the use of ^{14}N NMR spectroscopy from becoming a routine technique to investigate nitrogen-containing compounds. ^{14}N NMR spectra may be acquired directly due to the high natural abundance and the rapid relaxation of this quadrupolar nucleus. On the other hand, ^{14}N peaks are often broad due to the large quadrupole moment. In addition, the low resonance frequency of ^{14}N can result in "ringing" or acoustic resonance within the probe, a consequence of which is rolling baselines in the spectra, making broad signals even harder to detect.⁵ Although the development of antiringing pulse sequences can greatly improve baselines and dramatically reduce the time needed for acquisition of good quality spectra, ^{14}N NMR spectroscopy still remains poorly exploited.

To the best of our knowledge, biologically related ^{14}N NMR studies have been only reported to follow reactions of cisplatin in the blood plasma and cell culture media²³² and, more recently, to investigate the structure and bonding of Pt(IV) -azido complexes, which are being explored as potential photoactivatable anticancer agents,²³³ and to assess their photoinduced speciation.²³⁴

p-Block: Group 16 (O, S, and Se)**Oxygen**

Isotope	A (%)	I	γ ($\times 10^7$ rad T ⁻¹ s ⁻¹)	Q (fm ²)	Relative receptivity to ¹³ C	Reference sample
¹⁷ O	0.04	5/2	3.628	2.558	0.065	D ₂ O/neat

One of the main reasons for studying oxygen is its ubiquity in biology. Indeed, oxygen controls or participates in nearly every biological process, especially those involving aerobic metabolism. Oxygen occupies a key position at both structural and physiological level. In all macromolecules, including peptides, proteins, nucleic acids, and carbohydrates, oxygen plays a major role in the observed molecular conformation, owing to its involvement in H-bond formation. As such, oxygen atoms are involved in triggering, signaling, and activation mechanisms.²³⁵

¹⁷O is the only NMR-active oxygen isotope and shows several unfavorable properties. It has a small gyromagnetic ratio, so that the resonance frequency is about one-seventh that of protons, and low natural abundance, thus making isotopic enrichment often necessary. Finally, it is quadrupolar and frequently presents large EFGs. ¹⁷O exhibits a large NMR chemical shift range depending on the chemical function and the local environment, with the resonances being distributed over ~1000 ppm.

Although, due to these drawbacks, solid-state ¹⁷O NMR spectroscopy has been turning out to be better suited for biologically related studies,²³⁶ several applications of solution ¹⁷O NMR to biological systems have been reported to date, spanning from small compounds to macromolecules. For example, a recent paper has reported on the use of ¹⁷O NMR spectroscopy to detect an oxidized cysteine residue in the human Cu, Zn superoxide dismutase, the novelty of this work relying on the use of a directly

¹⁷O-labeled protein. Indeed, the protein was oxidized at a specific cysteine residue by ¹⁷O₂, and both the linewidth and the chemical shift of the observed signal resulted distinctly in different forms of the protein itself, that is, Cu²⁺, Cu⁺, and the peptide digested forms.²³⁷ Also, ¹⁷O NMR data provided evidences for the oxidation of H₂O to H₂O₂ and the simultaneous reduction of camphor to borneol catalyzed at low ¹⁷O₂ concentration by the bacterial monooxygenase P450_{cam},²³⁸ thus confirming the potential of ¹⁷O NMR in protein studies.

Pioneering works aimed at using ¹⁷O NMR in the study of ligand–protein interactions include the investigation, by both chemical shift and relaxation analysis of ¹⁷O-labeled carbon monoxide binding to several heme proteins.²³⁹

Recently, it was shown that ligand–protein interaction can be studied by means of quadruple central transition (QCT) spectroscopy. This approach relies on the multiexponential relaxation behavior of half-integer quadrupolar nuclei and on the possibility to detect a narrow signal for the central transition in the slow motion conditions. A detailed description of the theory and applications of ¹⁷O QCT spectroscopy to the study of the interaction between ¹⁷O-labeled oxalate, biotin, and palmitic acid with model proteins has been reported.²⁴⁰

Protein hydration dynamics is crucial, since it is strictly connected to correct folding, stability, and functioning of proteins. This phenomenon was studied by magnetic relaxation dispersion (MRD) of ¹⁷O in water molecules.²⁴¹ Moreover, protein conformational motions have been investigated by analyzing ¹⁷O MRD of internal water molecules for two model proteins.²⁴² The use of ¹⁷O NMR to monitor the interactions between water and proteins has also been previously reported.²⁴³ Similarly, ¹⁷O relaxation dispersion has been used to evaluate the residence time of water in minor and major grooves of DNA duplexes.²⁴⁴

The use of ¹⁷O NMR spectroscopy to assess the structure and dynamics of small molecules has been widely exploited. Examples related to biological systems include recent studies on internal carboxylate dynamics of DTPA (diethylenetriamine pentaacetic acid) and DOTA (tetraazacyclododecane tetraacetic acid) complexes of lanthanides, in particular Gd(III) analogues due to their use as MRI contrast agents (see text earlier).²⁴⁵ Moreover, owing to the possibility of using Mn(II) derivatives as contrast agents, detailed studies on Mn²⁺-containing macrocycles have been performed by means of different techniques, including ¹⁷O relaxation experiments.²⁴⁶

Finally, ¹⁷O NMR was used on ¹⁷O-labeled nucleobases to study the interactions within the bases themselves and with the solvents²⁴⁷ and also to evaluate ATP–metal ion interactions.²⁴⁸

A two-part comprehensive review on the theoretical principles and applications of ¹⁷O NMR, in both solution and solid state, from material to biological application, has been published in 2010,²⁴⁹ and subsequently expanded in recent years to include latest findings.²⁵⁰

Sulfur

Isotope	A (%)	I	γ ($\times 10^7$ rad T ⁻¹ s ⁻¹)	Q (fm ²)	Relative receptivity to ¹³ C	Reference sample
³³ S	0.76	3/2	2.056	6.78	0.101	(NH ₄) ₂ SO ₄ /D ₂ O (sat.)

Sulfur is essential for all living cells and may also serve as a chemical food source for some primitive organisms, such as some forms of bacteria using hydrogen sulfide in place of water as the electron donor in a primitive photosynthesis-like process. Sulfide forms a part of iron–sulfur clusters and the bridging ligand in the Cu_A site of cytochrome *c* oxidase, involved in the utilization of

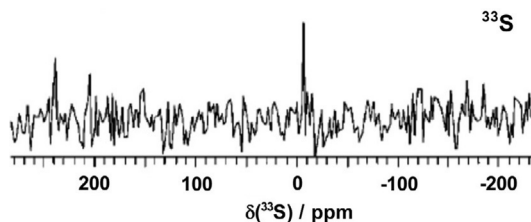


Fig. 22 In vivo ^{33}S NMR spectrum (referred to external aqueous 1 M Na_2SO_4 in a coaxial cell) of an *L. lithophaga* homogenate. The peak at 6.8 ppm is assigned to the amino acid taurine. Adapted from Musio, R.; Sciacovelli, O. *J. Magn. Reson.* **2001**, *153*, 259–261, with permission.

oxygen by all aerobic life. In plants and animals, sulfur is found in all peptides, proteins, and enzymes containing the amino acids cysteine and methionine. Homocysteine and taurine are other sulfur-containing acids that are similar in structure but which are not coded for by DNA and are not part of the primary structure of proteins. GSH is an important sulfur-containing tripeptide that plays a role in cells as a source of chemical reduction potential through its sulfhydryl group. Many important cellular enzymes use prosthetic groups ending with sulfhydryl groups to handle reactions involving acyl-containing biochemicals: two common examples from basic metabolism are coenzyme A and α -lipoic acid. Disulfide (S–S) bonds formed between cysteine residues in peptide chains are very important in protein assembly and structure. These strong covalent bonds between peptide chains give proteins a great deal of extra toughness and resilience.²⁵¹

^{33}S is a quadrupolar nucleus characterized by a low γ and scarce natural abundance, resulting in very low receptivity and low resonance frequency. These properties can increase the effects of spurious signals in the first part of the free induction decay signal, leading to severe distortions in the FT NMR spectrum. The moderate Q leads to an efficient quadrupolar relaxation and to broad NMR signals (from few to thousands hertz). Reasonably narrow resonances can be obtained only for small molecules in which the sulfur atom is located at sites with high electronic symmetry, such as the tetrahedral SO_4^{2-} anion and low-molecular-weight sulfones and sulfonates. In thiols, sulfides, sulfoxides, and other organic and inorganic functional groups with low symmetry, ^{33}S linewidths are often larger than 10 000 Hz, and the signals are observable only in a limited number of cases. Large linewidths prevent the accurate measurement of chemical shifts, may cause the overlap of resonances when more than one type of sulfur atom is present, and have a significant influence on the achievable signal-to-noise ratio, thus consequently affecting the experimental times needed to obtain reasonable spectra.

Consequently to these limitations, direct detection of ^{33}S signals is very challenging, although applications of ^{33}S NMR in solution exist and have been recently reviewed.²⁵²

To the best of our knowledge, the only exploitation of ^{33}S NMR spectroscopy for biochemical investigations is related to the detection of taurine in biological tissues.²⁵³ Taurine (2-aminoethanesulfonic acid) is a naturally occurring β -amino acid widely distributed in the biosphere. Despite the intensive studies, many mechanisms of the biochemical reactions involving taurine remain unknown or uncertain, probably because of the difficulty in detecting taurine in intact tissues. In this work, ^{33}S NMR spectra of biological tissues were reported for the first time. As shown in Fig. 22, the ^{33}S spectrum of *Lithophaga lithophaga* homogenates exhibits a single signal that was assigned to the $^{-33}\text{SO}_3^-$ group of taurine on the basis of its chemical shift value (-6.8 ppm). Remarkably, in the spectral range examined, no ^{33}S NMR signals were detected from other sulfur-containing biological molecules, for instance, cystine, cysteine, methionine, and hypotaurine.

Vale and coworkers carried out a detailed multinuclear NMR characterization of the antitubercular drug ethionamide.²⁵⁴ Notwithstanding the low symmetry of the thioamide sulfur atom, they succeeded in recording the corresponding ^{33}S peak of the drug at 190 ppm in $\text{DMSO}-d_6$ (relative to external 2 M aqueous solution of Cs_2SO_4) but only at 2.5 M concentration and after 14 days of data accumulation. On the other hand, Gale *et al.* developed a new techniques based on ^{33}S NMR to monitor the sulfate transport capability of synthetic transporters mimicking the lipid bilayer of cell membrane.²⁵⁵ The method relies on the use of ^{33}S -labeled sulfate anion and the exploitation of the relaxation properties of paramagnetic agents, such as Mn^{2+} and Fe^{3+} , to discriminate between intra- and extravascular sulfate. The corresponding ^{33}S peaks were observed in 162 mM solutions of $^{33}\text{SO}_4^{2-}$ and after only 3200 scans with a relaxation delay of 250 ms.

Currently, the increasing availability of high-field NMR spectrometers and the development of hardware and probe technology can improve the detection of ^{33}S signals. In this regard, by developing a 10 mm ^{33}S cryogenic NMR probe operating at 9–26 K, sensitivity was increased up to 9.8 times compared to conventional 5 mm broadband probes.²⁵⁶ This ^{33}S cryogenic probe was applied to biological samples, such as human urine, bile, chondroitin sulfate, and scallop tissue, allowing easy detection of sulfur compounds having $-\text{SO}_4^{2-}$ and $-\text{SO}_3^-$ groups.

Selenium

Isotope	A (%)	I	γ ($\times 10^7 \text{ rad T}^{-1} \text{ s}^{-1}$)	Q (fm^2)	Relative receptivity to ^{13}C	C Reference sample
^{77}Se	7.63	1/2	5.125	–	3.15	$\text{Se}(\text{CH}_3)_2/\text{C}_6\text{D}_6$ (90%) or neat

Selenium is a trace element essential for mammals. Low-molecular-weight selenium compounds present in the human body include selenocysteine (or selenocystine) and selenomethionine, with much lower abundance of their metabolic counterparts.

Diseases associated with selenium deficiency include asthma, Keshan disease, and HIV. Therefore, selenium-based agents are currently being investigated for their potential therapeutic applications. Moreover, selenium compounds have been shown to be of value as cancer chemoprotective agents.²⁵⁷ Selenium displays many similarities with its congener sulfur, that is, they have rather similar electronegativity and atom size and share the same major oxidation states. For these reasons, there are many sulfur compounds that have selenium analogs. However, in spite of these similarities, there are clearly differences between the two elements, and substitution for one another results in compounds with quite diverse chemical properties.²⁵⁸

Selenium has six natural isotopes, but only one, ⁷⁷Se, is NMR-active with $I = 1/2$, thus allowing high-resolution NMR spectroscopy to be carried out. ⁷⁷Se is approximately three times more sensitive than ¹³C and, taking into account that longitudinal relaxation times are in the range of seconds and that nuclear Overhauser enhancement (NOE) effects are nearly always absent, the sensitivity of ¹³C and ⁷⁷Se are comparable in routine NMR experiments.²⁵⁹

⁷⁷Se NMR spectroscopy has been successfully employed in several cases, including the characterization of selenium-based potential drugs²⁶⁰ the characterization of selenoproteins,²⁶¹ and their interaction with drugs.²⁶²

Interestingly, owing to the unfavorable nuclear properties of ³³S, ⁷⁷Se may be used as a surrogate in order to gain insights into the multifaceted roles of sulfur in biology. Unfortunately, in the past, such NMR studies were hindered by the low availability of selenium-rich proteins (in particular selenocysteine) and the low sensitivity in the absence of isotopic enrichment. In this regard, recent advances in ⁷⁷Se labeling of proteins, including selectivity and fine-tuning the percent of selenium incorporation, allowed the identification of multiple selenocysteine and selenomethionine residues in the sulfhydryl oxidase augmenter of liver regeneration²⁶³ and the visualization of disulfide bonds through diselenide proxies in a 37-residue spider toxin (κ -ACTX-Hv1c) containing four disulfide bonds, including a rare and functionally critical vicinal disulfide bridge between the adjacent cysteine residues Cys13 and Cys14.²⁶⁴

⁷⁷Se NMR has been also used to study the interaction between the nonenzymatic carbohydrate-binding proteins lectins and selenium-labeled glycosides,²⁶⁵ and to identify the 2-selenouridine moieties in the wobble position of the anticodon stem loop of three tRNA species.²⁶⁶

p-Block: Halogens (F, Cl, Br, and I)

Fluorine

Isotope	A (%)	I	γ ($\times 10^7 \text{ rad T}^{-1} \text{ s}^{-1}$)	Q (fm^2)	Relative receptivity to ¹³ C	Reference sample
¹⁹ F	100	1/2	25.181	–	4900	CFCl ₃ /neat

Fluorine is an essential trace element and is present in the human body mostly in the form of solid fluorides in the bones and teeth.

The ¹⁹F nucleus is a $I = 1/2$ species existing in 100% natural abundance and possessing a magnetogyric ratio that is 83% that of the proton. The large γ translates into both high sensitivity in 1D ¹⁹F NMR spectroscopy and strong dipolar couplings, allowing for the measurement of ¹⁹F–¹⁹F and ¹⁹F–¹H NOEs for distance restraints and the study of topology and contact with solvent.²⁶⁷

Fluorine chemistry is an expanding area of research that is attracting increasing interest, due to the impact of fluorine in the life sciences. Therefore, owing to the high receptivity and the inherent sensitivity of the fluorine resonances to the local environment, coupled with the virtual absence of background fluorine signals, it is not surprising that ¹⁹F NMR spectroscopy (a somewhat neglected technique within the bio-NMR community) in recent years has been emerging as a powerful tool in biological, pharmaceutical, and medicinal chemistry, as proved by the several publications continuously appearing in the literature.

The following applications of ¹⁹F NMR spectroscopy, exploiting several parameters such as chemical shift changes, relaxation rates, intermolecular magnetization transfer, and diffusion data, have been extensively reviewed²⁶⁸ and will not be further discussed in this article:

- Metabolic studies monitoring the biotransformation, pharmacokinetics, and metabolism of fluorinated xenobiotics and drugs²⁶⁹
- Binding studies involving protein–protein, protein–DNA, small molecule–protein, and small molecule–DNA interactions, crucial for drug screening^{269b,270}
- Structural analysis of protein structure and dynamics by incorporating fluorine-containing probes²⁷¹ and of protein cavities²⁷²
- Fluorine-based MRI contrast agents²⁷³

Among its uses, in recent years, ¹⁹F NMR spectroscopy has been successfully applied to RNA research. RNA is involved in many biological processes and is nowadays an acknowledged potential drug target.²⁷⁴ In order to be active, RNA must adopt specific secondary and tertiary structures, and RNA-based biological processes often rely on the ability of RNA to interconvert between several structures. In this regard, ¹⁹F NMR proved useful to study such conformational changes by incorporating a fluorine label either into a nucleobase, for example, by using 5-fluorouracil or 5-fluorocytosine,²⁷⁵ or at the sugar moiety.²⁷⁶ Micura and coworkers showed that the 2'-¹⁹F labeling of the ribose can be used to discriminate between double helical and single-stranded regions in RNAs,²⁷⁶ and to study RNA hairpin/duplex equilibria, providing accurate melting temperature values.²⁷⁷ More

recently, they also reported on the use of ^{19}F NMR spectroscopy for the evaluation of the ligand-induced conformational change of a riboswitch, that is, an RNA element located in the 5' untranslated region of mRNA that controls gene expression upon conformational change induced by ligand binding.²⁷⁸

In general, when a fluorine label is chosen, care should be taken in its positioning along the RNA structure to avoid modifications in the physicochemical properties of the RNA itself. In order to overcome this possible drawback, Tisné and coworkers have recently proposed the use of fluorinated diaminocyclopentanes as external probes for RNA structure.²⁷⁹

Besides its use in structure and conformational dynamics of RNA, ^{19}F NMR spectroscopy has been successfully employed also to evaluate the binding properties of small molecules toward RNA, crucial for the design of RNA-targeting drugs. For example, by incorporating a fluorinated label into the RNA itself, it was possible to identify site-specific RNA binding molecules.^{280a} Moreover, it was recently shown that binding competition studies involving fluorinated probes may open up new perspectives in the suitability of ^{19}F NMR to screen RNA–drug interaction.^{280b}

Overall, these studies have been opening up new perspectives in the use of ^{19}F NMR spectroscopy to study both the RNA–ligand interactions and the structure and dynamics of RNAs as already done currently with proteins (see text earlier).

Chlorine

Isotope	A (%)	I	γ ($\times 10^7 \text{ rad T}^{-1} \text{ s}^{-1}$)	Q (fm^2)	Relative receptivity to ^{13}C	Reference sample
^{35}Cl	75.78	3/2	2.624	8.165	21.0	NaCl/D ₂ O (0.1 M)
^{37}Cl	24.22	3/2	2.184	6.435	3.87	

Chlorine is an essential element for all living organisms largely as chloride, but hypochlorite is produced in some cell compartments to destroy invading organisms. Together with Na^+ , Cl^- is a major extracellular electrolyte. In conjunction with H^+ and monovalent alkali metal ions, it controls transmembrane potentials and regulates the equilibrium of cellular electrolytes and osmotic pressures. A defect in Cl transport causes cystic fibrosis, a genetic disorder resulting in a defect in the transmembrane chloride channel.²¹

All naturally occurring chlorine is found in two NMR-active isotopic forms, ^{35}Cl and ^{37}Cl , both quadrupolar. Owing to the higher natural abundance and receptivity, ^{35}Cl is the preferred isotope for NMR spectroscopic observation. Its relaxation is normally dominated by the contributions from interaction of the quadrupole moments with time-dependent EFG at the nucleus. Although both the natural abundance and receptivity are favorable, recording ^{35}Cl NMR spectra is often challenging as it gives rise to rather broad signals. Therefore, a very few papers report on the use of ^{35}Cl NMR techniques for specific biological purposes.

^{35}Cl NMR spectroscopy has been used in the past to monitor the chloride binding to proteins,²⁸¹ the anion distribution and transport in membranes,²⁸² also in presence of shift reagents to discriminate intra- and extracellular chloride signals,²⁸³ and the interaction between drugs and membranes.²⁸⁴ An interesting application involved the use of ^{35}Cl NMR spectroscopy to assess the mechanism through which chloride ions activate oxygen evolution in photosystem II of green plants.²⁸⁵

Although beyond the scope of this article, it is worth mentioning recent publications reporting on the use of solid-state ^{35}Cl NMR to study the polymorphism in hydrochloride pharmaceuticals,^{286a} and active pharmaceutical ingredients.^{286b}

Bromine and iodine

Isotope	A (%)	I	γ ($\times 10^7 \text{ rad T}^{-1} \text{ s}^{-1}$)	Q (fm^2)	Relative receptivity to ^{13}C	Reference sample
^{79}Br	50.69	3/2	6.725	31.3	237	NaBr/D ₂ O (0.01 M)
^{81}Br	49.31	3/2	7.250	26.2	288	2
^{127}I	100	5/2	5.390	-71.0	560	KI/D ₂ O (0.01 M)

Bromine is currently not thought to be an essential element for man, although it is present in blood at micromolar concentrations. As hypobromite, it has a potential role in the destruction of pathogenic organisms. Iodine is an essential micronutrient for humans, where it is required for incorporation into the thyroid hormones thyroxine and triiodothyronine.²¹

$^{79/81}\text{Br}$ and ^{127}I are the magnetically active quadrupolar isotopes and are characterized by a high sensitivity to detection by NMR spectroscopy. Although ^{79}Br has a slightly higher natural abundance, the preferred isotope for bromine NMR spectroscopic observation is ^{81}Br , due to its higher receptivity. Conversely, ^{127}I is the only NMR-active isotope of iodine at 100% natural abundance.

The use of ^{81}Br in biological systems has been poorly explored, with only few dated examples in the field of protein research.²⁸⁷ ^{127}I NMR spectroscopy has only rarely been utilized for studies of fluid systems partly because, for covalent environments, the ^{127}I signals are generally broadened beyond detection. On the other hand, the iodide ion may be conveniently detected. For example, ^{127}I has been used as a probe for the anion-binding properties of human serum albumin,²⁸⁸ and analogous studies have been

performed to investigate the binding of iodide to some peroxidases.²⁸⁹ The application of ¹²⁷I NMR spectroscopy to study the enzymatic degradation of κ -carrageenan has been recently reported.²⁹⁰

Acknowledgments

Financial support by the National University of Ireland Galway (*Millennium Fund* to LR; *Hardiman Research Scholarship* to EF) and the Irish Research Council (*Postgraduate Scholarship* to EF) is gratefully acknowledged.

References

- Chellani, P.; Sadler, P. J. *Phil. Trans. R. Soc. A* **2015**, *373*, 20140182.
- Crichton, R. R. *Biological Inorganic Chemistry*, 2nd edn.; Elsevier Science: Oxford, 2012.
- Unione, L.; Galante, S.; Diaz, D.; Cañada, F. J.; Jimenez-Barbero, J. *Med. Chem. Commun.* **2014**, *5*, 1280–1289.
- (a) Cohena, J. S.; Jaroszewski, J. W.; Kaplan, O.; Ruiz-Cabellod, J.; Collier, S. W. *Prog. Nucl. Magn. Reson. Spectrosc.* **1995**, *28*, 53–85; (b) Smith, I. C. P.; Stewart, L. C. *Prog. Nucl. Magn. Reson. Spectrosc.* **2002**, *40*, 1–34; (c) Dadiani, M.; Furman-Haran, E.; Degani, H. *Prog. Nucl. Magn. Reson. Spectrosc.* **2006**, *49*, 27–44; (d) Airoidi, C.; Merlo, S.; Sironi, E. *NMR Molecular Recognition Studies for the Elucidation of Protein and Nucleic Acid Structure and Function*. In *Applications of NMR Spectroscopy*; ur-Rahman, A., Iqbal Choudhary, M., Eds.; Bentham Science Publishers Ltd: Amsterdam, 2015; vol. 2, pp 147–219. Chapter 4.
- Mason, J. *Multinuclear NMR Spectroscopy*. Plenum Press: New York, 1987.
- (a) Ronconi, L.; Sadler, P. J. *Coord. Chem. Rev.* **2008**, *252*, 2239–2277; (b) Donghi, D.; Johannsen, S.; Sigel, R. K. O.; Freisinger, E. *Chimia* **2012**, *66*, 791–797.
- (a) Barker, P. B.; Lin, D. D. M. *Prog. Nucl. Magn. Reson. Spectrosc.* **2006**, *49*, 99–128; (b) Wind, R. A.; Hu, J. Z. *Prog. Nucl. Magn. Reson. Spectrosc.* **2006**, *49*, 207–259; (c) Rivera, M.; Caignan, G. A. *Anal. Bioanal. Chem.* **2004**, *378*, 1464–1483; (d) Bermel, W.; Bertini, I.; Felli, I. C.; Piccioli, M.; Pierattelli, R. *Prog. Nucl. Magn. Reson. Spectrosc.* **2006**, *48*, 25–45; (e) Henry, P.-G.; Adriany, G.; Deelchand, D.; Gruetter, R.; Marjanska, M.; Öz, G.; et al. *Magn. Reson. Imaging* **2006**, *24*, 527–539; (f) Marek, R.; Lycka, A. *Curr. Org. Chem.* **2002**, *6*, 35–66; (g) Berners-Price, S. J.; Ronconi, L.; Sadler, P. J. *Prog. Nucl. Magn. Reson. Spectrosc.* **2006**, *49*, 65–98; (h) Martino, R.; Gilard, V.; Desmoulin, F.; Malet-Martino, M. *J. Pharm. Biomed. Anal.* **2005**, *38*, 871–891; (i) Brindle, K. M. *J. Am. Chem. Soc.* **2015**, *137*, 6418–6427; (j) Heshari, K. R.; Wilson, D. M. *Chem. Soc. Rev.* **2014**, *43*, 1627–1659; (k) Ding, Y.; Yao, Y.; Marassi, F. M. *Acc. Chem. Res.* **2013**, *46*, 2182–2190; (l) Kumar, V.; Dwinedi, D. K.; Jagannathan, N. R. *NMR Biomed.* **2014**, *27*, 80–89.
- Harris, R. K.; Mann, B. E. *NMR and the Periodic Table*. Academic Press: London, 1978.
- Bertini, I.; Luchinat, C.; Parigi, G. *Solution NMR of Paramagnetic Molecules: Applications to Metallobiomolecules and Models*. Elsevier Science: Amsterdam, 2001.
- (a) Harris, R. K.; Becker, E. D.; Cabral de Menezes, S. M.; Goodfellow, R.; Granger, P. *Pure Appl. Chem.* **2001**, *73*, 305–332; (b) Harris, R. K.; Becker, E. D.; Cabral de Menezes, S. M.; Granger, P.; Hoffmann, R. E.; Zilm, K. W. *Pure Appl. Chem.* **2008**, *80*, 59–84.
- (a) Birch, H. J. *The Medical Use of Lithium*. In *Metal Ions in Biological Systems*; Sigel, A., Sigel, H., Eds.; 41; Marcel Dekker Inc.: New York, 2004; pp 221–238. Chapter 10; (b) Kozikowski, A. P.; Gaisina, I. N.; Yuan, H.; Petukhov, P. A.; Blond, S. Y.; Fedolak, A.; et al. *J. Am. Chem. Soc.* **2007**, *129*, 8328–8332.
- Gordji-Nejad, A.; Colell, J.; Glögler, S.; Blümich, B.; Appelt, S. *J. Magn. Reson.* **2012**, *214*, 10–14.
- Rehder, D.; Haupt, E. T. K.; Müller, A. *Magn. Reson. Chem.* **2008**, *46*, S24–S29.
- (a) Komoroski, R. A. *Magn. Reson. Imaging* **2000**, *18*, 103–116; (b) Komoroski, R. A. *NMR Biomed.* **2005**, *18*, 67–73; (c) Soares, J. C.; Boada, F.; Spencer, S.; Mallinger, A. G.; Dippold, C. S.; Forster Wells, K.; et al. *Biol. Psychiatry* **2001**, *49*, 437–443.
- Ramaprasad, S. *Prog. Nucl. Magn. Reson. Spectrosc.* **2005**, *47*, 111–121.
- Pierson, E.; Luterbach, K.; Rzepka, E.; Ramaprasad, S. *Magn. Reson. Imaging* **2004**, *22*, 123–126.
- Ardenkjaer-Larsen, J. H.; Fridlund, B.; Gram, A.; Hansson, G.; Hansson, L.; Lerche, M. H.; Servin, R.; Thaning, M.; Golman, K. *Proc. Natl. Acad. USA* **2003**, *100*, 10158–10163.
- van Heeswijk, R. B.; Uffmann, K.; Comment, A.; Kurdzesau, F.; Perazzolo, C.; Cudalbu, C.; Jonnin, S.; Konter, J. A.; Hautle, P.; van den Brandt, B.; Navon, G.; van der Klink, J. J.; Gruetter, R. *Magn. Reson. Med.* **2009**, *61*, 1489–1493.
- Balzan, R.; Mishkovsky, M.; Simonenko, Y.; van Heeswijk, R. B.; Gruetter, R.; Eliav, U.; Navon, G.; Comment, A. *Contrast Media Mol. Imaging* **2016**, *11*, 41–46.
- Wehrli, F. W. *J. Magn. Reson.* **1976**, *23*, 527–532.
- Frausto da Silva, J. J. R.; Williams, R. J. P. *Biological Chemistry of the Elements*. Oxford University Press: Oxford, 2001.
- Gupta, R. K.; Gupta, P. J. *Magn. Reson.* **1982**, *47*, 344–350.
- (a) Inserte, J.; Garcia-Dorado, D.; Hernando, V.; Barba, I.; Soler-Soler, J. *Cardiovasc. Res.* **2006**, *70*, 364–373; (b) Hoyer, K.; Song, Y.; Wang, D.; Phan, D.; Balschi, J.; Ingwall, J. S.; et al. *J. Pharmacol. Exp. Ther.* **2011**, *337*, 513–523; (c) Coman, D.; Trubel, H. K.; Hyder, F. *NMR Biomed.* **2010**, *23*, 277–285; (d) Milne, M.; Hudson, R. H. E. *Chem. Commun.* **2011**, *47*, 9194–9196; (e) Dignam, C. F.; Richards, C. J.; Zopf, J. J.; Wacker, L. S.; Wenzel, T. J. *Org. Lett.* **2005**, *7*, 1773–1776; (f) Zhang, X. M.; Patel, A. B.; de Graaf, A.; Behar, K. L. *Chem. Phys. Lipids* **2004**, *127*, 113–120; (g) Puckeridge, M.; Chapman, B. E.; Conigrave, A. D.; Kuchel, P. W. *J. Inorg. Biochem.* **2012**, *115*, 211–219. (errata corrigé: *J. Inorg. Biochem.* 2013, 121, 196); (h) Babsky, A. M.; Topper, S.; Zhang, H.; Gao, Y.; James, J. R.; Hekmatyar, S. K.; et al. *Magn. Reson. Chem.* **2008**, *59*, 485–490; (i) Delort, A. M.; Gaudet, G.; Forano, E. *Methods Biotechnol.* **2004**, *16*, 389–405; (j) Batista, A. P.; Marreiros, B. C.; Louro, R. O.; Pereira, M. M. *Biochim. Biophys. Acta* **2012**, *1817*, 1810–1816; (k) Puckeridge, M.; Chapman, B. E.; Conigrave, A. D.; Grieve, S. M.; Figtree, G. A.; Kuchel, P. W. *Biophys. J.* **2013**, *104*, 1676–1684.
- Laustsen, C.; Ringgaard, S.; Pedersen, M.; Nielsen, N. C. *J. Magn. Reson.* **2010**, *206*, 139–146.
- Torres, A. M.; Philp, D. J.; Kemp-Harper, R.; Garvey, C.; Kuchel, P. W. *Magn. Reson. Chem.* **2005**, *43*, 217–224.
- Fonseca, C. P.; Fonseca, L. L.; Montezinho, L. P.; Alves, P. M.; Santos, H.; Castro, M. M. C. A.; Geraldies, C. F. G. C. *Eur. Biophys. J.* **2013**, *42*, 503–519.
- (a) Dingley, A. J.; Peterson, R. D.; Grzesiek, S.; Feigon, J. *J. Am. Chem. Soc.* **2005**, *127*, 14466–14472; (b) Biffi, G.; Tannahill, D.; McCafferty, J.; Balasubramanian, S. *Nat. Chem.* **2013**, *5*, 182–186.
- Podbevsek, P.; Hud, N. V.; Plavec, J. *Nucleic Acids Res.* **2007**, *35*, 2554–2563.
- Wong, A.; Ida, R.; Wu, G. *Biochem. Biophys. Res. Commun.* **2005**, *337*, 363–366.
- (a) Ida, R.; Kwan, I. C. M.; Wu, G. *Chem. Commun.* **2007**, 795–797; (b) Snoussi, K.; Halle, B. *Biochemistry* **2008**, *47*, 12219–12229; (c) Ida, R.; Wu, G. *J. Am. Chem. Soc.* **2008**, *130*, 3590–3602; (d) Marincola, F. C.; Virno, A.; Randazzo, A.; Mucci, F.; Saba, G.; Lai, A. *Magn. Reson. Chem.* **2009**, *47*, 1036–1042.
- Augath, M.; Heiler, P.; Kirsch, S.; Schad, L. R. *J. Magn. Reson.* **2009**, *200*, 134–136.
- Rösler, M. B.; Nagel, A. M.; Umatham, R.; Bachert, P.; Benkhedah, N. *NMR Biomed.* **2016**, *29*, 451–457.
- Guttman, H. J.; Cayley, S.; Li, M.; Anderson, C. F.; Record, M. T., Jr. *Biochemistry* **1995**, *34*, 1393–1404.
- Xu, Q.; Deng, H.; Braunlin, W. H. *Biochemistry* **1993**, *32*, 13130–13137.
- (a) Seo, Y.; Murakami, M.; Suzuki, E.; Kuki, S.; Nagayama, K.; Watari, H. *Biochemistry* **1990**, *29*, 599–603; (b) Wellard, R. M.; Shehan, B. P.; Adam, W. R.; Craik, D. J. *Magn. Reson. Med.* **1993**, *29*, 68–76; (c) Rashid, S. A.; Adam, W. R.; Craik, D. J.; Shehan, B. P.; Wellard, R. M. *Magn. Reson. Med.* **1991**, *17*, 213–224.

36. Ogino, T.; Shulman, G. I.; Avison, M. J.; Gullanst, S. R.; den Hollander, J. A.; Shulman, R. G. *Proc. Natl. Acad. Sci. USA* **1985**, *82*, 1099–1103.
37. Kupriyanov, V. V.; Stewart, L. C.; Xiang, B.; Kwak, J.; Deslauriers, R. *Circ. Res.* **1995**, *76*, 839–851.
38. (a) Allis, J. L.; Snaith, C. D.; Seymour, A.-M. L.; Radda, G. K. *FEBS Lett.* **1989**, *242*, 215–217; (b) Allis, J. L.; Endre, Z. H.; Radda, G. K. *Ren. Physiol. Biochem.* **1989**, *12*, 171–180.
39. Jilkina, O.; Kuzio, B.; Rendell, J.; Xiang, B.; Kupriyanov, V. V. *J. Mol. Cell. Cardiol.* **2006**, *41*, 893–901.
40. Kupriyanov, V. V.; Xiang, B.; Sun, J. K.; Jilkina, O.; Dai, G. P.; Deslauriers, R. *Magn. Reson. Med.* **2001**, *46*, 963–973.
41. (a) Yushmanov, V. E.; Kharlamov, A.; Boada, F. E.; Jones, S. C. *Magn. Reson. Med.* **2007**, *57*, 494–500; (b) Yushmanov, V. E.; Kharlamov, A.; Ibrahim, T. S.; Zhaod, T.; Boada, F. E.; Jones, S. C. *NMR Biomed.* **2011**, *24*, 778–783.
42. Soong, L. L.; Leroi, G. E.; Popov, A. I. *Inorg. Chem.* **1990**, *29*, 1366–1370.
43. Goodman, J.; Neil, J. J.; Ackerman, J. J. H. *NMR Biomed.* **2005**, *18*, 125–134.
44. Davis, D. G.; Murphy, E.; London, R. E. *Biochemistry* **1988**, *27*, 3547–3551.
45. Lin, W.; Mota de Freitas, D.; Zhang, Q.; Olsen, K. W. *Arch. Biochem. Biophys.* **1999**, *369*, 78–88.
46. (a) Pfeffer, P. E.; Rolin, D. B.; Brauer, D.; Tu, S.-I.; Kumosinski, T. F. *Biochim. Biophys. Acta* **1990**, *1054*, 169–175; (b) Li, Y.; Neil, J.; Ackerman, J. J. *NMR Biomed.* **1995**, *8*, 183–189.
47. Freisinger, E.; Sigel, R. K. O. *Coord. Chem. Rev.* **2007**, *251*, 1834–1851.
48. Delva, P. The Role of Magnesium as a Metallotherapeutic Drug. In *Metallotherapeutic Drugs and Metal-Based Diagnostic Agents: The Use of Metals in Medicine*; Gielen, M., Tiekink, E. R. T., Eds.; Wiley-VCH: Weinheim, 2005; pp 51–64. Chapter 3.
49. Braunlin, W. H. *Adv. Biophys. Chem.* **1995**, *5*, 89–139.
50. Cowan, J. A. *Inorg. Chem.* **1991**, *30*, 2740–2747.
51. Donghi, D.; Sigel, R. K. O. *Methods Mol. Biol.* **2012**, *848*, 253–273.
52. Tsai, M.-D.; Drakenberg, T.; Thulin, E.; Forsen, S. *Biochemistry* **1987**, *26*, 3635–3643.
53. Yan, H.; Tsai, M.-D. *Biochemistry* **1991**, *30*, 5539–5546.
54. Xian, W.; Tang, J. X.; Janmey, P. A.; Braunlin, W. H. *Biochemistry* **1999**, *38*, 7219–7226.
55. Barbagallo, M.; Dominguez, L. J. The Role of Calcium as a Metallotherapeutic Drug. In *Metallotherapeutic Drugs and Metal-Based Diagnostic Agents: The Use of Metals in Medicine*; Gielen, M., Tiekink, E. R. T., Eds.; Wiley-VCH: Weinheim, 2005; pp 109–124. Chapter 6.
56. Kwan, I. C. M.; Wong, A.; She, Y.-M.; Smith, M. E.; Wu, G. *Chem. Commun.* **2008**, 682–684.
57. Vogel, H. J.; Forsen, S. *Biol. Magn. Reson.* **1987**, *7*, 249–309.
58. Andersson, T.; Drakenberg, T.; Forsen, S.; Thulin, E.; Swärd, M. *J. Am. Chem. Soc.* **1982**, *104*, 576–580.
59. Andersson, T.; Drakenberg, T.; Forsen, S.; Thulin, E. *Eur. J. Biochem.* **1982**, *126*, 501–505.
60. Aramini, J. M.; Drakenberg, T.; Hiraoki, T.; Ke, Y.; Nitta, K.; Vogel, H. J. *Biochemistry* **1992**, *31*, 6761–6768.
61. (a) Geninatti-Crich, S.; Deagostino, A.; Toppino, A.; Alberti, D.; Venturello, P.; Aime, S. *Anticancer Agents Med Chem.* **2012**, *12*, 543–553; (b) Barth, R. F. *J. Neurooncol* **2003**, *62*, 1–5; (c) Luderer, M. J.; de la Puente, P.; Abdel Kareem, A. *Pharm. Res.* **2015**, *32*, 2824–2836; (d) Quan, Z.; Xie, Z. *Chem. A Eur. J.* **2018**, <https://doi.org/10.1002/chem.201704937>.
62. (a) Bendel, P. *NMR Biomed.* **2005**, *18*, 74–82; (b) Bendel, P.; Sauerwein, W. *Med. Phys.* **2001**, *28*, 178–183.
63. Menichetti, L.; DeMarchi, D.; Calucci, L.; Ciofani, G.; Menciassi, A.; Forte, C. *Appl. Radiat. Isot.* **2011**, *69*, 1725–1727.
64. (a) Bonora, M.; Corti, M.; Borsa, F.; Bortolussi, S.; Protti, N.; Santoro, D.; et al. *Appl. Radiat. Isot.* **2011**, *69*, 1702–1705; (b) Geninatti-Crich, S.; Alberti, D.; Szabo, I.; Deagostino, A.; Toppino, A.; Barge, A.; et al. *Chem. A Eur. J.* **2011**, *17*, 8479–8486.
65. Tsilikounas, E.; Kettner, C. A.; Bachovchin, W. W. *Biochemistry* **1993**, *32*, 12651–12655.
66. Zhu Tang, P.-P. P.; Schweizer, M. P.; Bradshaw, K. M.; Bauer, W. F. *Biochem. Pharmacol.* **1995**, *49*, 625–632.
67. Taler, G.; Eliav, U.; Navon, G. *J. Magn. Reson.* **1999**, *141*, 228–238.
68. Leung, I. K. H.; Brown, T., Jr.; Schafeld, C. J.; Claridge, T. D. W. *Med. Chem. Commun.* **2011**, *2*, 390–395.
69. André, J. P.; Mäcke, H. R. *J. Inorg. Biochem.* **2003**, *97*, 315–323.
70. (a) Malakoff, D. *Science* **2000**, *288*, 1323–1324; (b) Salifoglou, T. Aluminum Metallotherapeutics. In *Metallotherapeutic Drugs and Metal-Based Diagnostic Agents: The Use of Metals in Medicine*; Gielen, M., Tiekink, E. R. T., Eds.; Wiley-VCH: Weinheim, 2005; pp 65–82. Chapter 4.
71. Harris, W. R.; Messori, L. *Coord. Chem. Rev.* **2002**, *228*, 237–262.
72. (a) Aramini, J. M.; Vogel, H. J. *J. Am. Chem. Soc.* **1993**, *115*, 245–252; (b) Aramini, J. M.; Vogel, H. J. *J. Am. Chem. Soc.* **1994**, *116*, 6971–6972; (c) Aramini, J. M.; Vogel, H. J. *J. Am. Chem. Soc.* **1994**, *116*, 11506–11511.
73. Aramini, J. M.; Germann, M. W.; Vogel, H. J. *J. Am. Chem. Soc.* **1993**, *115*, 9750–9753.
74. Dellavia, I.; Blixt, J.; Dupressoir, C.; Detellier, C. *Inorg. Chem.* **1994**, *33*, 2823–2829.
75. Wang, X.; Li, K.; Yang, X. D.; Wang, L. L.; Shen, R. F. *J. Inorg. Biochem.* **2009**, *103*, 657–665.
76. Yu, P.; Phillips, B. L.; Olmstead, M. M.; Casey, W. H. *J. Chem. Soc. Dalton Trans.* **2002**, 2119–2125.
77. (a) Cervini-Silva, J.; Nieto-Camacho, A.; Palacios, E.; Montoya, J. A.; Gomez-Vidales, V.; Ramirez-Apan, M. T. *Colloids Surf. B Biointerfaces* **2013**, *111*, 651–655; (b) Sazegar, M. R.; Mahmoudian, S.; Mahmoudi, A.; Triwahyono, S.; Jalil, A. A.; Mukti, R. R.; Nazirah Kamarudin, N. H.; Ghoreishi, M. K. *RSC Adv.* **2016**, *6*, 11023–11031.
78. Hayes, R. L. Gallium. In *Handbook of Toxicity of Inorganic Compounds*; Seiler, H. G., Sigel, H., Sigel, A., Eds.; Marcel Dekker: New York, 1988; pp 297–300.
79. (a) Blower, P. *J. Annu. Rep. Prog. Chem., Sect. A: Inorg. Chem.* **2002**, *98*, 615–633; (b) Mjos, K. D.; Orvig, C. *Chem. Rev.* **2014**, *114*, 4540–4563; (c) Ellahioui, Y.; Prashar, S.; Gomez-Ruiz, S. *Inorganics* **2017**, *5*, 4.
80. Clarke, M. J.; Zhu, F.; Frasca, D. R. *Chem. Rev.* **1999**, *99*, 2511–2534.
81. Chitambar, C. R. *Future Med. Chem.* **2012**, *4*, 1257–1272.
82. (a) Chaves, S.; Mendonça, A. C.; Marques, S. M.; Prata, M. I.; Santos, A. C.; Martins, A. F.; et al. *J. Inorg. Biochem.* **2011**, *105*, 31–38; (b) Garcia, R.; Fouskova, P.; Gano, L.; Paulo, A.; Campello, P.; Toth, E.; et al. *J. Biol. Inorg. Chem.* **2009**, *14*, 261–271.
83. (a) Prata, M. I.; André, J. P.; Kovács, Z.; Takács, A. I.; Tircsó, G.; Tóth, L.; Geraldes, C. F. G. C. *J. Inorg. Biochem.* **2017**, *177*, 8–16; (b) Bihari, Z.; Vultós, F.; Fernandes, C.; Gano, L.; Santos, I.; Correia, J. D. G.; Buglyó, P. *J. Inorg. Biochem.* **2016**, *160*, 189–197.
84. Burgess, J. *Chem. Soc. Rev.* **1996**, *25*, 85–92.
85. Bertini, I.; Luchinat, C.; Messori, L. *J. Am. Chem. Soc.* **1983**, *105*, 1347–1350.
86. Bertini, I.; Messori, L.; Pellacani, G. C.; Sola, M. *Inorg. Chem.* **1988**, *27*, 761–762.
87. Aramini, J. M.; Krygsmann, P. H.; Vogel, H. J. *Biochemistry* **1994**, *33*, 3304–3311.
88. Loria, J. P.; Nowak, T. *Biochemistry* **1998**, *37*, 6967–6974.
89. Resiga, D. S.; Nowak, T. *J. Biol. Chem.* **2003**, *278*, 40943–40952.
90. (a) Watts, S.; Meena, R.; Singh, R. V. *J. Chem. Pharm. Res.* **2013**, *5*, 260–265; (b) Zablotskaya, A.; Segal, I.; Popelis, Y.; Grinberga, S.; Shestakova, I.; Nikolajeva, V.; Eze, D. *Appl. Organomet. Chem.* **2013**, *27*, 114–124.
91. (a) Wang, X.; Liu, B.; Wang, X.; Sun, R. *Curr. Nanosci.* **2011**, *7*, 183–190; (b) Zhang, Z.; Santangelo, D. L.; Ten Brink, G.; Kooi, B. J.; Mouljin, J. A.; Melian-Cabrera, I. *Mater. Lett.* **2014**, *131*, 186–189; (c) Tagaya, M.; Abe, S.; Motozuka, S.; Shiba, K.; Takemura, T.; Hayashi, I.; Sakaguchi, Y. *RSC Adv.* **2017**, *7*, 13643–13652; (d) Miao, G.; Chen, X.; Dong, H.; Fang, L.; Mao, C.; Li, Y.; Li, Z.; Hu, Q. *Mater. Sci. Eng. C* **2013**, *33*, 4236–4243.

92. Poologasundarampillai, G.; Ionescu, C.; Tsigkou, O.; Murugesan, M.; Hill, R. G.; Stevens, M. M.; et al. *J. Mater. Chem.* **2010**, *20*, 8952–8961.
93. Haselhorst, R.; Scheffler, K.; Faletti, L.; Kaspar, A.; Prunte, C.; Seelig, J. *Magn. Reson. Med.* **1998**, *40*, 170–174.
94. Lukevics, E.; Ignatovich, L. Biological Activity of Organogermanium Compounds. In *Metallotherapeutic Drugs and Metal-Based Diagnostic Agents: The Use of Metals in Medicine*; Gielen, M., Tiekink, E. R. T., Eds.; Wiley-VCH: Weinheim, 2005; pp 279–295. Chapter 15.
95. DiMartino, M. J.; Lee, J. C.; Badger, M.; Muirhead, K. A.; Mirabelli, K.; Hanna, N. *J. Pharmacol. Exp. Ther.* **1986**, *236*, 103–110.
96. Takeuchi, Y.; Nishikawa, M.; Tanaka, K.; Takayama, T.; Imanari, M.; Deguchi, M.; et al. *Chem. Commun.* **2000**, 687–688.
97. Chaudhary, A.; Singh, R. V. *Main Group Met. Chem.* **2008**, *31*, 107–155.
98. Hadjikakou, S. K.; Hadjiladis, N. *Coord. Chem. Rev.* **2009**, *253*, 235–249.
99. Meurice, J.-C.; Vallier, M.; Ratier, M.; Duboudin, J. G.; Petraud, M. *J. Chem. Soc., Perkin Trans.* **1996**, *2*, 1311–1313.
100. Martins, J. C.; Biesemans, M.; Willem, R. *Prog. Nucl. Magn. Reson. Spectrosc.* **2000**, *36*, 271–322.
101. (a) Pellerito, L.; Nagy, L. *Coord. Chem. Rev.* **2002**, *224*, 111–150; (b) Wrackmeyer, B. NMR Spectroscopy of Tin Compounds. In *Tin Chemistry: Fundamentals, Frontiers, and Applications*; Gielen, M., Davies, A. G., Pannell, K., Tiekink, E. R. T., Eds.; Wiley-VCH: Weinheim, 2008; pp 17–52. Chapter 2.1.
102. See for example: (a) Camacho-Camacho, C.; Rojas-Oviedo, I.; Garza-Ortiz, A.; Toscano, R. A.; Sánchez-Sánchez, L.; Cardenas, J.; López-Muñoz, H. *Appl. Organomet. Chem.* **2016**, *30*, 199–207; (b) Galván-Hidalgo, J. M.; Chans, G. M.; Ramírez-Apan, T.; Nieto-Camacho, A.; Hernández-Ortega, S.; Gómez, E. *Appl. Organomet. Chem.* **2017**, *31*, e3704; (c) Basu Baul, T. S.; Kehie, P.; Duthie, A.; Guchhait, N.; Raviprakash, N.; Mokhamatam, R. B.; Manna, S. K.; Wang, R.; Englert, U. *J. Inorg. Biochem.* **2017**, *168*, 76–89; (d) Bhadra, P.; Sharma, J.; Sharma, R. A.; Singh, Y. *Appl. Organomet. Chem.* **2017**, *31*, e3639; (e) Lara-Cerón, J. A.; Jiménez-Pérez, V. M.; Molina-Paredes, A. A.; Rasika, D.; Chávez-Reyes, A.; Ram Paudel, H.; Ochoa, M. E.; Muñoz-Flores, B. M. *Eur. J. Inorg. Chem.* **2017**, (21), 2818–2827.
103. Deibler, K.; Basu, P. *Eur. J. Inorg. Chem.* **2013**, *2013*, 1086–1096.
104. Hassfjell, S. *Appl. Radiat. Isot.* **2001**, *55*, 433–439.
105. Yao, Z. S.; Garmestani, K.; Wong, K. J.; Park, L. S.; Dadachova, E.; Yordanov, A.; et al. *J. Nucl. Med.* **2001**, *42*, 1538–1544.
106. Wrackmeyer, B. *Annu. Rep. NMR Spectrosc.* **2002**, *47*, 1–37.
107. Goldstein, G. W. *Neurotoxicology* **1993**, *14*, 97–101.
108. Aramini, J. M.; Hiraoki, T.; Yazawa, M.; Yuan, T.; Zhang, M.; Vogel, H. J. *J. Biol. Inorg. Chem.* **1996**, *1*, 39–48.
109. Wrackmeyer, B.; Horchler, K. *Annu. Rep. NMR Spectrosc.* **1990**, *22*, 249–306.
110. Neupane, K. P.; Pecoraro, V. L. *Angew. Chem. Int. Ed.* **2010**, *49*, 8177–8180.
111. (a) Neupane, K. P.; Pecoraro, V. L. *J. Inorg. Biochem.* **2011**, *105*, 1030–1034; (b) Mah, V.; Jallilvand, F. *Inorg. Chem.* **2012**, *51*, 6285–6298.
112. Claudio, E. S.; ter Horst, M. A.; Forde, C. E.; Stern, C. L.; Zart, M. K.; Godwin, H. A. *Inorg. Chem.* **2000**, *39*, 1391–1397.
113. Ho, P. C. Metallotherapeutic Arsenic Compounds. In *Metallotherapeutic Drugs and Metal-Based Diagnostic Agents: The Use of Metals in Medicine*; Gielen, M., Tiekink, E. R. T., Eds.; Wiley-VCH: Weinheim, 2005; pp 297–312. Chapter 16.
114. Yan, S.; Jin, L.; Sun, H. Antimony in Medicine. In *Metallotherapeutic Drugs and Metal-Based Diagnostic Agents: The Use of Metals in Medicine*; Gielen, M., Tiekink, E. R. T., Eds.; Wiley-VCH: Weinheim, 2005; pp 441–462. Chapter 23.
115. (a) Witkowska, D.; Rowinska-Zyrek, M.; Valensin, G.; Kozlowski, H. *Coord. Chem. Rev.* **2012**, *256*, 133–148; (b) Burford, N.; Eelman, M. D. Bismuth-Based Pharmaceuticals. In *Metallotherapeutic Drugs and Metal-Based Diagnostic Agents: The Use of Metals in Medicine*; Gielen, M., Tiekink, E. R. T., Eds.; Wiley-VCH: Weinheim, 2005; pp 529–540. Chapter 27.
116. Yang, N.; Tanner, J. A.; Zheng, B.-J.; Watt, R. M.; He, M.-L.; Lu, L.-Y.; et al. *Angew. Chem. Int. Ed.* **2007**, *46*, 6464–6468.
117. Sredni, B.; Caspi, R. R.; Klein, A.; Kalechman, Y.; Danziger, Y.; Ben Ya'akov, M.; et al. *Nature* **1987**, *330*, 173–176.
118. (a) Singh, A. K.; Sharma, S. *Coord. Chem. Rev.* **2000**, *209*, 49–98; (b) Duddeck, H. Sulfur, Selenium and Tellurium NMR. In *Encyclopedia of NMR*; Harris, R. K., Wasylishen, R. E., Eds.; John Wiley & Sons Ltd.: Chichester, 2012; pp 4920–4933.
119. Albeck, A.; Weitman, H.; Sredni, B.; Albeck, M. *Inorg. Chem.* **1998**, *37*, 1704–1712.
120. Wadas, T. J.; Wong, E. H.; Weisman, G. R.; Anderson, C. J. *Chem. Rev.* **2010**, *110*, 2858–2902.
121. Aramini, J. M.; Vogel, H. J. *J. Am. Chem. Soc.* **1994**, *116*, 1988–1993.
122. Huclier-Markai, S.; Sabatie, A.; Ribet, S.; Kubicek, V.; Paris, M.; Vidaud, C.; et al. *Radiochim. Acta* **2011**, *99*, 653–662.
123. White, R. E.; Hanusa, T. P. *Organometallics* **2006**, *25*, 5621–5630.
124. Ardenkjær-Larsen, J. H.; Fridlund, B.; Gram, A.; Hansson, G.; Hansson, L.; Lerche, M. H.; et al. *Proc. Natl. Acad. Sci. USA* **2003**, *100*, 10158–10163.
125. Merrit, M. E.; Harrison, C.; Kovacs, Z.; Kshirsagar, P.; Malloy, C. R.; Sherry, A. D. *J. Am. Chem. Soc.* **2007**, *129*, 12942–12943.
126. Mieville, P.; Jannin, S.; Helm, L.; Bodenhauser, G. *J. Am. Chem. Soc.* **2010**, *132*, 5006–5007.
127. (a) Yaghoubi, S.; Schwietert, C. W.; McCue, J. P. *Biol. Trace Elem. Res.* **2000**, *78*, 205–217; (b) Dubler, E. The Biochemistry of Titanium. In *Metallotherapeutic Drugs and Metal-Based Diagnostic Agents: The Use of Metals in Medicine*; Gielen, M., Tiekink, E. R. T., Eds.; Wiley-VCH: Weinheim, 2005; pp 125–142. Chapter 27.
128. Abeyasinghe, P. M.; Harding, M. M. *Dalton Trans.* **2007**, 3474–3482.
129. (a) Gassman, P. G.; Campbell, W. H.; Macomber, D. W. *Organometallics* **1984**, *3*, 385–387; (b) Finch, W. C.; Anslын, E. V.; Grubbs, R. H. *J. Am. Chem. Soc.* **1988**, *110*, 2406–2413.
130. Maurya, R. C.; Rajput, S. *J. Mol. Struct.* **2007**, *833*, 133–144.
131. Clague, M. J.; Butler, A. *Adv. Inorg. Biochem.* **1994**, *9*, 219–243.
132. Jakusch, T.; Costa Pessoa, J.; Kiss, T. *Coord. Chem. Rev.* **2011**, *255*, 2218–2226.
133. Kostova, I. *Anticancer Agents Med Chem.* **2009**, *9*, 827–842.
134. Barrio, D. A.; Etcheverry, S. B. *Curr. Med. Chem.* **2010**, *17*, 3632–3642.
135. (a) Gorzsás, A.; Andersson, I.; Pettersson, L. *J. Inorg. Biochem.* **2009**, *103*, 517–526; (b) Postal, K.; Maluf, D. F.; Valdameri, G.; Rüdiger, A. L.; Hughes, D. L.; De Sá, E. L.; Ribeiro, R. R.; De Souza, E. M.; Soares, J. F.; Nunes, G. G. *RSC Adv.* **2016**, *6*, 114955–114968.
136. Rehder, D. J. *J. Inorg. Biochem.* **2015**, *147*, 25–31.
137. (a) Miranda, C. T.; Carvalho, S.; Yamaki, R. T.; Paniago, E. B.; Borges, R. H. U.; De Bellis, V. M. *Inorg. Chim. Acta* **2010**, *363*, 3776–3783; (b) Fautsch, J. M.; Wilker, J. J. *Inorg. Chem.* **2010**, *49*, 4791–4801; (c) Gonzalez Baro, A.; Andersson, I.; Pettersson, L.; Gorzsás, A. *Dalton Trans.* **2008**, 1095–1102; (d) Gorzsás, A.; Getty, K.; Andersson, I.; Pettersson, L. *Dalton Trans.* **2004**, 2873–2882.
138. (a) Caravan, P.; Gelmini, L.; Glover, N.; Herring, F. G.; Li, H.; McNeill, J. H.; et al. *J. Am. Chem. Soc.* **1995**, *117*, 12759–12770; (b) Yuen, V. G.; Caravan, P.; Gelmini, L.; Glover, N.; McNeill, J. H.; Setyawati, I. A.; et al. *J. Inorg. Biochem.* **1997**, *68*, 109–116; (c) Yraola, F.; Garcia-Vicente, S.; Marti, L.; Albericio, F.; Zorzano, A.; Royo, M. *Chem. Biol. Drug Des.* **2007**, *69*, 423–428.
139. (a) Butler, A.; Danzitz, M. J. *J. Am. Chem. Soc.* **1987**, *109*, 1864–1865; (b) Butler, A.; Eckert, H. J. *J. Am. Chem. Soc.* **1989**, *111*, 2802–2809; (c) Saponja, J. A.; Vogel, H. J. *J. Inorg. Biochem.* **1996**, *62*, 253–270.
140. Ramos, S.; Moura, J. J. G.; Aureliano, M. *Metalomics* **2012**, *4*, 16–22.
141. Delgado, T. C.; Tomaz, A. I.; Correia, I.; Costa Pessoa, J.; Jones, J. G.; Galdes, C. F. G. C.; et al. *J. Inorg. Biochem.* **2005**, *99*, 2328–2339.
142. Aureliano, M.; Tiago, T.; Gandara, R. M. C.; Sousa, A.; Moderno, A.; Kaliva, M.; et al. *J. Inorg. Biochem.* **2005**, *99*, 2355–2361.
143. (a) Patra, D.; Biswas, N.; Kumari, B.; Das, P.; Sepay, N.; Chatterjee, S.; Drew, M. G. B.; Ghosh, T. *RSC Adv.* **2015**, *5*, 92456–92472; (b) Holder, A. A.; Taylor, P.; Magnusen, A. R.; Moffett, E. T.; Meyer, K.; Hong, Y.; Ramsdale, S. E.; Gordon, M.; Stubbs, J.; Seymour, L. A.; Acharya, D.; Weber, R. T.; Smith, P. F.; Dismukes, G. C.; Ji, P.; Menocal, L.; Bay, F.; Williams, J. L.; Cropek, D. M.; Jarrett, W. L. *Dalton Trans.* **2013**, *42*, 11881–11899; (c) Maurya, M. R.; Sarkar, B.; Avcilla, F.; Tariq, S.; Azam, A.

- Correia, I. *Eur. J. Inorg. Chem.* **2016**, 2016, 1430–1441; (d) Benitez, J.; Correia, I.; Becco, L.; Fernandez, M.; Garat, B.; Gallardo, H.; Conte, G.; Kuznetsov, M. L.; Neves, A.; Moreno, V.; Costa Pessoa, J.; Gambino, D. Z. *Anorg. Allg. Chem.* **2013**, 639, 1417–1425; (e) Maurya, M. R.; Kumar, N.; Chaudhary, N. *Polyhedron* **2015**, 97, 103–111.
144. (a) Zhang, Z.; Gao, Y.; Luo, H.; Kang, L.; Chen, Z.; Du, J.; Kaneshira, M.; Zhang, Y.; Wang, Z. L. *Energy Environ. Sci.* **2011**, 4, 4290–4297; (b) Sharifi, S.; Laurent, S.; Laird Forrest, M.; Straeve, P.; Mahmoudi, M. *Chem. Soc. Rev.* **2012**, 41, 2323–2343; (c) Zhou, H.; Li, J.; Bao, S.; Wang, D.; Liu, X.; Jin, P. *RSC Adv.* **2015**, 5, 106315–106324.
145. Vincent, J. B. *Acc. Chem. Res.* **2000**, 33, 503–510.
146. Mendel, R. R. *J. Biol. Chem.* **2013**, 288, 13165–13172.
147. Gomez-Ruiz, S.; Maksimovic-Ivanic, D.; Mijatovic, S.; Kaluderovic, G. N. *Bioinorg. Chem. Appl.* **2012**, 2012, 140284.
148. Hille, R. *Trends Biochem. Sci.* **2002**, 27, 360–367.
149. (a) Hafner, A.; Hegedus, L. S.; DeWeck, G.; Hawkins, B.; Doetz, K. H. *J. Am. Chem. Soc.* **1988**, 110, 8413–8421; (b) Dove, M. F. A.; Jones, E. M. L.; Clark, R. *J. Magn. Reson. Chem.* **1989**, 27, 973–979; (c) Kuroki, S.; Matsukawa, S.; Yasunaga, H. Applications of Nuclear Shielding. In *Nuclear Magnetic Resonance*; Kamienska-Trela, K., Ed.; 44; Royal Society of Chemistry: Cambridge, 2015; pp 76–149.
150. Bristow, S.; Garner, C. D.; Hagyard, S. K.; Morris, G. A.; Nicholson, J. R.; Mills, C. F. *J. Chem. Soc. Chem. Commun.* **1985**, 479–481.
151. Absillis, G.; van Deun, R.; Paract-Vogt, T. N. *Inorg. Chem.* **2011**, 50, 11552–11560.
152. Kim, G.-S.; Judd, D. A.; Hill, C. L.; Schinazi, R. F. *J. Med. Chem.* **1994**, 37, 816–820.
153. Wang, L.; Zhou, B.-B.; Yu, K.; Su, Z.-H.; Gao, S.; Chu, L.-L.; Liu, J.-R.; Yang, G.-Y. *Inorg. Chem.* **2013**, 52, 5119–5127.
154. (a) Barsukova-Stuckart, M.; Piedra-Garza, L. F.; Gautam, B.; Alfaro-Espinoza, G.; Izarova, N. V.; Banerjee, A.; et al. *Inorg. Chem.* **2012**, 51, 12015–12022; (b) Yang, P.; Lin, Z.; Alfaro-Espinoza, G.; Ullrich, M. S.; Raj, C. I.; Silvestru, C.; Kortz, U. *Inorg. Chem.* **2016**, 55, 251–258.
155. Reed, G. H.; Poyner, R. R. *Met. Ions Biol. Syst.* **2000**, 37, 183–207.
156. Crowley, J. D.; Traynor, D. A.; Weatherburn, D. C. *Met. Ions Biol. Syst.* **2000**, 37, 209–278.
157. Horsburgh, M. J.; Wharton, S. J.; Karavolos, M.; Foster, S. J. *Trends Microbiol.* **2002**, 10, 496–501.
158. Freeland-Graves, J. H.; Bose, T.; Karbassian, A. Manganese Metallotherapeutics. In *Metallotherapeutic Drugs and Metal-Based Diagnostic Agents: The Use of Metals in Medicine*; Gielen, M., Tiekink, E. R. T., Eds.; Wiley-VCH: Weinheim, 2005; pp 159–178. Chapter 9.
159. Ooms, K. J.; Feindel, K. W.; Tersikh, V. V.; Wasylishen, R. E. *Inorg. Chem.* **2006**, 45, 8492–8499.
160. (a) Cave, A.; Daures, M. F.; Parello, J.; Saint-Yves, A.; Sempere, R. *Biochimie* **1979**, 61, 755–765; (b) Sheats, J. E.; Czernuszewicz, R. S.; Dismukes, G. C.; Rheingold, A. L.; Petrouleas, V.; Stubbe, J.-A.; et al. *J. Am. Chem. Soc.* **1987**, 109, 1435–1444; (c) Yorkovsky, Y.; Silver, B. L. *J. Inorg. Biochem.* **1997**, 65, 35–43; (d) Li, F.; Li, H.; Hu, L.; Kwan, M.; Chen, G.; He, Q.-Y.; Sun, H. *J. Am. Chem. Soc.* **2005**, 127, 1414–1423; (e) Gaggelli, E.; Bernardi, F.; Molteni, E.; Pogni, R.; Valensin, D.; Valensin, G.; et al. *J. Am. Chem. Soc.* **2005**, 127, 996–1006.
161. Mikhalev, V. A. *Radiochemistry* **2005**, 47, 319–333.
162. (a) Baltzer, L.; Landergrén, M. *J. Am. Chem. Soc.* **1990**, 112, 2804–2805; (b) Baltzer, L.; Becker, E. D.; Averill, B. A.; Hutchinson, J. M.; Gansow, O. A. *J. Am. Chem. Soc.* **1984**, 106, 2444–2446; (c) Meier, E. J. M.; Kozminski, W.; Linden, A.; Lustenberger, P.; von Philipsborn, W. *Organometallics* **1996**, 15, 2469–2477.
163. (a) Baltzer, L.; Becker, E. D.; Tschudin, R. G.; Gansow, O. A. *J. Chem. Soc. Chem. Commun.* **1985**, 1040–1041; (b) Lee, H. C.; Gard, J. K.; Brown, T. L.; Oldfield, E. *J. Am. Chem. Soc.* **1985**, 107, 4087–4088; (c) Baltzer, L. *J. Am. Chem. Soc.* **1987**, 109, 3479–3481; (d) Chung, J.; Lee, H. C.; Oldfield, E. *J. Magn. Reson.* **1990**, 90, 148–157.
164. (a) Baltzer, L.; Landergrén, M. *J. Chem. Soc. Chem. Commun.* **1987**, 32–34; (b) Gerotheranassis, I. P.; Kalodimos, C. G.; Hawkes, G. E.; Haycock, P. *J. Magn. Reson.* **1998**, 131, 163–165.
165. Bergamo, A.; Gaiddon, C.; Schellens, J. H. M.; Beijnen, J. H.; Sava, G. *J. Inorg. Biochem.* **2012**, 106, 90–99.
166. (a) Smith, G. S.; Therrien, B. *Dalton Trans.* **2011**, 40, 10793–10800; (b) Süß-Fink, G. *Dalton Trans.* **2010**, 39, 1673–1688.
167. Peacock, A. F. A.; Sadler, P. J. *Chem. Asian J.* **2008**, 3, 1890–1899.
168. Gaemers, S.; van Slageren, J.; O'Connor, C. M.; Vos, J. G.; Hage, R.; Elsevier, C. *J. Organometallics* **1999**, 18, 5238–5244.
169. (a) Xiaoming, X.; Matsumura-Inoue, T.; Mizutani, S. *Chem. Lett.* **1997**, 241–242; (b) Orellana, G.; Kirsch-De Mesmaeker, A.; Turro, N. J. *Inorg. Chem.* **1990**, 29, 882–885; (c) Steel, P. J.; Lahousse, F.; Lerner, D.; Marzin, C. *Inorg. Chem.* **1983**, 22, 1488–1493.
170. Kaufmann, J.; Schwenk, A. *Phys. Lett.* **1967**, 24A, 115–116.
171. (a) Benn, R.; Jousen, E.; Lehmkühl, H.; Lopez Ortiz, F.; Rufinska, A. *J. Am. Chem. Soc.* **1989**, 111, 8754–8756; (b) Benn, R.; Brenneke, H.; Jousen, E.; Lehmkühl, H.; Lopez Ortiz, F. *Organometallics* **1990**, 9, 756–761; (c) Bell, A. G.; Kozminski, W.; Linden, A.; von Philipsborn, W. *Organometallics* **1996**, 15, 3124–3135; (d) Gray, J. C.; Pagelot, A.; Collins, A.; Fabbiani, F. P. A.; Parsons, S.; Sadler, P. J. *Eur. J. Inorg. Chem.* **2009**, (18), 2673–2677.
172. (a) Gherasim, C.; Lofgren, M.; Banerjee, R. *J. Biol. Chem.* **2013**, 288, 13186–13193; (b) Chao, H.; Ji, L.-N. Cobalt Complexes as Potential Pharmaceutical Agents. In *Metallotherapeutic Drugs and Metal-Based Diagnostic Agents: The Use of Metals in Medicine*; Gielen, M., Tiekink, E. R. T., Eds.; Wiley-VCH: Weinheim, 2005; pp 201–218. Chapter 11.
173. Drennan, C. L.; Huang, S.; Drummond, J. T.; Matthews, R. G.; Ludwig, M. L. *Science* **1994**, 266, 1669–1674.
174. Medek, A.; Frydman, V.; Frydman, L. *Proc. Natl. Acad. Sci. USA* **1997**, 94, 14237–14242.
175. (a) Power, W. P.; Kirby, C. W.; Taylor, N. J. *J. Am. Chem. Soc.* **1998**, 120, 9428–9434; (b) Medek, A.; Frydman, L. *J. Am. Chem. Soc.* **2000**, 122, 684–691.
176. Pruchnik, F. P. Rhodium in Medicine. In *Metallotherapeutic Drugs and Metal-Based Diagnostic Agents: The Use of Metals in Medicine*; Gielen, M., Tiekink, E. R. T., Eds.; Wiley-VCH: Weinheim, 2005; pp 379–398. Chapter 20.
177. Fedotov, M. A. *J. Struct. Chem.* **2016**, 57, 563–613.
178. (a) Dixon, N. E.; Gazzola, T. C.; Blakeley, R. L.; Zerner, B. *J. Am. Chem. Soc.* **1975**, 97, 4131–4133; (b) Farrugia, M. A.; Macomber, L.; Hausinger, R. P. *J. Biol. Chem.* **2013**, 288, 13178–13185.
179. Bühl, M.; Peters, D.; Herges, R. *Dalton Trans.* **2009**, 6037–6044.
180. Garoufis, A.; Hadjikakou, S. K.; Hadjilias, N. *Coord. Chem. Rev.* **2009**, 253, 1384–1397.
181. (a) Wheate, N. J.; Walker, S.; Craig, G. E.; Oun, R. *Dalton Trans.* **2010**, 39, 8113–8127; (b) Medici, S.; Peana, M.; Nurchi, V. M.; Lachowicz, J. I.; Crisponi, G.; Zoroddu, M. A. *Coord. Chem. Rev.* **2015**, 284, 329–350.
182. Becker, M.; Port, R. E.; Zabel, H.-J.; Zeller, W. J.; Bachert, P. *J. Magn. Reson.* **1998**, 133, 115–122.
183. (a) Gabano, E.; Marengo, E.; Bobba, M.; Robotti, E.; Cassino, C.; Botta, M.; et al. *Coord. Chem. Rev.* **2006**, 250, 2158–2174; (b) Still, B. M.; Kumar, P. G. A.; Aldrich-Wright, J. R.; Price, W. S. *Chem. Soc. Rev.* **2007**, 36, 665–686; (c) Vinje, J.; Sletten, E. *Anticancer Agents Med Chem.* **2007**, 7, 35–54.
184. (a) Tsiapis, A. C.; Karapetsas, I. N. *Dalton Trans.* **2014**, 43, 5409–5426; (b) Tsiapis, A. C.; Karapetsas, I. N. *Magn. Reson. Chem.* **2017**, 55, 145–153; (c) Tsiapis, A. C.; Karapetsas, I. N. *Magn. Reson. Chem.* **2017**, 55, 662–669.
185. (a) Harper, B. W. J.; Morris, T. T.; Gailer, J.; Aldrich-Wright, J. R. *J. Inorg. Biochem.* **2016**, 163, 95–102; (b) Kumar, R.; Rosenberg, E.; Feske, M. I.; DiPasquale, A. G. *J. Organomet. Chem.* **2013**, 734, 53–60; (c) Qu, K.; Farrell, N. P. *Dalton Trans.* **2015**, 44, 3563–3572; (d) Bernardes, V. H. F.; Qu, Y.; Du, Z.; Beaton, J.; Vargas, M. D.; Farrell, N. P. *Inorg. Chem.* **2016**, 55, 11396–11407; (e) Hosni, Z.; Bessrou, R.; Tangour, B. *J. Comput. Theor. Nanosci.* **2014**, 11, 318–323.
186. Burkitt, M. J. *Methods Enzymol.* **1994**, 234, 66–79.
187. (a) Wang, W.; Billen, L. P.; Li, Y. *Chem. Biol.* **2002**, 9, 507–517; (b) Carmi, N.; Shultz, L. A.; Breaker, R. R. *Chem. Biol.* **1996**, 3, 1039–1046.
188. (a) Szymanski, P.; Fraczek, T.; Markowicz, M.; Mikiciuk-Olasik, E. *Biomaterials* **2012**, 25, 1089–1112; (b) Leon, I. E.; Cadavid-Vargas, J. F.; Di Virgilio, A. L.; Etcheverry, S. B. *Curr. Med. Chem.* **2017**, 24, 112–148.
189. Kroneck, P.; Lutz, O.; Nolle, A.; Oehler, H. *Z. Naturforsch. A* **1980**, 35, 221–225.
190. Kujime, M.; Kurahashi, T.; Tomura, M.; Fujii, H. *Inorg. Chem.* **2007**, 46, 541–551.

191. (a) Yang, E.-J.; Jang, J.; Kim, S.; Choi, I.-H. *J. Bacteriol. Virol.* **2012**, *42*, 177–179; (b) Gordon, O.; Slenters, T. V.; Brunetto, P. S.; Villaruz, A. E.; Sturdevant, D. E.; Otto, M.; et al. *Antimicrob. Agents Chemother.* **2010**, *54*, 4208–4218.
192. (a) Tiekink, E. R. T. *Inflammopharmacology* **2008**, *16*, 138–142; (b) Ott, I. *Coord. Chem. Rev.* **2009**, *253*, 1670–1681.
193. (a) Nobili, S.; Mini, E.; Landini, I.; Gabbiani, C.; Casini, A.; Messori, L. *Med. Chem. Res.* **2010**, *30*, 550–580; (b) Berners-Price, S. J.; Filipovska, A. *Metallomics* **2011**, *3*, 863–873; (c) Nagy, E. M.; Ronconi, L.; Nardon, C.; Fregona, D. *Mini-Rev. Med. Chem.* **2012**, *12*, 1216–1229.
194. (a) Henrichs, P. M. Silver-109. In *NMR of Newly Accessible Nuclei*; Laszlo, P., Ed.; Chemically and Biochemically Important Elements 2; Academic Press: New York, 1983; pp 319–336. Chapter 12; (b) Penner, G. H.; Li, W. *Inorg. Chem.* **2004**, *43*, 5588–5597.
195. (a) Granger, P. Elements of Column 11: Cu, Ag, Au. In *Transition Metal Nuclear Magnetic Resonance*; Pregosin, P. S., Ed.; Elsevier: Amsterdam, 1991; pp 264–346; (b) Jameson, C. J. Spin–Spin Coupling. In *Multinuclear NMR*; Mason, J., Ed.; Plenum Press: New York, 1987; pp 89–131.
196. (a) Nomiyama, K.; Tsuda, K.; Tanabe, Y.; Nagano, H. *J. Inorg. Biochem.* **1998**, *69*, 9–14; (b) Nomiyama, K.; Takahashi, S.; Noguchi, R.; Nemoto, S.; Takayama, T.; Oda, M. *Inorg. Chem.* **2000**, *39*, 3301–3311; (c) Barreiro, E.; Casas, J. S.; Couce, M. D.; Sanchez, A.; Seoane, R.; Sordo, J.; et al. *Dalton Trans.* **2007**, 3074–3085; (d) Kasuga, N. C.; Yoshikawa, R.; Sakai, Y.; Nomiyama, K. *Inorg. Chem.* **2012**, *51*, 1640–1647.
197. Berners-Price, S. J.; Bowen, R. J.; Harvey, P. J.; Healy, P. C.; Koutsantonis, G. A. *J. Chem. Soc. Dalton Trans.* **1998**, 1743–1750.
198. Penner, G. H.; Liu, X. *Prog. Nucl. Magn. Reson. Spectrosc.* **2006**, *49*, 151–167.
199. (a) Narula, S. S.; Mehra, R. K.; Winge, D. R.; Armitage, I. M. *J. Am. Chem. Soc.* **1991**, *113*, 9354–9358; (b) Narula, S. S.; Winge, D. R.; Armitage, I. M. *Biochemistry* **1993**, *32*, 6773–6787.
200. Leung, B. O.; Jallilvand, F.; Mah, V.; Parvez, M.; Wu, Q. *Inorg. Chem.* **2013**, *52*, 4593–4602.
201. (a) Stulz, E. *Chem. A Eur. J.* **2012**, *18*, 4456–4469; (b) Megger, D. M.; Megger, N.; Müller, J. *Met. Ions Life Sci.* **2012**, *10*, 295–317.
202. Johannsen, S.; Megger, N.; Böhme, D.; Sigel, R. K. O.; Müller, J. *Nat. Chem.* **2010**, *2*, 229–234.
203. Dairaku, T.; Furuta, K.; Sato, H.; Sebera, J.; Nakashima, K.; Kondo, J.; Yamanaka, D.; Kondo, Y.; Okamoto, I.; Ono, A.; Sychrovsky, V.; Kojima, C.; Tanaka, Y. *Chem. A Eur. J.* **2016**, *22*, 13028–13031.
204. Zangger, K.; Armitage, I. M. *Met. Based Drugs* **1999**, *6*, 239–245.
205. (a) Shimizu, T.; Hatano, M. *Biochem. Biophys. Res. Commun.* **1982**, *104*, 1356–1362; (b) Shimizu, T.; Hatano, M. *Biochem. Biophys. Res. Commun.* **1983**, *115*, 22–28; (c) Shimizu, T.; Hatano, M. *Inorg. Chem.* **1985**, *24*, 2003–2009; (d) Ogoma, Y.; Kobayashi, H.; Fujii, T.; Kondo, Y.; Hachimori, A.; Shimizu, T.; et al. *Int. J. Biol. Macromol.* **1992**, *14*, 279–286.
206. (a) Lipton, A. S.; Sears, J. A.; Ellis, P. D. *J. Magn. Reson.* **2001**, *151*, 48–59; (b) Lipton, A. S.; Buchko, G. W.; Sears, J. A.; Kennedy, M. A.; Ellis, P. D. *J. Am. Chem. Soc.* **2001**, *123*, 992–993.
207. (a) Lipton, A. S.; Bergquist, C.; Parkin, G.; Ellis, P. D. *J. Am. Chem. Soc.* **2003**, *125*, 3768–3772; (b) Lipton, A. S.; Ellis, P. D. *J. Am. Chem. Soc.* **2007**, *129*, 9192–9200; (c) Lipton, A. S.; Heck, R. W.; Staeheli, G. R.; Valiev, M.; De Jong, W. A.; Ellis, P. D. *J. Am. Chem. Soc.* **2008**, *130*, 6224–6230; (d) Lipton, A. S.; Heck, R. W.; Hernick, M.; Fierke, C. A.; Ellis, P. D. *J. Am. Chem. Soc.* **2008**, *130*, 12671–12679; (e) Huang, Y.; Sutrisno, A. *Annu. Rep. NMR Spectrosc.* **2014**, *81*, 1–46.
208. Nordberg, G. F. *Toxicol. Appl. Pharmacol.* **2009**, *238*, 192–200.
209. Remelli, M.; Nurchi, V. M.; Lachowicz, J. I.; Medici, S.; Zoroddu, M. A.; Peana, M. *Coord. Chem. Rev.* **2016**, *327*, 55–69.
210. (a) Henehan, C. J.; Pountney, D. L.; Zerbe, O.; Vasak, M. *Protein Sci.* **1993**, *2*, 1756–1764; (b) Li, H.; Otvos, J. D. *Biochemistry* **1996**, *35*, 13929–13936; (c) Öz, G.; Pountney, D. L.; Armitage, I. M. *Biochem. Cell Biol.* **1998**, *76*, 223–234; (d) Daniels, M. J.; Turner-Cavet, J. S.; Selkirk, R.; Sun, H.; Parkinson, J. A.; Sadler, P. J.; Robinson, N. J. *J. Biol. Chem.* **1998**, *273*, 22957–22961; (e) Munoz, A.; Laib, F.; Petering, D. H.; Shaw, C. F., III. *J. Biol. Inorg. Chem.* **1999**, *4*, 495–507; (f) Ejnik, J. W.; Munoz, A.; DeRose, E.; Shaw, C. F., III; Petering, D. H. *Biochemistry* **2003**, *42*, 8403–8410; (g) Stewart, A. J.; Blindauer, C. A.; Berezenko, S.; Sleep, D.; Sadler, P. J. *Proc. Natl. Acad. Sci. U. S. A.* **2003**, *100*, 3701–3706; (h) Meloni, G.; Zovo, K.; Kazantseva, J.; Palumaa, P.; Vasak, M. *J. Biol. Chem.* **2006**, *281*, 14588–14595; (i) Digilio, G.; Bracco, C.; Vergani, L.; Botta, M.; Osella, D.; Viarengo, A. *J. Biol. Inorg. Chem.* **2009**, *14*, 167–178; (j) Loebus, J.; Peroza, E. A.; Blüthgen, N.; Fox, T.; Meyer-Klaucke, W.; Zerbe, O.; et al. *J. Biol. Inorg. Chem.* **2011**, *16*, 683–694; (k) Sutherland, D. E. K.; Willans, M. J.; Stillman, M. J. *J. Am. Chem. Soc.* **2012**, *134*, 3290–3299; (l) Armitage, I. M.; Drakenberg, T.; Reilly, B. *Met. Ions Life Sci.* **2013**, *11*, 117–144; (m) Stachura, M.; Chakraborty, S.; Gottberg, A.; Ruckthong, L.; Pecoraro, V. L.; Hemmingsen, L. *J. Am. Chem. Soc.* **2017**, *139*, 79–82; (n) van Roon, A.-M. M.; Yang, J.-C.; Mathieu, D.; Bermel, W.; Nagai, K.; Neuhaus, D. *Angew. Chem. Int. Ed.* **2015**, *54*, 4861–4864.
211. Maiti, B. K.; Aviles, T.; Matzapetakis, M.; Moura, I.; Pauleta, S. R.; Moura, J. G. E. *Eur. J. Inorg. Chem.* **2012**, (26), 4159–4166.
212. (a) Matzapetakis, M.; Pecoraro, V. L. *J. Am. Chem. Soc.* **2005**, *127*, 18229–18233; (b) Łuczowski, M.; Stachura, M.; Schirf, V.; Demeler, B.; Hemmingsen, L.; Pecoraro, V. L. *Inorg. Chem.* **2008**, *47*, 10875–10888; (c) Iranzo, O.; Jakusch, T.; Lee, K.-H.; Hemmingsen, L.; Pecoraro, V. L. *Chem. A Eur. J.* **2009**, *15*, 3761–3772; (d) Iranzo, O.; Chakraborty, S.; Hemmingsen, L.; Pecoraro, V. L. *J. Am. Chem. Soc.* **2011**, *133*, 239–251; (e) Chakraborty, S.; Iranzo, O.; Zuidenweg, E. R. P.; Pecoraro, V. L. *J. Am. Chem. Soc.* **2012**, *134*, 6191–6203; (f) Peacock, A. F. A.; Pecoraro, V. L. *Met. Ions Life Sci.* **2013**, *11*, 303–337.
213. Gonzalez, R. L., Jr.; Tinoco, I., Jr. *Methods Enzymol.* **2001**, *338*, 421–443.
214. Vogtherr, M.; Limmer, S. *FEBS Lett.* **1998**, *433*, 301–306.
215. (a) Tanaka, Y.; Taira, K. *Chem. Commun.* **2005**, 2069–2079; (b) Tanaka, Y.; Ono, A. *Dalton Trans.* **2008**, 4965–4974.
216. Biagini, S.; Casu, M.; Lai, A.; Caminiti, R.; Crisponi, G. *Chem. Phys.* **1985**, *93*, 461–473.
217. Bernhoft, R. A. *J. Environ. Public Health* **2012**, *2012*, 460–508.
218. Bebout, D. C.; Berry, S. M. *Struct. Bonding (Berlin)* **2006**, *120*, 81–105.
219. (a) Watton, S. P.; Wright, J. G.; Macdonnell, F. M.; Bryson, J. W.; Sabat, M.; O'Halloran, T. V. *J. Am. Chem. Soc.* **1990**, *112*, 2824–2826; (b) Natan, M. J.; Millikan, C. F.; Wright, J. G.; O'Halloran, T. V. *J. Am. Chem. Soc.* **1990**, *112*, 3255–3257; (c) Santos, R. A.; Gruff, E. S.; Koch, S. A.; Harbison, G. S. *J. Am. Chem. Soc.* **1991**, *113*, 469–475; (d) Utschig, L. M.; Bryson, J. W.; O'Halloran, T. V. *Science* **1995**, *268*, 380–385; (e) Huffman, D. L.; Utschig, L. M.; O'Halloran, T. V. *Met. Ions Biol. Syst.* **1997**, *34*, 503–526; (f) Pufahl, R. A.; Singer, C. P.; Peariso, K. L.; Lin, S. J.; Schmidt, P. J.; Fahmi, R. J.; et al. *Science* **1997**, *278*, 853–856; (g) Veglia, G.; Porcellini, F.; DeSilva, T.; Prantner, A.; Opella, S. J. *J. Am. Chem. Soc.* **2000**, *122*, 2389–2390; (h) Warner, T.; Jallilvand, F. *Can. J. Chem.* **2016**, *94*, 373–379.
220. (a) Iranzo, O.; Thulstrup, P. W.; Ryu, S.-B.; Hemmingsen, L.; Pecoraro, V. L. *Chem. A Eur. J.* **2007**, *13*, 9178–9190; (b) Pecoraro, V. L.; Peacock, A. F. A.; Iranzo, O.; Łuczowski, M. *ACS Symp. Ser.* **2009**, *1012*, 183–197.
221. Łuczowski, M.; Zeider, B. A.; Hinz, A. V. H.; Stachura, M.; Chakraborty, S.; Hemmingsen, L.; et al. *Chem. A Eur. J.* **2013**, *19*, 9042–9049.
222. (a) Leung, B. O.; Jallilvand, F.; Mah, V. *Dalton Trans.* **2007**, 4666–4674; (b) Mah, V.; Jallilvand, F. *J. Biol. Inorg. Chem.* **2008**, *13*, 541–553; (c) Mah, V.; Jallilvand, F. *Chem. Res. Toxicol.* **2010**, *23*, 1815–1823; (d) Pujol, A. M.; Lebrun, C.; Gateau, C.; Manceau, A.; Delangle, P. *Eur. J. Inorg. Chem.* **2012**, 3835–3843.
223. Sletten, E.; Nerdal, W. *Met. Ions Biol. Syst.* **1997**, *34*, 479–501.
224. Zamora, F.; Sabat, M.; Lippert, B. *Inorg. Chem.* **1996**, *35*, 4858–4864.
225. Tanaka, Y.; Oda, S.; Yamaguchi, H.; Kondo, Y.; Kojima, C.; Ono, A. *J. Am. Chem. Soc.* **2007**, *129*, 244–245.
226. Johannsen, S.; Paulus, S.; Düpre, N.; Müller, J.; Sigel, R. K. O. *J. Inorg. Biochem.* **2008**, *102*, 1141–1151.
227. New, E. J.; Parker, D.; Smith, D. G.; Walton, J. W. *Curr. Opin. Chem. Biol.* **2010**, *14*, 238–246.
228. (a) Aime, S.; Geninatti Crich, S.; Gianolio, E.; Giovannana, G. B.; Tei, L.; Terreno, E. *Coord. Chem. Rev.* **2006**, *250*, 1562–1579; (b) Yang, C.-T.; Chuang, K.-H. *Med. Chem. Commun.* **2012**, *3*, 552–565.
229. (a) Lacerda, S.; Toth, E. *ChemMedChem* **2017**, *12*, 883–894; (b) Bonnet, C. S.; Toth, E. *Adv. Inorg. Chem.* **2016**, *68*, 43; (c) Bonnet, C. S.; Toth, E. *Chimia* **2016**, *70*, 102–108.

220. Gerdal, C. F. G. C. Lanthanide Shift Reagents. In *The Rare Earth Elements: Fundamentals and Applications*; Atwood, D. A., Ed.; John Wiley & Sons: Chichester, 2012; pp 501–520.
221. Otting, G. *J. Biomol. NMR* **2008**, *42*, 1–9.
222. Norman, R. E.; Sadler, P. J. *Inorg. Chem.* **1988**, *27*, 3583–3587.
223. Farrer, N. J.; Gierth, P.; Sadler, P. J. *Chem. A Eur. J.* **2011**, *17*, 12059–12066.
224. (a) Ronconi, L.; Sadler, P. J. *Chem. Commun.* **2008**, 235–237; (b) Phillips, H. I. A.; Ronconi, L.; Sadler, P. J. *Chem. A Eur. J.* **2009**, *15*, 1588–1596; (c) Ronconi, L.; Sadler, P. J. *Dalton Trans.* **2011**, 40, 262–268.
225. Cleland, W. W.; Kreevoy, M. M. *Science* **1994**, *264*, 1887–1890.
226. (a) Zhu, J.; Ye, E.; Tersikh, V.; Wu, G. *Angew. Chem. Int. Ed.* **2010**, *49*, 8399–8402; (b) Wu, G. *Prog. Nucl. Magn. Reson. Spectrosc.* **2008**, *52*, 118–169.
227. Hanashima, S.; Fujiwara, N.; Matsumoto, K.; Iwasaki, N.; Zheng, G.; Torigo, H.; et al. *Chem. Commun.* **2013**, 49, 1449–1451.
228. Prasad, B.; Mah, D. J.; Lewis, A. R.; Plettner, E. *PLoS One* **2013**, *8*, e61897.
229. (a) Lee, H. C.; Cummings, K.; Hall, K.; Hager, L. P.; Oldfield, E. *J. Biol. Chem.* **1988**, *263*, 16118–16124; (b) Park, K. D.; Guo, K.; Adebodun, F.; Chiu, M. L.; Sligar, S. G.; Oldfield, E. *Biochemistry* **1991**, *30*, 2333–2347.
240. (a) Zhu, J.; Wu, G. *J. Am. Chem. Soc.* **2011**, *133*, 920–932; (b) Zhu, J.; Kwan, I. C. M.; Wu, G. *J. Am. Chem. Soc.* **2009**, *131*, 14206–14207.
241. Modig, K.; Liepinsh, E.; Otting, G.; Halle, B. *J. Am. Chem. Soc.* **2004**, *126*, 102–114.
242. Persson, E.; Halle, B. *J. Am. Chem. Soc.* **2008**, *130*, 1774–1787.
243. (a) Baguet, E.; Hennebert, N. *Biophys. Chem.* **1999**, *77*, 111–121; (b) Torres, A. M.; Grieve, S. M.; Chapman, B. E.; Kuchel, P. W. *Biophys. Chem.* **1997**, *67*, 187–198.
244. Phan, A. T.; Leroy, J. L.; Gueron, M. *J. Mol. Biol.* **1999**, *286*, 505–519.
245. (a) Mayer, F.; Platas-Iglesias, C.; Helm, L.; Peters, J. A.; Djanashvili, K. *Inorg. Chem.* **2012**, *51*, 170–178; (b) Fusaro, L.; Mocchi, F.; Muller, R. N.; Luhmer, M. *Inorg. Chem.* **2012**, *51*, 8455–8461; (c) Elhabiri, M.; Abada, S.; Sy, M.; Nonat, A.; Choquet, P.; Esteban-Gómez, D.; Cassino, C.; Platas-Iglesias, C.; Botta, M.; Charbonnière, L. *J. Chem. A Eur. J.* **2015**, *21*, 6535–6546; (d) Peters, J. A. *Contrast Media Mol. Imaging* **2016**, *11*, 160–168; (e) Tei, L.; Barge, A.; Galli, M.; Pinali, R.; Lattuada, L.; Gianolio, E.; Aime, S. *RSC Adv.* **2015**, *5*, 74734–74743.
246. (a) Drahoš, B.; Koteč, J.; Čisářová, I.; Hermann, P.; Helm, L.; Lukeš, I.; et al. *Inorg. Chem.* **2011**, *50*, 12785–12801; (b) Molnar, E.; Camus, N.; Patinec, V.; Rolla, G. A.; Botta, M.; Tircso, G.; Kaiman, F. K.; Fodor, T.; Tripiet, R.; Platas-Iglesias, C. *Inorg. Chem.* **2014**, *53*, 5136–5149; (c) Forgács, A.; Regueiro-Figueroa, M.; Barriada, J. L.; Esteban-Gómez, D.; De Blas, A.; Rodríguez-Blas, T.; Botta, M.; Platas-Iglesias, C. *Inorg. Chem.* **2015**, *54*, 9576–9587; (d) Gale, E. M.; Mukherjee, S.; Liu, C.; Loving, G. S.; Caravan, P. *Inorg. Chem.* **2014**, *53*, 10748–10761; (e) Kenkel, I.; Franke, A.; Dürr, M.; Zahl, A.; Dücker-Benfer, C.; Langer, J.; Filipović, M. R.; Yu, M.; Puchta, R.; Fiedler, S. R.; Shores, M. P.; Goldsmith, C. R.; Ivanović-Burmazović, I. *J. Am. Chem. Soc.* **2017**, *139*, 1472–1484.
247. Burgar, M. I.; Dhawan, D.; Fiat, D. *Org. Magn. Reson.* **1982**, *20*, 184–190.
248. Shyy, Y.-J.; Tsai, T.-C.; Tsai, M. D. *J. Am. Chem. Soc.* **1985**, *107*, 3478–3484.
249. (a) Gerotheranassis, I. P. *Prog. Nucl. Magn. Reson. Spectrosc.* **2010**, *56*, 95–197; (b) Gerotheranassis, I. P. *Prog. Nucl. Magn. Reson. Spectrosc.* **2010**, *57*, 1–110.
250. (a) Castiglione, F.; Mele, A.; Raos, G. *Annu. Rep. NMR Spectrosc.* **2015**, *85*, 143–192; (b) Wu, G. *Solid State Nucl. Magn. Reson.* **2016**, *73*, 1–14.
251. Kessler, D. *FEMS Microbiol. Rev.* **2006**, *30*, 825–840.
252. Musio, R. *Annu. Rep. NMR Spectrosc.* **2009**, *68*, 1–88.
253. Musio, R.; Sciacovelli, O. *J. Magn. Reson.* **2001**, *153*, 259–261.
254. Vale, N.; Correia, A.; Figueiredo, P.; Santos, H. A. *J. Mol. Struct.* **2016**, *1105*, 286–292.
255. Busschaert, N.; Karagiannidis, L. E.; Wenzel, M.; Haynes, C. J. E.; Wells, N. J.; Young, P. G.; Makuc, D.; Plavec, J.; Jolliffe, K. A.; Gale, P. A. *Chem. Sci.* **2014**, *5*, 1118–1127.
256. Hobo, F.; Takahashi, M.; Saito, Y.; Sato, N.; Takao, T.; Koshihara, S.; et al. *Rev. Sci. Instrum.* **2010**, *81*, 054302/1–054302/7.
257. Carland, M.; Fenner, T. The Use of Selenium-Based Drugs in Medicine. In *Metallotherapeutic Drugs and Metal-Based Diagnostic Agents: The Use of Metals in Medicine*; Gielen, M.; Tiekink, E. R. T., Eds.; Wiley-VCH: Weinheim, 2005; pp 313–332. Chapter 17.
258. Wessjohann, L. A.; Schneider, A.; Abbas, M.; Brandt, W. *Biol. Chem.* **2007**, *388*, 997–1006.
259. Glass, R. S.; Berry, M. J.; Block, E.; Boakye, H. T.; Carlson, B. A.; Gailer, J.; et al. *Phosphorus Sulfur Silicon Relat. Elem.* **2008**, *183*, 924–930.
260. (a) Antoniadis, C. D.; Hadjikakou, S. K.; Hadjiiladis, N.; Papakyriakou, A.; Baril, M.; Butler, I. S. *Chem. A Eur. J.* **2006**, *12*, 6888–6897; (b) Roy, G.; Das, D.; Mughesh, G. *Inorg. Chim. Acta* **2007**, *360*, 303–316; (c) Bhabak, K. P.; Mughesh, G. *Chem. A Eur. J.* **2007**, *13*, 4594–4601; (d) Roy, G.; Mughesh, G. *Phosphorus Sulfur Silicon Relat. Elem.* **2008**, *183*, 908–923; (e) Hill, D. T.; Isab, A. A.; Griswold, D. E.; Di Martino, M. J.; Matz, E. D.; Figueroa, A. L.; et al. *Inorg. Chem.* **2010**, *49*, 7663–7675; (f) Prabhur, P.; Singh, B. G.; Noguchi, M.; Phadnis, P. P.; Jain, V. K.; Iwaoka, M.; Priyadarsini, K. I. *Org. Biomol. Chem.* **2014**, *12*, 2404–2412; (g) Rizvi, M. A.; Zaki, M.; Afzal, M.; Mane, M.; Kumar, M.; Shah, B. A.; Srivastav, S.; Srikrishna, S.; Peerzada, G. M.; Tabassum, S. *Eur. J. Med. Chem.* **2015**, *90*, 876–888; (h) Piovani, L.; Milani, P.; Silva, M. S.; Moraes, P. G.; Demasi, M.; Andrade, L. H. *Eur. J. Med. Chem.* **2014**, *73*, 280–285; (i) Zeng, L.; Li, Y.; Li, T.; Cao, W.; Yi, Y.; Geng, W.; Sun, Z.; Xu, H. *Chem. Asian J.* **2014**, *9*, 2295–2302; (j) Asatkar, A. K.; Tripathi, M.; Panda, S.; Pande, R.; Zade, S. S. *Spectrochim. Acta A* **2017**, *171*, 18–24; (k) Seliman, A. A. A.; Altaf, M.; Odewunmi, N. A.; Kawde, A.-N.; Zierkiewicz, W.; Ahmad, S.; Altuwaijri, S.; Isab, A. A. *Polyhedron* **2017**, *137*, 197–206.
261. (a) Gettins, P.; Crews, B. C. *J. Biol. Chem.* **1991**, *266*, 4804–4809; (b) Boles, J. O.; Tolleson, W. H.; Schmidt, J. C.; Dunlap, R. B.; Odom, J. D. *J. Biol. Chem.* **1992**, *267*, 22217–22223; (c) Stocking, E.; Schwarz, J.; Senn, H.; Salzmann, M.; Silks, L. *J. Chem. Soc. Perkin Trans.* **1997**, 2443–2447; (d) Potrzebowski, M. J.; Katarzynski, R.; Ciesielski, W. *Magn. Reson. Chem.* **1999**, *37*, 173–181; (e) Bayse, C. A. *Inorg. Chem.* **2004**, *43*, 1208–1210; (f) Mobli, M.; Morgenstern, D.; King, G. F.; Alewood, P. F.; Muttenthaler, M. *Angew. Chem. Int. Ed.* **2011**, *50*, 11952–11955; (g) Schaefer, S. A.; Dong, M.; Rubenstein, R. P.; Wilkie, W. A.; Bahnson, B. J.; Thorpe, C.; et al. *J. Mol. Biol.* **2013**, *425*, 222–231; (h) Li, F.; Lutz, P. B.; Pepelyayeva, Y.; Arnér, E. S. J.; Bayse, C. A.; Rozovsky, S. *Proc. Natl. Acad. Sci. USA* **2014**, *111*, 6976–6981; (i) Fehér, K.; Timári, I.; Rákosi, K.; Szolomájer, J.; Illyés, T. Z.; Bartok, A.; Varga, Z.; Panyi, G.; Tóth, G. K.; Kövér, K. E. *Chem. Sci.* **2016**, *7*, 1666–2673.
262. Di Sarra, F.; Fresch, B.; Bini, R.; Saielli, G.; Bagno, A. *Eur. J. Inorg. Chem.* **2013**, (15), 2718–2727.
263. Schaefer, S. A.; Dong, M.; Rubenstein, R. P.; Wilkie, W. A.; Bahnson, B. J.; Thorpe, C.; et al. *J. Mol. Biol.* **2013**, *425*, 222–231.
264. Mobli, M.; Dantas de Araffjo, A.; Lambert, L. K.; Pierens, G. K.; Windley, M. J.; Nicholson, G. M.; et al. *Angew. Chem. Int. Ed.* **2009**, *48*, 9312–9314.
265. (a) Hamark, C.; Landström, J.; Widmalm, G. *Chem. A Eur. J.* **2014**, *20*, 13905–13908; (b) Pérez-Victoria, I.; Boutoureira, O.; Claridge, T. D. W.; Davis, B. G. *Chem. Commun.* **2015**, 51, 12208–12211.
266. Payne, N. C.; Geissler, A.; Button, A.; Sasuclark, A. R.; Schroll, A. L.; Ruggles, E. L.; Gladyshev, V. N.; Hondal, R. J. *J. Free Radic. Biol. Med.* **2017**, *104*, 249–261.
267. (a) Loewen, M. C.; Klein-Seetharaman, J.; Getmanova, E. V.; Reeves, P. J.; Schwalbe, H.; Khorana, H. G. *Proc. Natl. Acad. Sci. USA* **2001**, *98*, 4888–4892; (b) Martinez, D.; Gerig, J. T. *J. Magn. Reson.* **2001**, *152*, 269–275; (c) Campos-Olivas, R.; Aziz, R.; Helms, G. L.; Evans, J. N. S.; Gronenborn, A. M. *FEBS Lett.* **2002**, *517*, 55–60; (d) Wang, X.; Mercier, P.; Letouneau, P.-J.; Sykes, B. D. *Protein Sci.* **2005**, *14*, 2447–2460.
268. Chen, H.; Viel, S.; Ziarelli, F.; Peng, L. *Chem. Soc. Rev.* **2013**, *42*, 7971–7982.
269. (a) Dalvit, C. *Drug Discov. Today* **2009**, *14*, 1051–1057; (b) Cobb, S. L.; Murphy, C. D. *J. Fluorine Chem.* **2009**, *130*, 132–143; (c) Dalvit, C. Fluorine NMR Spectroscopy for Biochemical Screening in Drug Discovery. In *NMR of Biomolecules*; Bertini, I., McGreevy, K. S., Parigi, G., Eds.; Wiley-Blackwell: Weinheim, 2012; pp 315–327; (d) Dalvit, C.; Vulpetti, A. *Magn. Reson. Chem.* **2012**, *50*, 592–597; (e) Takemami, S.; Kitamura, K.; Ohsugi, M.; Konishi, A.; Kitade, T. *AAPS PharmSciTech* **2016**, *17*, 1500–1506; (f) James, A. D.; Marvalín, C.; Luneau, A.; Meissner, A.; Camenisch, G. *Drug Metab. Dispos.* **2017**, *45*, 900–907; (g) Dastjerdi, L. S.; Shamsipur, M. *Trop. J. Pharm. Res.* **2016**, *15*, 2675–2682; (h) Wu, D.; Yan, J.; Sun, P.; Xu, K.; Li, S.; Yang, H.; Li, H. *J. Pharm. Biomed. Anal.* **2016**, *129*, 15–20; (i) Ojima, I. *J. Fluor. Chem.* **2017**, *198*, 10–23; (j) Norton, R. S.; Leung, E. W. W.; Chandrashekar, I. R.; MacRaild, C. A. *Molecules* **2016**, *21*, 860.
270. (a) Dalvit, C. *Prog. Nucl. Magn. Reson. Spectrosc.* **2007**, *51*, 243–271; (b) Matei, E.; André, S.; Glinschert, A.; Infantino, A. S.; Oscarson, S.; Gabius, H.-J.; Gronenborn, A. M. *Chem. A Eur. J.* **2013**, *19*, 5364–5374; (c) Bao, H.-L.; Ishizuka, T.; Sakamoto, T.; Fujimoto, K.; Uechi, T.; Kenmochi, N.; Xu, Y. *Nucleic Acids Res.* **2017**, *45*, 5501–5511;

- (d) Takechi-Haraya, Y.; Aki, K.; Tohyama, Y.; Harano, Y.; Kawakami, T.; Saito, H.; Okamura, E. *Pharmaceuticals* **2017**, *10*, 42; (e) Gee, C. T.; Arntson, K. E.; Urlick, A. K.; Mishra, N. K.; Hawk, L. M. L.; Wisniewski, A. J.; Pomerantz, W. C. K. *Nat. Protoc.* **2016**, *11*, 1414–1427.
271. (a) Kitevski-LeBlanc, J. L.; Prosser, R. S. *Prog. Nucl. Magn. Reson. Spectrosc.* **2012**, *62*, 1–33; (b) Sharaf, N. G.; Gronenborn, A. M. *Methods Enzymol.* **2015**, *565*, 67–95; (c) Marsh, E. N. G.; Suzuki, Y. *ACS Chem. Biol.* **2014**, *9*, 1242–1250; (d) Arntson, K. E.; Pomerantz, W. C. K. *J. Med. Chem.* **2016**, *59*, 5158–5171; (e) Matei, E.; Gronenborn, A. M. *Angew. Chem. Int. Ed.* **2016**, *55*, 150–154; (f) Michurin, O. M.; Afonin, S.; Berditsch, M.; Daniliuc, C. G.; Ulrich, A. S.; Komarov, I. V.; Radchenko, D. S. *Angew. Chem. Int. Ed.* **2016**, *55*, 14595–14599.
272. (a) Fusaro, L.; Locci, E.; Lai, A.; Luhmer, M. *J. Phys. Chem. B* **2010**, *114*, 3398–3403; (b) Liu, D.; Wüthrich, K. *J. Biomol. NMR* **2016**, *65*, 1–5.
273. (a) Srinivas, M.; Heerschap, A.; Ahrens, E. T.; Figdor, C. G.; de Vries, I. J. M. *Trends Biotechnol.* **2010**, *28*, 363–370; (b) Ruiz-Cabello, J.; Barnett, B. P.; Bottomley, P. A.; Bulte, J. W. M. *NMR Biomed.* **2011**, *24*, 114–129; (c) Srinivas, M.; Boehm-Sturm, P.; Figdor, C. G.; de Vries, I. J.; Hoehn, M. *Biomaterials* **2012**, *33*, 8830–8840; (d) Matsushita, H.; Mizukami, S.; Mori, Y.; Sugihara, F.; Shirakawa, M.; Yoshioka, Y.; et al. *ChemBioChem* **2012**, *13*, 1579–1583; (e) Wolters, M.; Mohades, S. G.; Hackeng, T. M.; Post, M. J.; Kooi, M. E.; Backes, W. H. *Invest. Radiol.* **2013**, *48*, 341–359; (f) Gonzales, C.; Yoshihara, H. A. I.; Dilek, N.; Leignadier, J.; Irving, M.; Mievil, P.; Helm, L.; Michielin, O.; Schwitter, J. *PLoS One* **2016**, *11*, e0164557; (g) Zhang, C.; Moonshi, S. S.; Han, Y.; Puttick, S.; Peng, H.; Magoling, B. J. A.; Reid, J. C.; Bernardi, S.; Searles, D. J.; Král, P.; Whittaker, A. K. *Macromolecules* **2017**, *50*, 5953–5963; (h) Chubarov, A. S.; Zakharova, O. D.; Koval, O. A.; Romaschenko, A. V.; Akulov, A. E.; Zavljalov, E. L.; Razumov, I. A.; Koptuyg, I. V.; Knorre, D. G.; Godovikova, T. S. *Bioorg. Med. Chem.* **2015**, *23*, 6943–6954; (i) Zhang, C.; Moonshi, S. S.; Peng, H.; Puttick, S.; Reid, J.; Bernardi, S.; Searles, D. J.; Whittaker, A. K. *ACS Sensors* **2016**, *1*, 757–765; (j) Zheng, Z.; Sun, H.; Hu, C.; Li, G.; Liu, X.; Chen, P.; Cui, Y.; Liu, J.; Wang, J.; Liang, G. *Anal. Chem.* **2016**, *88*, 3363–3368.
274. Guan, L.; Disney, M. D. *ACS Chem. Biol.* **2012**, *7*, 73–86.
275. (a) Puffer, B.; Kreutz, C.; Rieder, U.; Ebert, M.-O.; Konrat, R.; Micura, R. *Nucleic Acids Res.* **2009**, *37*, 7728–7740; (b) Zhao, C.; Anklin, C.; Greenbaum, N. L. *Methods Enzymol.* **2014**, *549*, 267–285.
276. Kreutz, C.; Kählig, H.; Konrat, R.; Micura, R. *J. Am. Chem. Soc.* **2005**, *127*, 11558–11559.
277. Graber, D.; Moroder, H.; Micura, R. *J. Am. Chem. Soc.* **2008**, *130*, 17230–17231.
278. Rieder, U.; Kreutz, C.; Micura, R. *Proc. Natl. Acad. Sci. U. S. A.* **2010**, *107*, 10804–10809.
279. Moumné, R.; Pasco, M.; Prost, E.; Lecourt, T.; Micouin, L.; Tisné, C. *J. Am. Chem. Soc.* **2010**, *132*, 13111–13113.
280. (a) Kreutz, C.; Kählig, H.; Konrat, R.; Micura, R. *Angew. Chem. Int. Ed.* **2006**, *45*, 3450–3453; (b) Lombès, T.; Moumné, R.; Larue, V.; Prost, E.; Catala, M.; Lecourt, T.; et al. *Angew. Chem. Int. Ed.* **2012**, *51*, 9530–9534.
281. (a) Lundberg, P.; Vogel, H.; Drakenberg, T.; Forsen, S.; Amiconi, G.; Forlani, L.; et al. *Biochem. Biophys. Acta* **1989**, *999*, 12–18; (b) Gettins, P.; Sottrup-Jensen, L. *J. Biol. Chem.* **1990**, *265*, 7268–7272; (c) Bahar, S.; Gunter, C. T.; Wu, C.; Kennedy, S.; Knauf, P. A. *Am. J. Physiol. Cell Physiol.* **1999**, *277*, C791–C799; (d) Wolf-Watz, M.; Bäckström, S.; Grundström, T.; Sauer, U.; Härd, T. *FEBS Lett.* **2001**, *488*, 81–84; (e) Maret, W.; Heffron, G.; Hill, H. A. O.; Djuricic, D.; Jiang, L.-J.; Vallee, B. L. *Biochemistry* **2002**, *41*, 1689–1694.
282. (a) Falke, J. J.; Kanes, K. J.; Chan, S. I. *J. Biol. Chem.* **1985**, *260*, 9545–9551; (b) Brauer, M.; Spread, C. Y.; Reithmeier, R. A. F.; Sykes, B. *J. Biol. Chem.* **1985**, *260*, 11643–11650; (c) Gilbowicka, M.; Wincler, B.; Aranibar, N.; Schuster, M.; Hanssum, H.; Rüterjans, H.; et al. *Biochim. Biophys. Acta* **1988**, *946*, 345–358; (d) Müller-Berger, S.; Karbach, D.; Kang, D.; Aranibar, N.; Wood, P. G.; Rüterjans, H.; et al. *Biochemistry* **1995**, *34*, 9325–9332; (e) Liu, D.; Kennedy, S. D.; Knauf, P. A. *Biochemistry* **1996**, *35*, 15228–15235; (f) Koulov, A. V.; Mahoney, J. M.; Smith, B. D. *Org. Biomol. Chem.* **2003**, *1*, 27–29.
283. Diven, C. F.; Wang, F.; Abukhdeir, A. M.; Salah, W.; Layden, B. T.; Gerald, C. F. G. C.; et al. *Inorg. Chem.* **2003**, *42*, 2774–2782.
284. Eriksson, L. E. G. *Biophys. Chem.* **1987**, *26*, 9–18.
285. (a) Coleman, W. J.; Govindjee, J.; Gutowsky, H. S. *Biochim. Biophys. Acta* **1987**, *894*, 443–452.
286. (a) Hamaed, H.; Pawlowski, J. M.; Cooper, B. F. T.; Fu, R.; Eichhorn, S. H.; Schurko, R. W. *J. Am. Chem. Soc.* **2008**, *130*, 11056–11065; (b) Hirsh, D. A.; Rossini, A. J.; Emsley, L.; Schurko, R. W. *Phys. Chem. Chem. Phys.* **2016**, *18*, 25893–25904.
287. (a) Stengle, T. R.; Baldeschwieler, J. D. *Proc. Natl. Acad. Sci. USA* **1966**, *55*, 1020–1025; (b) Zeppezauer, M.; Lindman, B.; Forsen, S.; Lindqvist, I. *Biochem. Biophys. Res. Commun.* **1969**, *37*, 137–142; (c) Collins, T. R.; Starcuk, Z.; Burr, A. H.; Wells, E. J. *J. Am. Chem. Soc.* **1973**, *95*, 1649–1656; (d) Pesek, J. J.; Ronen, S. M.; Alcaraz, A. *Appl. Spectrosc.* **1987**, *41*, 865–869.
288. None, J.-E.; Hjalmarsson, S.-G.; Lindman, B.; Zeppezauer, M. *Biochemistry* **1975**, *14*, 3401–3408.
289. (a) Sakurada, J.; Hosoya, T.; Shimizu, T.; Hatano, M. *Chem. Lett.* **1985**, *2*, 211–214; (b) Sakurada, J.; Takahashi, S.; Shimizu, T.; Hatano, M.; Nakamura, S.; Hosoya, T. *Biochemistry* **1987**, *26*, 6478–6483; (c) Fukuyama, K.; Sato, K.; Itakura, H.; Takahashi, S.; Hosoya, T. *J. Biol. Chem.* **1997**, *272*, 5752–5756.
290. Collén, P. N.; Lemoine, M.; Daniellou, R.; Guegan, J.-P.; Paoletti, S.; Helbert, W. *Biomacromolecules* **2009**, *10*, 1757–1767.